7

Filter Design Techniques

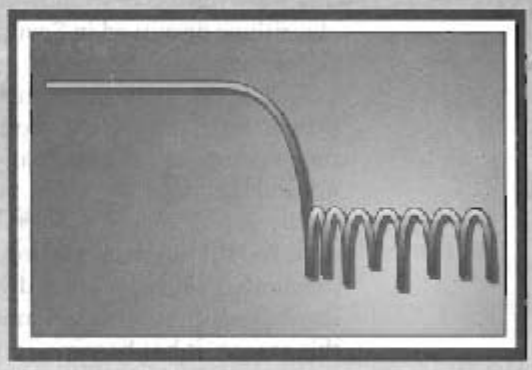

7.0 INTRODUCTION

Filters are a particularly important class of LTI systems. Strictly speaking, the term *frequency-selective filter* suggests a system that passes certain frequency components of an input signal and totally rejects all others, but in a broader context, any system that modifies certain frequencies relative to others is also called a filter. While the primary emphasis in this chapter is on the design of frequency-selective filters, some of the techniques are more broadly applicable. We concentrate on the design of causal filters, although in many contexts, filters need not be restricted to causal designs. Very often, noncausal filters are designed and implemented by modifying causal designs.

The design of discrete-time filters corresponds to determining the parameters of a transfer function or difference equation that approximates a desired impulse response or frequency response within specified tolerances. As discussed in Chapter 2, discrete-time systems implemented with difference equations fall into two basic categories: infinite impulse response (IIR) systems and finite impulse response (FIR) systems. Designing IIR filters implies obtaining an approximating transfer function that is a rational function of z, whereas designing FIR filters implies polynomial approximation. The commonly used design techniques for these two classes take different forms. When discrete-time filters first came into common use, their designs were based on mapping well-formulated and well-understood continuous-time filter designs to discrete-time designs through techniques such as impulse invariance and the bilinear transformation, as we will discuss in Sections 7.2.1 and 7.2.2. These always resulted in IIR filters and remain at the core of the design of frequency selective discrete-time IIR filters. In contrast, since there is not a body of FIR design techniques in continuous time that could be adapted to

the discrete-time case, design techniques for that class of filters emerged only after they became important in practical systems. The most prevalent approaches to designing FIR filters are the use of windowing, as we will discuss in Section 7.5 and the class of iterative algorithms discussed in Section 7.7 and collectively referred to as the Parks–McClellan algorithm.

The design of filters involves the following stages: the specification of the desired properties of the system, the approximation of the specifications using a causal discrete-time system, and the realization of the system. Although these three steps are certainly not independent, we focus our attention primarily on the second step, the first being highly dependent on the application and the third dependent on the technology to be used for the implementation. In a practical setting, the desired filter is generally implemented with digital hardware and often used to filter a signal that is derived from a continuous-time signal by means of periodic sampling followed by A/D conversion. For this reason, it has become common to refer to discrete-time filters as *digital filters*, even though the underlying design techniques most often relate only to the discrete-time nature of the signals and systems. The issues associated with quantization of filter coefficients and signals inherent in digital representations is handled separately, as already discussed in Chapter 6.

In this chapter, we will discuss a wide range of methods for designing both IIR and FIR filters. In any practical context, there are a variety of trade offs between these two classes of filters, and many factors that need to be considered in choosing a specific design procedure or class of filters. Our goal in this chapter is to discuss and illustrate some of the most widely used design techniques and to suggest some of the trade offs involved. The projects and problems on the companion website provide an opportunity to explore in more depth the characteristics of the various filter types and classes and the associated issues and trade offs.

7.1 FILTER SPECIFICATIONS

In our discussion of filter design techniques, we will focus primarily on frequency-selective lowpass filters, although many of the techniques and examples generalize to other types of filters. Furthermore, as discussed in Section 7.4, lowpass filter designs are easily transformed into other types of frequency-selective filters.

Figure 7.1 depicts the typical representation of the tolerance limits associated with approximating a discrete-time lowpass filter that ideally has unity gain in the passband and zero gain in the stopband. We refer to a plot such as Figure 7.1 as a "tolerance scheme."

Since the approximation cannot have an abrupt transition from passband to stopband, a transition region from the passband edge frequency ω_p to the beginning of the stopband at ω_s is allowed, in which the filter gain is unconstrained.

Depending somewhat on the application, and the historical basis for the design technique, the passband tolerance limits may vary symmetrically around unity gain in which case $\delta_{p_1} = \delta_{p_2}$, or the passband may be constrained to have maximum gain of unity, in which case $\delta_{p_1} = 0$.

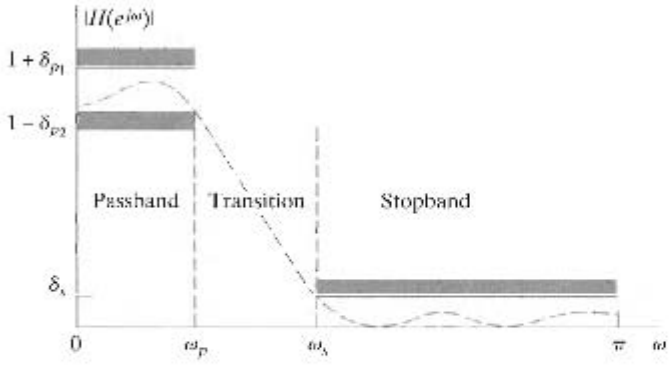

Figure 7.1 Lowpass filter tolerance scheme.

Many of the filters used in practice are specified by a tolerance scheme similar to that which is presented below in Example 7.1, with no constraints on the phase response other than those imposed implicitly by requirements of stability and causality. For example, the poles of the system function for a causal and stable IIR filter must lie inside the unit circle. In designing FIR filters, we often impose the constraint of linear phase. This removes the phase of the signal from consideration in the design process.

Example 7.1 Determining Specifications for a Discrete-Time Filter

Consider a discrete-time lowpass filter that is to be used to filter a continuous-time signal using the basic configuration of Figure 7.2. As shown in Section 4.4, if an LTI discrete-time system is used as in Figure 7.2, and if the input is bandlimited and the sampling frequency is high enough to avoid aliasing, then the overall system behaves as an LTI continuous-time system with frequency response

$$H_{\text{eff}}(j\Omega) = \begin{cases} H(e^{j\Omega T}), & |\Omega| < \pi/T, \\ 0, & |\Omega| \geq \pi/T. \end{cases} \tag{7.1a}$$

In such cases, it is straightforward to convert from specifications on the effective continuous-time filter to specifications on the discrete-time filter through the relation $\omega = \Omega T$. That is, $H(e^{j\omega})$ is specified over one period by the equation

$$H(e^{j\omega}) = H_{\text{eff}}\left(j\frac{\omega}{T}\right), \qquad |\omega| < \pi. \tag{7.1b}$$

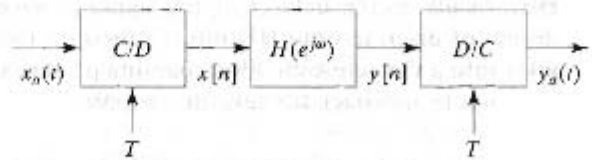

Figure 7.2 Basic system for discrete-time filtering of continuous-time signals.

For this example, the overall system of Figure 7.2 is to have the following properties when the sampling rate is 10^4 samples/s ($T = 10^{-4}$ s):

1. The gain $|H_{\text{eff}}(j\Omega)|$ should be within ± 0.01 of unity in the frequency band $0 \leq \Omega \leq 2\pi(2000)$.
2. The gain should be no greater than 0.001 in the frequency band $2\pi(3000) \leq \Omega$.

Since Eq. (7.1a) is a mapping between the continuous-time and discrete-time frequencies, it only affects the passband and stopband edge frequencies and not the tolerance limits on frequency response magnitude. For this specific example, the parameters would be

$$\begin{aligned} \delta_{p1} = \delta_{p2} &= 0.01 \\ \delta_s &= 0.001 \\ \omega_p &= 0.4\pi \text{ radians} \\ \omega_s &= 0.6\pi \text{ radians.} \end{aligned}$$

Therefore, in this case, the ideal passband magnitude is unity and is allowed to vary between $(1+\delta_{p1})$ and $(1-\delta_{p2})$, and the stopband magnitude is allowed to vary between 0 and δ_s. Expressed in units of decibels,

$$\begin{aligned} \text{ideal passband gain in decibels} &= 20\log_{10}(1) &&= 0 \text{ dB} \\ \text{maximum passband gain in decibels} &= 20\log_{10}(1.01) &&= 0.0864 \text{ dB} \\ \text{minimum passband gain at passband edge in decibels} &= 20\log_{10}(0.99) &&= -0.873 \text{ dB} \\ \text{maximum stopband gain in decibels} &= 20\log_{10}(0.001) &&= -60 \text{ dB} \end{aligned}$$

Example 7.1 was phrased in the context of using a discrete-time filter to process a continuous-time signal after periodic sampling. There are many applications in which a discrete-time signal to be filtered is not derived from a continuous-time signal, and there are a variety of means besides periodic sampling for representing continuous-time signals in terms of sequences. Also, in most of the design techniques that we discuss, the sampling period plays no role whatsoever in the approximation procedure. For these reasons, we take the point of view that the filter design problem begins from a set of desired specifications in terms of the discrete-time frequency variable ω. Depending on the specific application or context, these specifications may or may not have been obtained from a consideration of filtering in the framework of Figure 7.2.

7.2 DESIGN OF DISCRETE-TIME IIR FILTERS FROM CONTINUOUS-TIME FILTERS

Historically, as the field of digital signal processing was emerging, techniques for the design of discrete-time IIR filters relied on the transformation of a continuous-time filter into a discrete-time filter meeting prescribed specifications. This was and still is a reasonable approach for several reasons:

- The art of continuous-time IIR filter design is highly advanced, and since useful results can be achieved, it is advantageous to use the design procedures already developed for continuous-time filters.

- Many useful continuous-time IIR design methods have relatively simple closed-form design formulas. Therefore, discrete-time IIR filter design methods based on such standard continuous-time design formulas are simple to carry out.
- The standard approximation methods that work well for continuous-time IIR filters do not lead to simple closed-form design formulas when these methods are applied directly to the discrete-time IIR case, because the frequency response of a discrete-time filter is periodic, and that of a continuous-time filter is not.

The fact that continuous-time filter designs can be mapped to discrete-time filter designs is totally unrelated to, and independent of, whether the discrete-time filter is to be used in the configuration of Figure 7.2 for processing continuous-time signals. We emphasize again that the design procedure for the discrete-time system begins from a set of discrete-time specifications. Henceforth, we assume that these specifications have been appropriately determined. We will use continuous-time filter approximation methods only as a convenience in determining the discrete-time filter that meets the desired specifications. Indeed, the continuous-time filter on which the approximation is based may have a frequency response that is vastly different from the effective frequency response when the discrete-time filter is used in the configuration of Figure 7.2.

In designing a discrete-time filter by transforming a prototype continuous-time filter, the specifications for the continuous-time filter are obtained by a transformation of the specifications for the desired discrete-time filter. The system function $H_c(s)$ or impulse response $h_c(t)$ of the continuous-time filter is then obtained through one of the established approximation methods used for continuous-time filter design, such as those which are discussed in Appendix B. Next, the system function $H(z)$ or impulse response $h[n]$ for the discrete-time filter is obtained by applying to $H_c(s)$ or $h_c(t)$ a transformation of the type discussed in this section.

In such transformations, we generally require that the essential properties of the continuous-time frequency response be preserved in the frequency response of the resulting discrete-time filter. Specifically, this implies that we want the imaginary axis of the s-plane to map onto the unit circle of the z-plane. A second condition is that a stable continuous-time filter should be transformed to a stable discrete-time filter. This means that if the continuous-time system has poles only in the left half of the s-plane, then the discrete-time filter must have poles only inside the unit circle in the z-plane. These constraints are basic to all the techniques discussed in this section.

7.2.1 Filter Design by Impulse Invariance

In Section 4.4.2, we discussed the concept of *impulse invariance*, wherein a discrete-time system is defined by sampling the impulse response of a continuous-time system. We showed that impulse invariance provides a direct means of computing samples of the output of a bandlimited continuous-time system for bandlimited input signals. In some contexts, it is particularly appropriate and convenient to design a discrete-time filter by sampling the impulse response of a continuous-time filter. For example, if the overall objective is to simulate a continuous-time system in a discrete-time setting, we might typically carry out the simulation in the configuration of Figure 7.2, with the discrete-time system design such that its impulse response corresponds to samples of the

continuous-time filter to be simulated. In other contexts, it might be desirable to maintain, in a discrete-time setting, certain time-domain characteristics of well-developed continuous-time filters, such as desirable time-domain overshoot, energy compaction, controlled time-domain ripple, and so on. Alternatively, in the context of filter design, we can think of impulse invariance as a method for obtaining a discrete-time system whose frequency response is determined by the frequency response of a continuous-time system.

In the impulse invariance design procedure for transforming continuous-time filters into discrete-time filters, the impulse response of the discrete-time filter is chosen proportional to equally spaced samples of the impulse response of the continuous-time filter; i.e.,

$$h[n] = T_d h_c(nT_d), \tag{7.2}$$

where T_d represents a sampling interval. As we will see, because we begin the design problem with the discrete-time filter specifications, the parameter T_d in Eq. (7.2) in fact has no role whatsoever in the design process or the resulting discrete-time filter. However, since it is customary to specify this parameter in defining the procedure, we include it in the following discussion. Even if the filter is used in the basic configuration of Figure 7.2, the design sampling period T_d need not be the same as the sampling period T associated with the C/D and D/C conversion.

When impulse invariance is used as a means for designing a discrete-time filter with a specified frequency response, we are especially interested in the relationship between the frequency responses of the discrete-time and continuous-time filters. From the discussion of sampling in Chapter 4, it follows that the frequency response of the discrete-time filter obtained through Eq. (7.2) is related to the frequency response of the continuous-time filter by

$$H(e^{j\omega}) = \sum_{k=-\infty}^{\infty} H_c\left(j\frac{\omega}{T_d} + j\frac{2\pi}{T_d}k\right). \tag{7.3}$$

If the continuous-time filter is bandlimited, so that

$$H_c(j\Omega) = 0, \qquad |\Omega| \geq \pi/T_d, \tag{7.4}$$

then

$$H(e^{j\omega}) = H_c\left(j\frac{\omega}{T_d}\right), \qquad |\omega| < \pi; \tag{7.5}$$

i.e., the discrete-time and continuous-time frequency responses are related by a linear scaling of the frequency axis, namely, $\omega = \Omega T_d$ for $|\omega| < \pi$. Unfortunately, any practical continuous-time filter cannot be exactly bandlimited, and consequently, interference between successive terms in Eq. (7.3) occurs, causing aliasing, as illustrated in Figure 7.3. However, if the continuous-time filter approaches zero at high frequencies, the aliasing may be negligibly small, and a useful discrete-time filter can result from sampling the impulse response of a continuous-time filter.

When the impulse invariance design procedure is used to utilize continuous-time filter design procedures for the design of a discrete-time filter with given frequency response specifications, the discrete-time filter specifications are first transformed to continuous-time filter specifications through the use of Eq. (7.5). Assuming that the

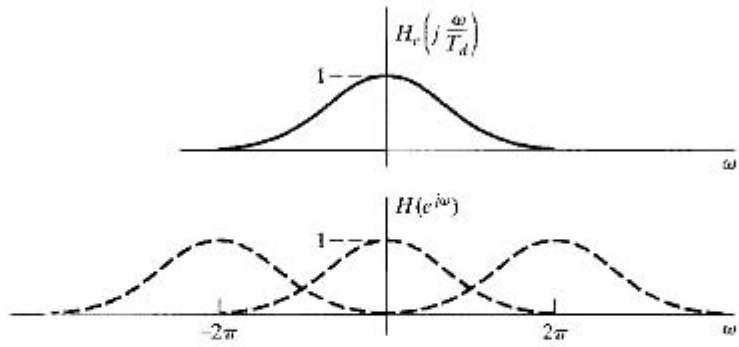

Figure 7.3 Illustration of aliasing in the impulse invariance design technique.

aliasing involved in the transformation from $H_c(j\Omega)$ to $H(e^{j\omega})$ is negligible, we obtain the specifications on $H_c(j\Omega)$ by applying the relation

$$\Omega = \omega/T_d \tag{7.6}$$

to obtain the continuous-time filter specifications from the specifications on $H(e^{j\omega})$. After obtaining a continuous-time filter that meets these specifications, the continuous-time filter with system function $H_c(s)$ is transformed to the desired discrete-time filter with system function $H(z)$. We develop the algebraic details of the transformation from $H_c(s)$ to $H(z)$ shortly. Note, however, that in the transformation back to discrete-time frequency, $H(e^{j\omega})$ will be related to $H_c(j\Omega)$ through Eq. (7.3), which again applies the transformation of Eq. (7.6) to the frequency axis. As a consequence, the "sampling" parameter T_d cannot be used to control aliasing. Since the basic specifications are in terms of discrete-time frequency, if the sampling rate is increased (i.e., if T_d is made smaller), then the cutoff frequency of the continuous-time filter must increase in proportion. In practice, to compensate for aliasing that might occur in the transformation from $H_c(j\Omega)$ to $H(e^{j\omega})$, the continuous-time filter may be somewhat overdesigned, i.e., designed to exceed the specifications, particularly in the stopband.

While the impulse invariance transformation from continuous time to discrete time is defined in terms of time-domain sampling, it is easy to carry out as a transformation on the system function. To develop this transformation, we consider the system function of a causal continuous-time filter expressed in terms of a partial fraction expansion, so that[1]

$$H_c(s) = \sum_{k=1}^{N} \frac{A_k}{s - s_k}. \tag{7.7}$$

The corresponding impulse response is

$$h_c(t) = \begin{cases} \displaystyle\sum_{k=1}^{N} A_k e^{s_k t}, & t \geq 0, \\ 0, & t < 0. \end{cases} \tag{7.8}$$

[1]For simplicity, we assume in the discussion that all poles of $H(s)$ are single order. In Problem 7.41, we consider the modifications required for multiple-order poles.

The impulse response of the causal discrete-time filter obtained by sampling $T_d h_c(t)$ is

$$\begin{aligned} h[n] = T_d h_c(nT_d) &= \sum_{k=1}^{N} T_d A_k e^{s_k n T_d} u[n] \\ &= \sum_{k=1}^{N} T_d A_k (e^{s_k T_d})^n u[n]. \end{aligned} \tag{7.9}$$

The system function of the causal discrete-time filter is therefore given by

$$H(z) = \sum_{k=1}^{N} \frac{T_d A_k}{1 - e^{s_k T_d} z^{-1}}. \tag{7.10}$$

In comparing Eqs. (7.7) and (7.10), we observe that a pole at $s = s_k$ in the s-plane transforms to a pole at $z = e^{s_k T_d}$ in the z-plane and the coefficients in the partial fraction expansions of $H_c(s)$ and $H(z)$ are equal, except for the scaling multiplier T_d. If the continuous-time causal filter is stable, corresponding to the real part of s_k being less than zero, then the magnitude of $e^{s_k T_d}$ will be less than unity, so that the corresponding pole in the discrete-time filter is inside the unit circle. Therefore, the causal discrete-time filter is also stable. Although the poles in the s-plane map to poles in the z-plane according to the relationship $z_k = e^{s_k T_d}$, it is important to recognize that the impulse invariance design procedure does not correspond to a simple mapping of the s-plane to the z-plane by that relationship. In particular, the zeros in the discrete-time system function are a function of the poles $e^{s_k T_d}$ and the coefficients $T_d A_k$ in the partial fraction expansion, and they will not in general be mapped in the same way the poles are mapped. We illustrate the impulse invariance design procedure of a lowpass filter with the following example.

Example 7.2 Impulse Invariance with a Butterworth Filter

In this example we consider the design of a lowpass discrete-time filter by applying impulse invariance to an appropriate continuous-time filter. The class of filters that we choose for this example is referred to as Butterworth filters, which we discuss in more detail in Section 7.3 and in Appendix B.[2] The specifications for the discrete-time filter correspond to passband gain between 0 dB and -1 dB, and stopband attenuation of at least -15 dB, i.e.,

$$0.89125 \le |H(e^{j\omega})| \le 1, \qquad 0 \le |\omega| \le 0.2\pi, \tag{7.11a}$$

$$|H(e^{j\omega})| \le 0.17783, \qquad 0.3\pi \le |\omega| \le \pi. \tag{7.11b}$$

Since the parameter T_d cancels in the impulse invariance procedure, we can just as well choose $T_d = 1$, so that $\omega = \Omega$. In Problem 7.2, this same example is considered, but with the parameter T_d explicitly included to illustrate how and where it cancels.

In designing the filter using impulse invariance on a continuous-time Butterworth filter, we must first transform the discrete-time specifications to specifications on the continuous-time filter. For this example, we will assume that the effect of aliasing in Eq. (7.3) is negligible. After the design is complete, we can evaluate the resulting frequency response against the specifications in Eqs. (7.11a) and (7.11b).

[2] Continuous-time Butterworth and Chebyshev filters are discussed in Appendix B.

Because of the preceding considerations, we want to design a continuous-time Butterworth filter with magnitude function $|H_c(j\Omega)|$ for which

$$0.89125 \leq |H_c(j\Omega)| \leq 1, \qquad 0 \leq |\Omega| \leq 0.2\pi, \tag{7.12a}$$

$$|H_c(j\Omega)| \leq 0.17783, \qquad 0.3\pi \leq |\Omega| \leq \pi. \tag{7.12b}$$

Since the magnitude response of an analog Butterworth filter is a monotonic function of frequency, Eqs. (7.12a) and (7.12b) will be satisfied if $H_c(j0) = 1$,

$$|H_c(j0.2\pi)| \geq 0.89125 \tag{7.13a}$$

and

$$|H_c(j0.3\pi)| \leq 0.17783. \tag{7.13b}$$

The magnitude-squared function of a Butterworth filter is of the form

$$|H_c(j\Omega)|^2 = \frac{1}{1+(\Omega/\Omega_c)^{2N}}, \tag{7.14}$$

so that the filter design process consists of determining the parameters N and Ω_c to meet the desired specifications. Using Eq. (7.14) in Eqs. (7.13) with equality leads to the equations

$$1+\left(\frac{0.2\pi}{\Omega_c}\right)^{2N} = \left(\frac{1}{0.89125}\right)^2 \tag{7.15a}$$

and

$$1+\left(\frac{0.3\pi}{\Omega_c}\right)^{2N} = \left(\frac{1}{0.17783}\right)^2. \tag{7.15b}$$

The simultaneous solution of these two equations is $N = 5.8858$ and $\Omega_c = 0.70474$. The parameter N, however, must be an integer. In order that the specifications are met or exceeded, we must round N up to the nearest integer, $N = 6$, in which case the filter will not exactly satisfy both Eqs. (7.15a) and (7.15b) simultaneously. With $N = 6$, the filter parameter Ω_c can be chosen to exceed the specified requirements (i.e., have lower approximation error) in either the passband, the stopband, or both. Specifically, as the value of Ω_c varies, there is a trade-off in the amount by which the stopband and passband specifications are exceeded. If we substitute $N = 6$ into Eq. (7.15a), we obtain ($\Omega_c = 0.7032$). With this value, the passband specifications (of the continuous-time filter) will be met exactly, and the stopband specifications (of the continuous-time filter) will be exceeded. This allows some margin for aliasing in the discrete-time filter. With ($\Omega_c = 0.7032$) and with $N = 6$, the 12 poles of the magnitude-squared function $H_c(s)H_c(-s) = 1/[1+(s/j\Omega_c)^{2N}]$ are uniformly distributed in angle on a circle of radius ($\Omega_c = 0.7032$), as indicated in Figure 7.4. Consequently, the poles of $H_c(s)$ are the three pole pairs in the left half of the s-plane with the following coordinates:

Pole pair 1: $-0.182 \pm j(0.679)$,

Pole pair 2: $-0.497 \pm j(0.497)$,

Pole pair 3: $-0.679 \pm j(0.182)$.

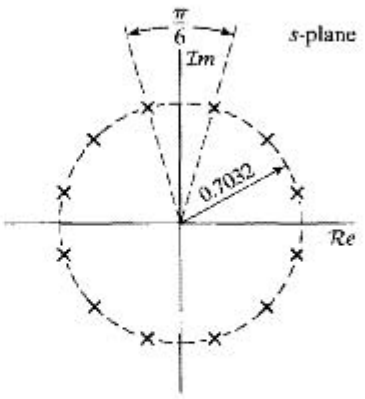

Figure 7.4 s-plane locations for poles of $H_c(s)H_c(-s)$ for 6th-order Butterworth filter in Example 7.2.

Therefore,

$$H_c(s) = \frac{0.12093}{(s^2 + 0.3640s + 0.4945)(s^2 + 0.9945s + 0.4945)(s^2 + 1.3585s + 0.4945)}. \tag{7.16}$$

If we express $H_c(s)$ as a partial fraction expansion, perform the transformation of Eq. (7.10), and then combine complex-conjugate terms, the resulting system function of the discrete-time filter is

$$H(z) = \frac{0.2871 - 0.4466z^{-1}}{1 - 1.2971z^{-1} + 0.6949z^{-2}} + \frac{-2.1428 + 1.1455z^{-1}}{1 - 1.0691z^{-1} + 0.3699z^{-2}} + \frac{1.8557 - 0.6303z^{-1}}{1 - 0.9972z^{-1} + 0.2570z^{-2}}. \tag{7.17}$$

As is evident from Eq. (7.17), the system function resulting from the impulse invariance design procedure may be realized directly in parallel form. If either the cascade or direct form is desired, the separate 2nd-order terms are first combined in an appropriate way.

The frequency-response functions of the discrete-time system are shown in Figure 7.5. The prototype continuous-time filter had been designed to meet the specifications exactly at the passband edge and to exceed the specifications at the stopband edge, and this turns out to be true for the resulting discrete-time filter. This is an indication that the continuous-time filter was sufficiently bandlimited so that aliasing presented no problem. Indeed, the difference between $20\log_{10}|H(e^{j\omega})|$ and $20\log_{10}|H_c(j\Omega)|$ would not be visible on this plotting scale, except for a slight deviation around $\omega = \pi$. (Recall that $T_d = 1$, so $\Omega = \omega$.) Sometimes, aliasing is much more of a problem. If the resulting discrete-time filter fails to meet the specifications because of aliasing, there is no alternative with impulse invariance but to try again with a higher-order filter or with different filter parameters, holding the order fixed.

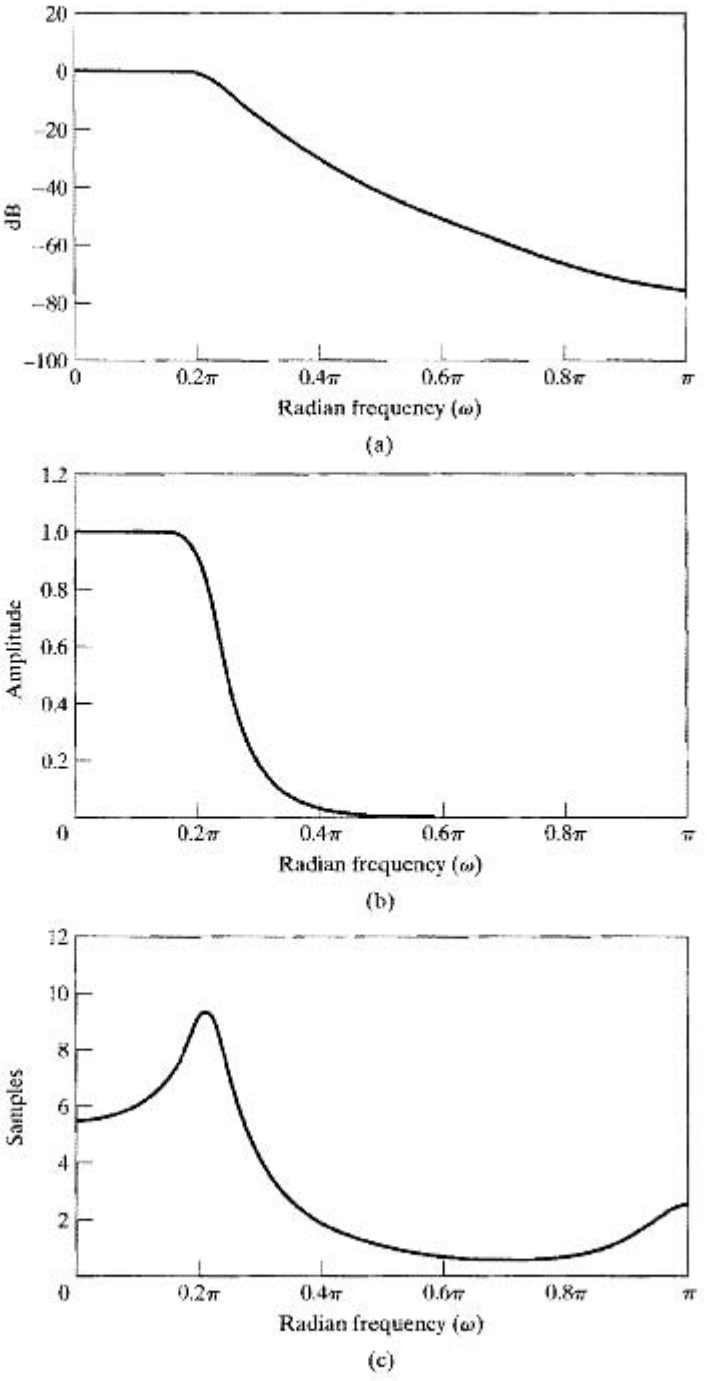

Figure 7.5 Frequency response of 6th-order Butterworth filter transformed by impulse invariance. (a) Log magnitude in dB. (b) Magnitude. (c) Group delay.

The basis for impulse invariance is to choose an impulse response for the discrete-time filter that is similar in some sense to the impulse response of the continuous-time filter. The use of this procedure may be motivated by a desire to maintain the shape of the impulse response or by the knowledge that if the continuous-time filter is bandlimited, consequently the discrete-time filter frequency response will closely approximate the continuous-time frequency response. When the primary objective is to control some aspect of the time response, such as the impulse response or the step response, a natural approach might be to design the discrete-time filter by impulse invariance or by step invariance. In the latter case, the response of the filter to a sampled unit step function is defined to be the sequence obtained by sampling the continuous-time step response. If the continuous-time filter has good step response characteristics, such as a small rise time and low peak overshoot, these characteristics will be preserved in the discrete-time filter. Clearly, this concept of waveform invariance can be extended to the preservation of the output waveshape for a variety of inputs, as illustrated in Problem 7.1. The problem points out the fact that transforming the same continuous-time filter by impulse invariance and also by step invariance (or some other waveform invariance criterion) does not lead to the same discrete-time filter in the two cases.

In the impulse invariance design procedure, the relationship between continuous-time and discrete-time frequency is linear; consequently, except for aliasing, the shape of the frequency response is preserved. This is in contrast to the procedure discussed next, which is based on an algebraic transformation. In concluding this subsection we iterate that the impulse invariance technique is appropriate only for bandlimited filters; highpass or bandstop continuous-time filters, for example, would require additional bandlimiting to avoid severe aliasing distortion if impulse invariance design is used.

7.2.2 Bilinear Transformation

The technique discussed in this subsection uses the bilinear transformation, an algebraic transformation between the variables s and z that maps the entire $j\Omega$-axis in the s-plane to one revolution of the unit circle in the z-plane. Since with this approach, $-\infty \leq \Omega \leq \infty$ maps onto $-\pi \leq \omega \leq \pi$, the transformation between the continuous-time and discrete-time frequency variables is necessarily nonlinear. Therefore, the use of this technique is restricted to situations in which the corresponding nonlinear warping of the frequency axis is acceptable.

With $H_c(s)$ denoting the continuous-time system function and $H(z)$ the discrete-time system function, the bilinear transformation corresponds to replacing s by

$$s = \frac{2}{T_d}\left(\frac{1 - z^{-1}}{1 + z^{-1}}\right); \tag{7.18}$$

that is,

$$H(z) = H_c\left(\frac{2}{T_d}\left(\frac{1 - z^{-1}}{1 + z^{-1}}\right)\right). \tag{7.19}$$

As in impulse invariance, a "sampling" parameter T_d is often included in the definition of the bilinear transformation. Historically, this parameter has been included, because the difference equation corresponding to $H(z)$ can be obtained by applying the trapezoidal integration rule to the differential equation corresponding to $H_c(s)$, with T_d

representing the step size of the numerical integration. (See Kaiser, 1966, and Problem 7.49.) However, in filter design, our use of the bilinear transformation is based on the properties of the algebraic transformation given in Eq. (7.18). As with impulse invariance, the parameter T_d is of no consequence in the design procedure, since we assume that the design problem always begins with specifications on the discrete-time filter $H(e^{j\omega})$. When these specifications are mapped to continuous-time specifications, and the continuous-time filter is then mapped back to a discrete-time filter, the effect of T_d will cancel. We will retain the parameter T_d in our discussion for historical reasons; in specific problems and examples, any convenient value can be chosen.

To develop the properties of the algebraic transformation specified in Eq. (7.18), we solve for z to obtain

$$z = \frac{1 + (T_d/2)s}{1 - (T_d/2)s}, \tag{7.20}$$

and, substituting $s = \sigma + j\Omega$ into Eq. (7.20), we obtain

$$z = \frac{1 + \sigma T_d/2 + j\Omega T_d/2}{1 - \sigma T_d/2 - j\Omega T_d/2}. \tag{7.21}$$

If $\sigma < 0$, then, from Eq. (7.21), it follows that $|z| < 1$ for any value of Ω. Similarly, if $\sigma > 0$, then $|z| > 1$ for all Ω. That is, if a pole of $H_c(s)$ is in the left-half s-plane, its image in the z-plane will be inside the unit circle. Therefore, causal stable continuous-time filters map into causal stable discrete-time filters.

Next, to show that the $j\Omega$-axis of the s-plane maps onto the unit circle, we substitute $s = j\Omega$ into Eq. (7.20), obtaining

$$z = \frac{1 + j\Omega T_d/2}{1 - j\Omega T_d/2}. \tag{7.22}$$

From Eq. (7.22), it is clear that $|z| = 1$ for all values of s on the $j\Omega$-axis. That is, the $j\Omega$-axis maps onto the unit circle, so Eq. (7.22) takes the form

$$e^{j\omega} = \frac{1 + j\Omega T_d/2}{1 - j\Omega T_d/2}. \tag{7.23}$$

To derive a relationship between the variables ω and Ω, it is useful to return to Eq. (7.18) and substitute $z = e^{j\omega}$. We obtain

$$s = \frac{2}{T_d}\left(\frac{1 - e^{-j\omega}}{1 + e^{-j\omega}}\right), \tag{7.24}$$

or, equivalently,

$$s = \sigma + j\Omega = \frac{2}{T_d}\left[\frac{2e^{-j\omega/2}(j \sin \omega/2)}{2e^{-j\omega/2}(\cos \omega/2)}\right] = \frac{2j}{T_d}\tan(\omega/2). \tag{7.25}$$

Equating real and imaginary parts on both sides of Eq. (7.25) leads to the relations $\sigma = 0$ and

$$\Omega = \frac{2}{T_d}\tan(\omega/2), \tag{7.26}$$

or

$$\omega = 2\arctan(\Omega T_d/2). \tag{7.27}$$

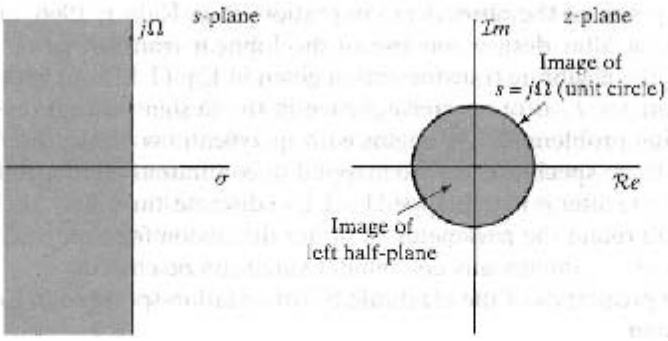

Figure 7.6 Mapping of the s-plane onto the z-plane using the bilinear transformation.

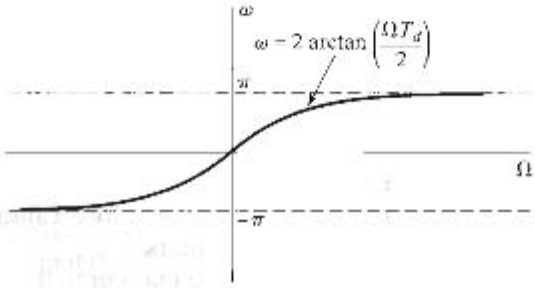

Figure 7.7 Mapping of the continuous-time frequency axis onto the discrete-time frequency axis by bilinear transformation.

These properties of the bilinear transformation as a mapping from the s-plane to the z-plane are summarized in Figures 7.6 and 7.7. From Eq. (7.27) and Figure 7.7, we see that the range of frequencies $0 \leq \Omega \leq \infty$ maps to $0 \leq \omega \leq \pi$, while the range $-\infty \leq \Omega \leq 0$ maps to $-\pi \leq \omega \leq 0$. The bilinear transformation avoids the problem of aliasing encountered with the use of impulse invariance, because it maps the entire imaginary axis of the s-plane onto the unit circle in the z-plane. The price paid for this, however, is the nonlinear compression of the frequency axis, as depicted in Figure 7.7. Consequently, the design of discrete-time filters using the bilinear transformation is useful only when this compression can be tolerated or compensated for, as in the case of filters that approximate ideal piecewise-constant magnitude-response characteristics. This is illustrated in Figure 7.8, wherein we show how a continuous-time frequency response and tolerance scheme maps to a corresponding discrete-time frequency response and tolerance scheme through the frequency warping of Eqs. (7.26) and (7.27). If the critical frequencies (such as the passband and stopband edge frequencies) of the continuous-time filter are prewarped according to Eq. (7.26) then, when the continuous-time filter is transformed to the discrete-time filter using Eq. (7.19), the discrete-time filter will meet the desired specifications.

Although the bilinear transformation can be used effectively in mapping a piecewise-constant magnitude-response characteristic from the s-plane to the z-plane, the distortion in the frequency axis also manifests itself as a warping of the phase response of the filter. For example, Figure 7.9 shows the result of applying the bilinear transformation to an ideal linear-phase factor $e^{-s\alpha}$. If we substitute Eq. (7.18) for s and evaluate the result on the unit circle, the phase angle is $-(2\alpha/T_d)\tan(\omega/2)$. In Figure 7.9, the

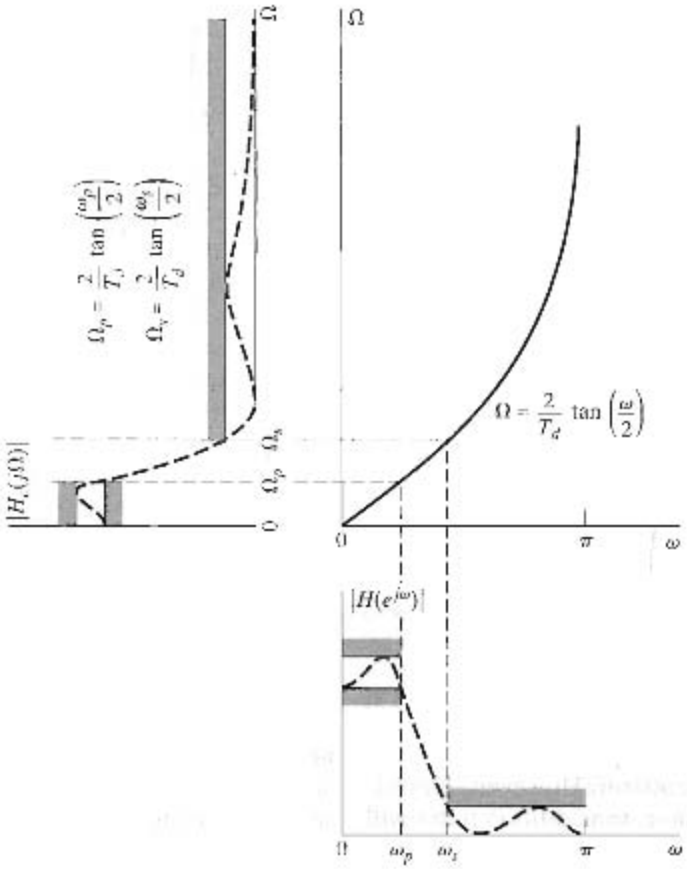

Figure 7.8 Frequency warping inherent in the bilinear transformation of a continuous-time lowpass filter into a discrete-time lowpass filter. To achieve the desired discrete-time cutoff frequencies, the continuous-time cutoff frequencies must be prewarped as indicated.

solid curve shows the function $-(2\alpha/T_d)\tan(\omega/2)$, and the dotted curve is the periodic linear-phase function $-(\omega\alpha/T_d)$, which is obtained by using the small-angle approximation $\omega/2 \approx \tan(\omega/2)$. From this, it should be evident that if we desire a discrete-time lowpass filter with a linear-phase characteristic, we cannot obtain such a filter by applying the bilinear transformation to a continuous-time lowpass filter with a linear-phase characteristic.

As mentioned previously, because of the frequency warping, the bilinear transformation is most useful in the design of approximations to filters with piecewise-constant frequency magnitude characteristics, such as highpass, lowpass and bandpass filters. As demonstrated in Example 7.2, impulse invariance can also be used to design lowpass filters. However, impulse invariance cannot be used to map highpass continuous-time designs to highpass discrete-time designs, since highpass continuous-time filters are not bandlimited.

In Example 4.4, we discussed a class of filters often referred to as discrete-time differentiators. A significant feature of the frequency response of this class of filters is that it is linear with frequency. The nonlinear warping of the frequency axis introduced by the bilinear transformation will not preserve that property. Consequently, the

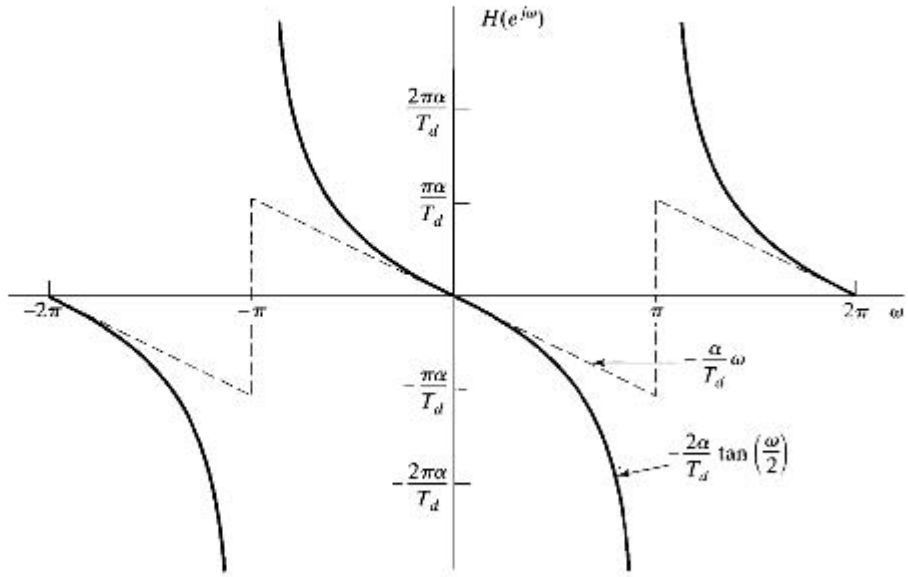

Figure 7.9 Illustration of the effect of the bilinear transformation on a linear-phase characteristic. (Dashed line is linear phase and solid line is phase resulting from bilinear transformation.)

bilinear transformation applied to a continuous-time differentiator will not result in a discrete-time differentiator. However, impulse invariance applied to an appropriately bandlimited continuous-time differentiator will result in a discrete-time differentiator.

7.3 DISCRETE-TIME BUTTERWORTH, CHEBYSHEV AND ELLIPTIC FILTERS

Historically, the most widely used classes of frequency-selective continuous-time filters are those referred to as Butterworth, Chebyshev and elliptic filter designs. In Appendix B we briefly summarize the characteristics of these three classes of continuous-time filters. The associated closed-form design formulas make the design procedure relatively straightforward. As discussed in Appendix B, the magnitude of the frequency response of a Butterworth continuous-time filter is monotonic in the passband and the stopband. A type I Chebyshev filter has an equiripple frequency response in the passband and varies monotonically in the stopband. A type II Chebyshev filter is monotonic in the passband and equiripple in the stopband. An elliptic filter is equiripple in both the passband and the stopband. Clearly, these properties will be preserved when the filter is mapped to a digital filter with the bilinear transformation. This is illustrated by the dashed approximation shown in Figure 7.8. The filters resulting from applying the bilinear transformation to these classes of continuous-time filters, referred to respectively as discrete-time Butterworth, Chebyshev and elliptic filters have similarly become widely used as discrete-time frequency selective filters.

As a first step in the design procedure for any of these classes of filters, the critical frequencies, i.e., the band edge frequencies, must be prewarped to the continuous-time frequencies using Eq. (7.26) so that the frequency distortion inherent in the bilinear transformation will map the continuous-time frequencies back to the correct discrete-time frequencies. This prewarping will be illustrated in more detail in Example 7.3. The allowed tolerances in the passbands and stopbands will be the same for the discrete-time and continuous-time filters since the bilinear mapping only distorts the frequency axis, not the amplitude scale. In using a discrete-time filter design package such as found in MATLAB and LabVIEW, the typical inputs would be the desired tolerances and the discrete-time critical frequencies. The design program explicitly or implicitly handles any necessary prewarping of the frequencies.

In advance of illustrating these classes of filters with several examples, it is worth commenting on some general characteristics to expect. We have noted above that we expect the discrete-time Butterworth, Chebyshev and elliptic filter frequency responses to retain the monotonicity and ripple characteristics of the corresponding continuous-time filters. The N^{th}-order continuous-time lowpass Butterworth filter has N zeros at $\Omega = \infty$. Since the bilinear transformation maps $s = \infty$ to $z = -1$, we would expect any Butterworth design utilizing the bilinear transformation to result in N zeros at $z = -1$. The same is also true for the Chebyshev type I lowpass filter.

7.3.1 Examples of IIR Filter Design

In the following discussion, we present a number of examples to illustrate IIR filter design. The purpose of Example 7.3 is to illustrate the steps in the design of a Butterworth filter using the bilinear transformation, in comparison with the use of impulse invariance. Example 7.4 presents a set of examples comparing the design of a Butterworth, Chebyshev I, Chebyshev II, and elliptic filter. Example 7.5 illustrates, with a different set of specifications, the design of a Butterworth, Chebyshev I, Chebyshev II and elliptic filter. These designs will be compared in Section 7.8.1 with FIR designs. For both Example 7.4 and 7.5 the filter design package in the signal processing toolbox of MATLAB was used.

Example 7.3 Bilinear Transformation of a Butterworth Filter

Consider the discrete-time filter specifications of Example 7.2, in which we illustrated the impulse invariance technique for the design of a discrete-time filter. The specifications for the discrete-time filter are

$$0.89125 \leq |H(e^{j\omega})| \leq 1, \qquad 0 \leq \omega \leq 0.2\pi, \tag{7.28a}$$

$$|H(e^{j\omega})| \leq 0.17783, \qquad 0.3\pi \leq \omega \leq \pi. \tag{7.28b}$$

In carrying out the design using the bilinear transformation applied to a continuous-time design, the critical frequencies of the discrete-time filter are first prewarped to the corresponding continuous-time frequencies using Eq. (7.26) so that the frequency distortion inherent in the bilinear transformation will map the continuous-time frequencies back to the correct discrete-time critical frequencies. For this specific filter, with $|H_c(j\Omega)|$ representing the magnitude-response function of the continuous-time filter, we require that

$$0.89125 \le |H_c(j\Omega)| \le 1, \qquad 0 \le \Omega \le \frac{2}{T_d}\tan\left(\frac{0.2\pi}{2}\right), \tag{7.29a}$$

$$|H_c(j\Omega)| \le 0.17783, \qquad \frac{2}{T_d}\tan\left(\frac{0.3\pi}{2}\right) \le \Omega \le \infty. \tag{7.29b}$$

For convenience, we choose $T_d = 1$. Also, as with Example 7.2, since a continuous-time Butterworth filter has a monotonic magnitude response, we can equivalently require that

$$|H_c(j2\tan(0.1\pi))| \ge 0.89125 \tag{7.30a}$$

and

$$|H_c(j2\tan(0.15\pi))| \le 0.17783. \tag{7.30b}$$

The form of the magnitude-squared function for the Butterworth filter is

$$|H_c(j\Omega)|^2 = \frac{1}{1+(\Omega/\Omega_c)^{2N}}. \tag{7.31}$$

Solving for N and Ω_c with the equality sign in Eqs. (7.30a) and (7.30b), we obtain

$$1+\left(\frac{2\tan(0.1\pi)}{\Omega_c}\right)^{2N} = \left(\frac{1}{0.89}\right)^2 \tag{7.32a}$$

and

$$1+\left(\frac{2\tan(0.15\pi)}{\Omega_c}\right)^{2N} = \left(\frac{1}{0.178}\right)^2, \tag{7.32b}$$

and solving for N in Eqs. (7.32a) and (7.32b) gives

$$N = \frac{\log\left[\left(\left(\frac{1}{0.178}\right)^2-1\right)\Big/\left(\left(\frac{1}{0.89}\right)^2-1\right)\right]}{2\log[\tan(0.15\pi)/\tan(0.1\pi)]} \tag{7.33}$$

$$= 5.305.$$

Since N must be an integer, we choose $N = 6$. Substituting $N = 6$ into Eq. (7.32b), we obtain $\Omega_c = 0.766$. For this value of Ω_c, the passband specifications are exceeded and the stopband specifications are met exactly. This is reasonable for the bilinear transformation, since we do not have to be concerned with aliasing. That is, with proper prewarping, we can be certain that the resulting discrete-time filter will meet the specifications exactly at the desired stopband edge.

In the s-plane, the 12 poles of the magnitude-squared function are uniformly distributed in angle on a circle of radius 0.766, as shown in Figure 7.10. The system function of the causal continuous-time filter obtained by selecting the left half-plane poles is

$$H_c(s) = \frac{0.20238}{(s^2 + 0.3996s + 0.5871)(s^2 + 1.0836s + 0.5871)(s^2 + 1.4802s + 0.5871)}. \tag{7.34}$$

The system function for the discrete-time filter is then obtained by applying the bilinear transformation to $H_c(s)$ with $T_d = 1$. The result is

$$H(z) = \frac{0.0007378(1 + z^{-1})^6}{(1 - 1.2686z^{-1} + 0.7051z^{-2})(1 - 1.0106z^{-1} + 0.3583z^{-2})} \times \frac{1}{(1 - 0.9044z^{-1} + 0.2155z^{-2})}. \tag{7.35}$$

The magnitude, log magnitude, and group delay of the frequency response of the discrete-time filter are shown in Figure 7.11. At $\omega = 0.2\pi$ the log magnitude is -0.56 dB, and at $\omega = 0.3\pi$ the log magnitude is exactly -15 dB.

Since the bilinear transformation maps the entire $j\Omega$-axis of the s-plane onto the unit circle in the z-plane, the magnitude response of the discrete-time filter falls off much more rapidly than that of the continuous-time filter or the Butterworth discrete-time filter designed by impulse invariance. In particular, the behavior of $H(e^{j\omega})$ at $\omega = \pi$ corresponds to the behavior of $H_c(j\Omega)$ at $\Omega = \infty$. Therefore, since the continuous-time Butterworth filter has a 6^{th}-order zero at $s = \infty$, the resulting discrete-time filter has a 6^{th}-order zero at $z = -1$.

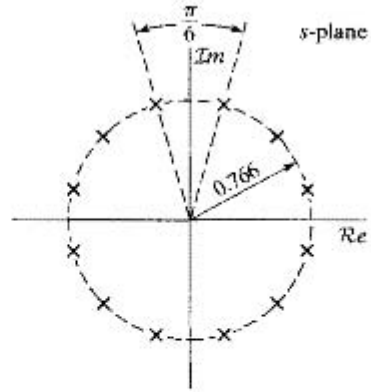

Figure 7.10 s-plane locations for poles of $H_c(s)H_c(-s)$ for 6^{th}-order Butterworth filter in Example 7.3.

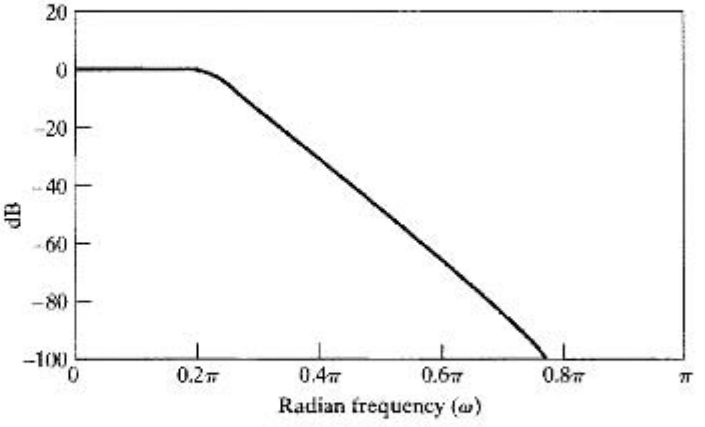

(a)

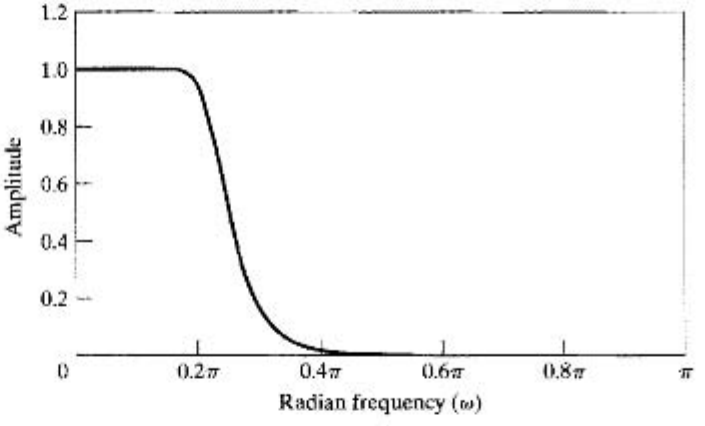

(b)

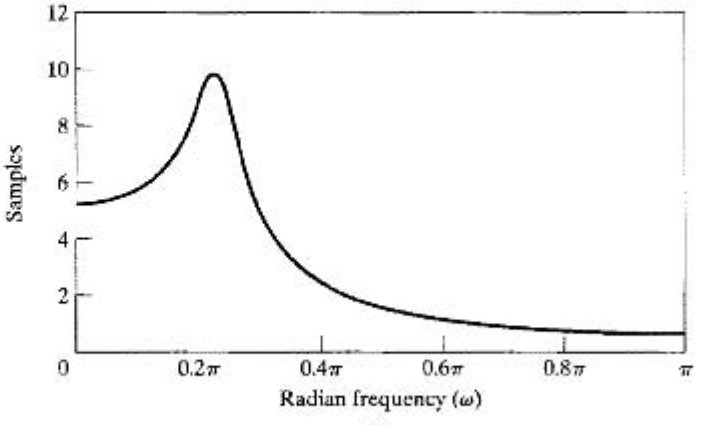

(c)

Figure 7.11 Frequency response of 6th-order Butterworth filter transformed by bilinear transform. (a) Log magnitude in dB. (b) Magnitude. (c) Group delay.

Since the general form of the magnitude-squared of the N^{th}-order Butterworth continuous-time filter is as given by Eq. (7.31), and since ω and Ω are related by Eq. (7.26), it follows that the general N^{th}-order Butterworth discrete-time filter has the magnitude-squared function

$$|H(e^{j\omega})|^2 = \frac{1}{1 + \left(\dfrac{\tan(\omega/2)}{\tan(\omega_c/2)}\right)^{2N}}, \tag{7.36}$$

where $\tan(\omega_c/2) = \Omega_c T_d/2$. The frequency-response function of Eq. (7.36) has the same properties as the continuous-time Butterworth response; i.e., it is maximally flat[3] and $|H(e^{j\omega_c})|^2 = 0.5$. However, the function in Eq. (7.36) is periodic with period 2π and falls off more sharply than the continuous-time Butterworth response.

Discrete-time Butterworth filters are not typically designed directly by starting with Eq. (7.36), because it is not straightforward to determine the z-plane locations of the poles (all the zeros are at $z = -1$) associated with the magnitude-squared function of Eq. (7.36). It is necessary to determine the poles so as to factor the magnitude-squared function into $H(z)H(z^{-1})$ and thereby determine $H(z)$. It is much easier to factor the continuous-time system function, and then transform the left half-plane poles by the bilinear transformation as we did in Example 7.3.

Equations of the form of Eq. (7.36) may also be obtained for discrete-time Chebyshev and elliptic filters. However, the details of the design computations for these commonly used classes of filters are best carried out by computer programs that incorporate the appropriate closed-form design equations.

In the next example, we compare the design of a lowpass filter based on Butterworth, Chebyshev I, Chebyshev II and elliptic filter designs. There are some specific characteristics of the frequency response magnitude and the pole–zero patterns for each of these four discrete-time lowpass filter types, and these characteristics will be evident in the designs in Example 7.4 and Example 7.5 that follow.

For a Butterworth lowpass filter, the frequency response magnitude decreases monotonically in both the passband and stopband, and all the zeros of the transfer function are at $z = -1$. For a Chebyshev Type I lowpass filter, the frequency response magnitude will always be equiripple in the passband, i.e., will oscillate with equal maximum error on either side of the desired gain and will be monotonic in the stopband. All the zeros of the corresponding transfer function will be at $z = -1$. For a Chebyshev Type II lowpass filter, the frequency response magnitude will be monotonic in the passband and equiripple in the stopband, i.e., oscillates around zero gain. Because of this equiripple stopband behavior, the zeros of the transfer function will correspondingly be distributed on the unit circle.

In both cases of Chebyshev approximation, the monotonic behavior in either the stopband or the passband suggests that perhaps a lower-order system might be obtained if an equiripple approximation were used in both the passband and the stopband. Indeed, it can be shown (see Papoulis, 1957) that for fixed values of δ_{p_1}, δ_{p_2}, δ_s, ω_p, and ω_s in the tolerance scheme of Figure 7.1, the lowest order filter is obtained when the approximation error ripples equally between the extremes of the two approximation bands. This equiripple behavior is achieved with the class of filters referred to as elliptic

[3]The first $(2N-1)$ derivatives of $|H(e^{j\omega})|^2$ are zero at $\omega = 0$.

filters. Elliptic filters, like the Chebyshev type II filter, has its zeros arrayed in the stopband region of the unit circle. These properties of Butterworth, Chebyshev, and elliptic filters are illustrated by the following example.

Example 7.4 Design Comparisons

For the four filter designs that follow, the signal processing toolbox in MATLAB was used. This and other typical design programs for IIR lowpass filter design, assume tolerance specifications as indicated in Figure 7.1 with $\delta_{p1} = 0$. Although the resulting designs correspond to what would result from applying the bilinear transformation to appropriate continuous-time designs, any required frequency prewarping and incorporation of the bilinear transformation, are internal to these design programs and transparent to the user. Consequently the specifications are given to the design program directly in terms of the discrete-time parameters. For this example, the filter has been designed to meet or exceed the following specifications:

passband edge frequency ω_p	$= 0.5\pi$
stopband edge frequency ω_s	$= 0.6\pi$
maximum passband gain	$= 0$ dB
minimum passband gain	$= -0.3$ dB
maximum stopband gain	$= -30$ dB

Referring to Figure 7.1, the corresponding passband and stopband tolerance limits are

$$20\log_{10}(1 + \delta_{p_1}) = 0 \quad \text{or equivalently } \delta_{p_1} = 0$$
$$20\log_{10}(1 - \delta_{p_2}) = -0.3 \text{ or equivalently } \delta_{p_2} = 0.0339$$
$$20\log_{10}(\delta_s) = -30 \quad \text{or equivalently } \delta_s = 0.0316.$$

Note that the specifications are only on the magnitudes of the frequency response. The phase is implicitly determined by the nature of the approximating functions.

Using the filter design program, it is determined that for a Butterworth design, the minimum (integer) filter order that meets or exceeds the given specifications is a 15^{th}-order filter. The resulting frequency response magnitude, group delay, and pole-zero plot are shown in Figure 7.12. As expected, all of the zeros of the Butterworth filter are at $z = -1$.

For a Chebyshev type I design, the minimum filter order is 7. The resulting frequency response magnitude and group delay, and the corresponding pole–zero plot are shown in Figure 7.13. As expected, all of the zeros of the transfer function are at $z = -1$ and the frequency response magnitude is equiripple in the passband and monotonic in the stopband.

For a Chebyshev type II design, the minimum filter order is again 7. The resulting frequency response magnitude, group delay and pole–zero plot are shown in Figure 7.14. Again as expected, the frequency response magnitude is monotonic in the passband and equiripple in the stopband. The zeros of the transfer function are arrayed on the unit circle in the stopband.

In comparing the Chebyshev I and Chebyshev II designs it is worth noting that for both, the order of the denominator polynomial in the transfer function corresponding to the poles is 7, and the order of the numerator polynomial is also 7. In the implementation of the difference equation for both the Chebyshev I design and the Butterworth design, significant advantage can be taken of the fact that all the zeros

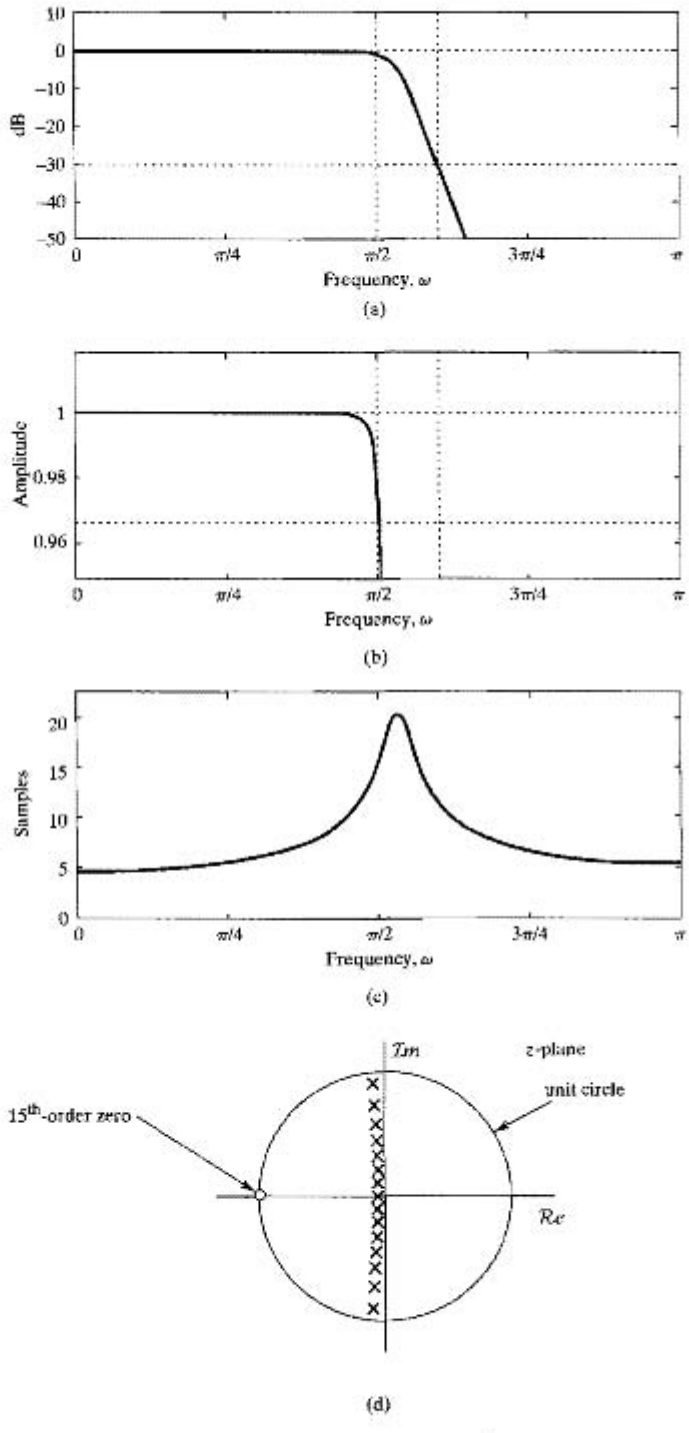

Figure 7.12 Butterworth filter, 15th-order.

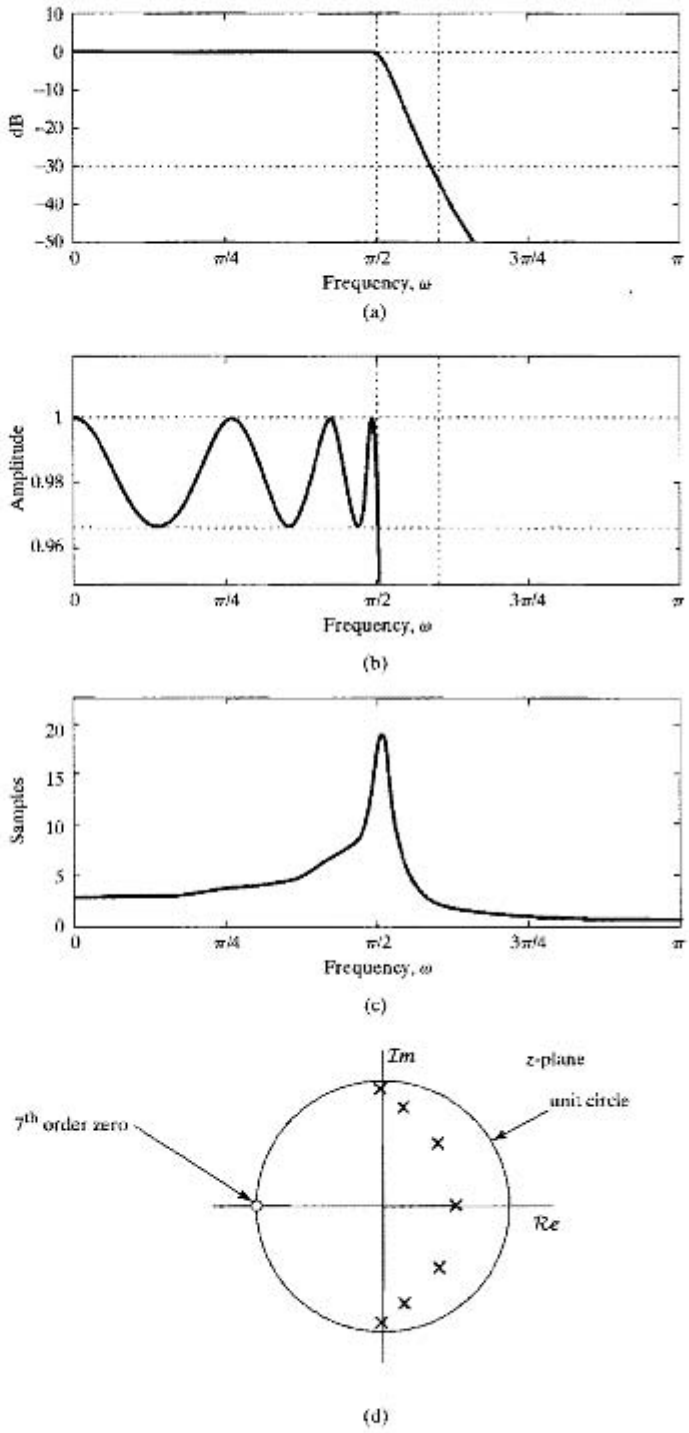

Figure 7.13 Chebyshev Type I filter, 7th-order.

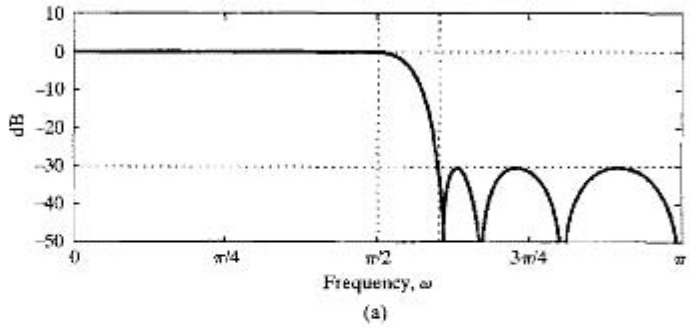

(a)

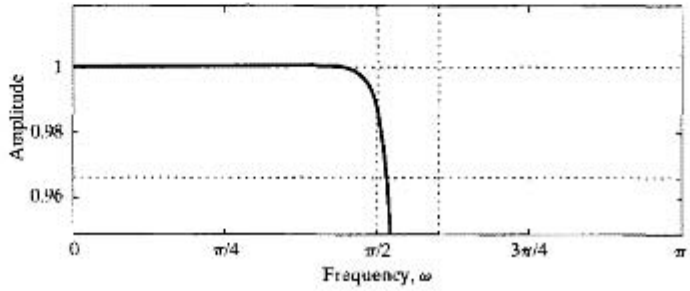

(b)

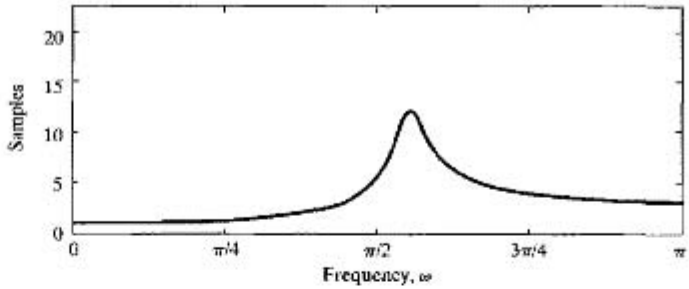

(c)

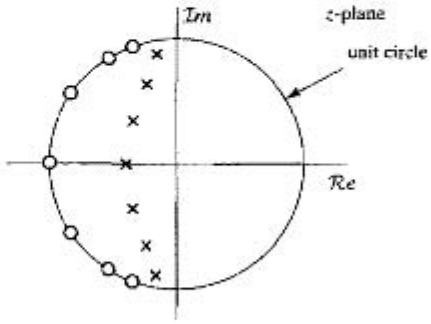

(d)

Figure 7.14 Chebyshev Type II filter, 7th-order.

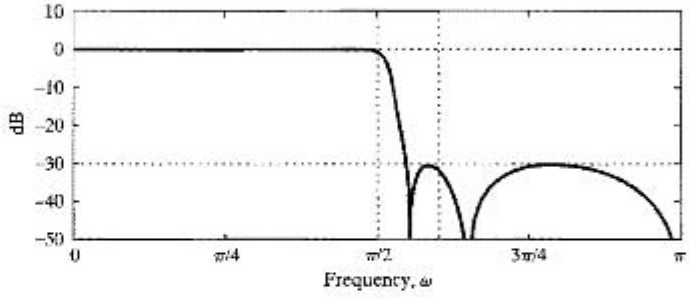

(a)

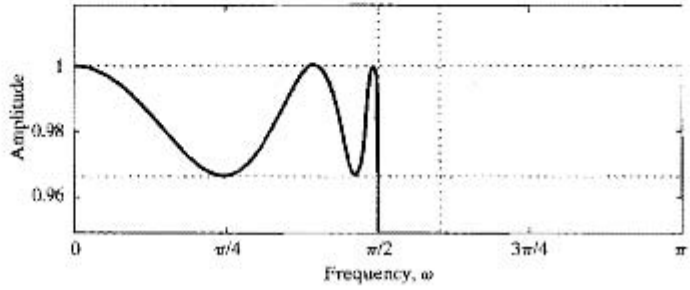

(b)

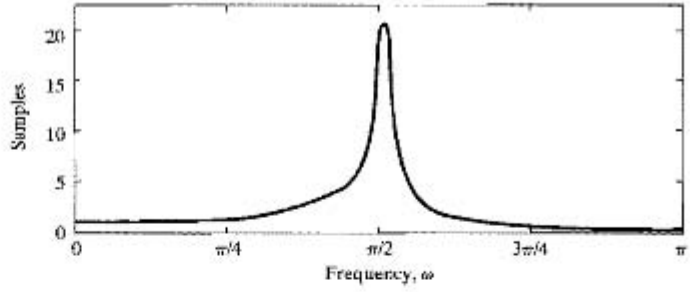

(c)

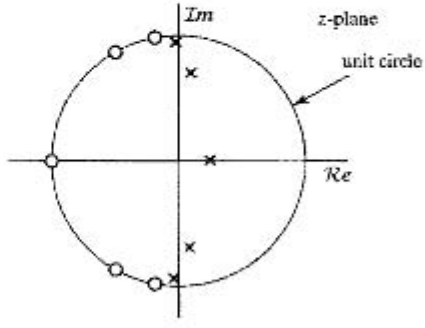

(d)

Figure 7.15 Elliptic filter, 5th-order, exceeds design specifications.

occur at $z = -1$. This is not the case for the Chebyshev II filter. Consequently, in an implementation of the filter, the Chebyshev II design will require more multiplications than the Chebyshev I design. For the Butterworth design, while advantage can be taken of the clustered zeros at $z = -1$, the filter order is more than twice that of the Chebyshev designs and consequently requires more multiplications.

For the design of an elliptic filter to meet the given specifications, a filter of at least 5^{th}-order is required. Figure 7.15 shows the resulting design. As with previous examples, in designing a filter with given specifications, the minimum specifications are likely to be exceeded, since the filter order is necessarily an integer. Depending on the application, the designer may choose which of the specifications to exactly meet and which to exceed. For example, with the elliptic filter design we may choose to exactly meet the passband and stopband edge frequencies and the passband variation and minimize the stopband gain. The resulting filter, which achieves 43 dB of attenuation in the stopband, is shown in Figure 7.16. Alternately, the added flexibility can be used to narrow the transition band or reduce the deviation from 0 dB gain in the passband. Again as expected, the frequency response of the elliptic filter is equiripple in both the passband and the stopband.

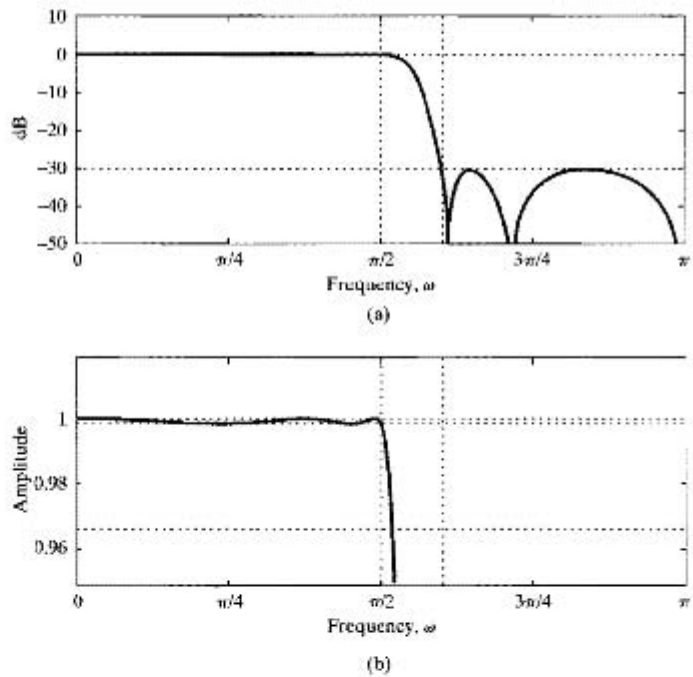

Figure 7.16 Elliptic filter, 5^{th}-order, minimizing the passband ripple.

Example 7.5 Design Example for Comparison with FIR Designs

In this example we return to the specifications of Example 7.1 and illustrate the realization of this filter specification with a Butterworth, Chebyshev I, Chebyshev II,

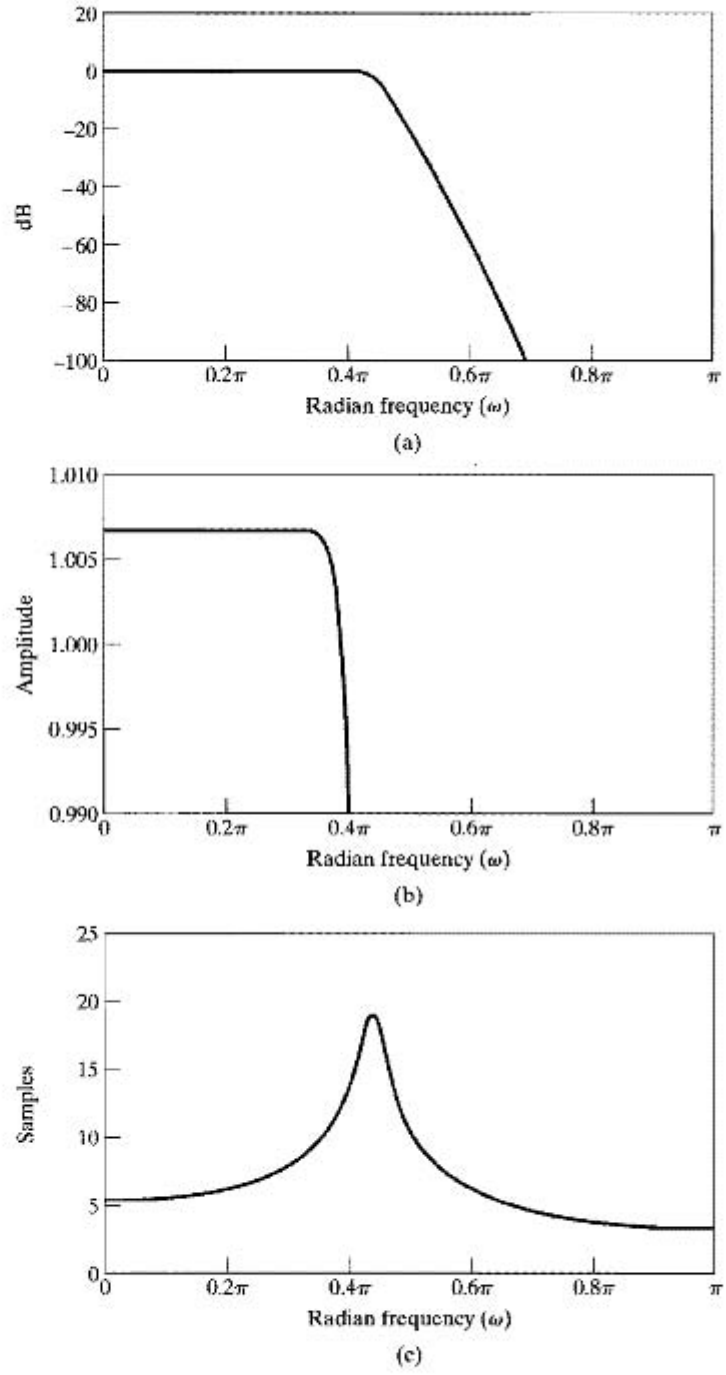

Figure 7.17 Frequency response of 14th-order Butterworth filter in Example 7.5. (a) Log magnitude in dB. (b) Detailed plot of magnitude in passband. (c) Group delay.

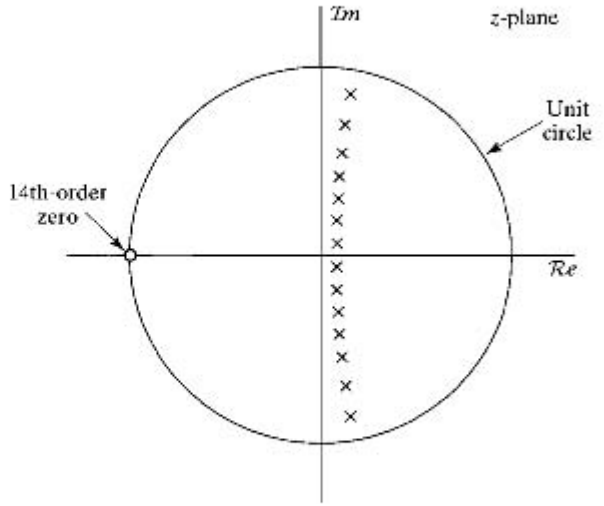

(d)

Figure 7.17 (*continued*) (d) Pole–zero plot of 14th-order Butterworth filter in Example 7.5.

and elliptic designs. The designs are again carried out using the filter design program in the MATLAB signal processing toolbox. In Section 7.8.1 we will compare these IIR designs with FIR designs with the same specifications. Typical design programs for FIR filters require the passband tolerance limits in Figure 7.1 to be specified with $\delta_{p1} = \delta_{p2}$, whereas for IIR filters, it is typically assumed that $\delta_{p1} = 0$. Consequently to carry out a comparison of IIR and FIR designs, some renormalization of the passband and stopband specifications may need to be carried out (see, for example, Problem 7.3), as will be done in Example 7.5.

The lowpass discrete-time filter specifications as used for this example are:

$$0.99 \leq |H(e^{j\omega})| \leq 1.01, \qquad |\omega| \leq 0.4\pi, \tag{7.37a}$$

and

$$|H(e^{j\omega})| \leq 0.001, \qquad 0.6\pi \leq |\omega| \leq \pi. \tag{7.37b}$$

In terms of the tolerance scheme of Figure 7.1, $\delta_{p_1} = \delta_{p_2} = 0.01$, $\delta_s = 0.001$, $\omega_p = 0.4\pi$, and $\omega_s = 0.6\pi$. Rescaling these specifications so that $\delta_{p1} = 0$ corresponds to scaling the filter by $1/(1 + \delta_{p1})$ to obtain: $\delta_{p1} = 0$, $\delta_{p2} = 0.0198$ and $\delta_s = .00099$.

The filters are first designed using the filter design program with these specifications and the filter designs returned by the filter design program are then rescaled by a factor of 1.01 to satisfy the specifications in Eqs. (7.37a) and (7.37b).

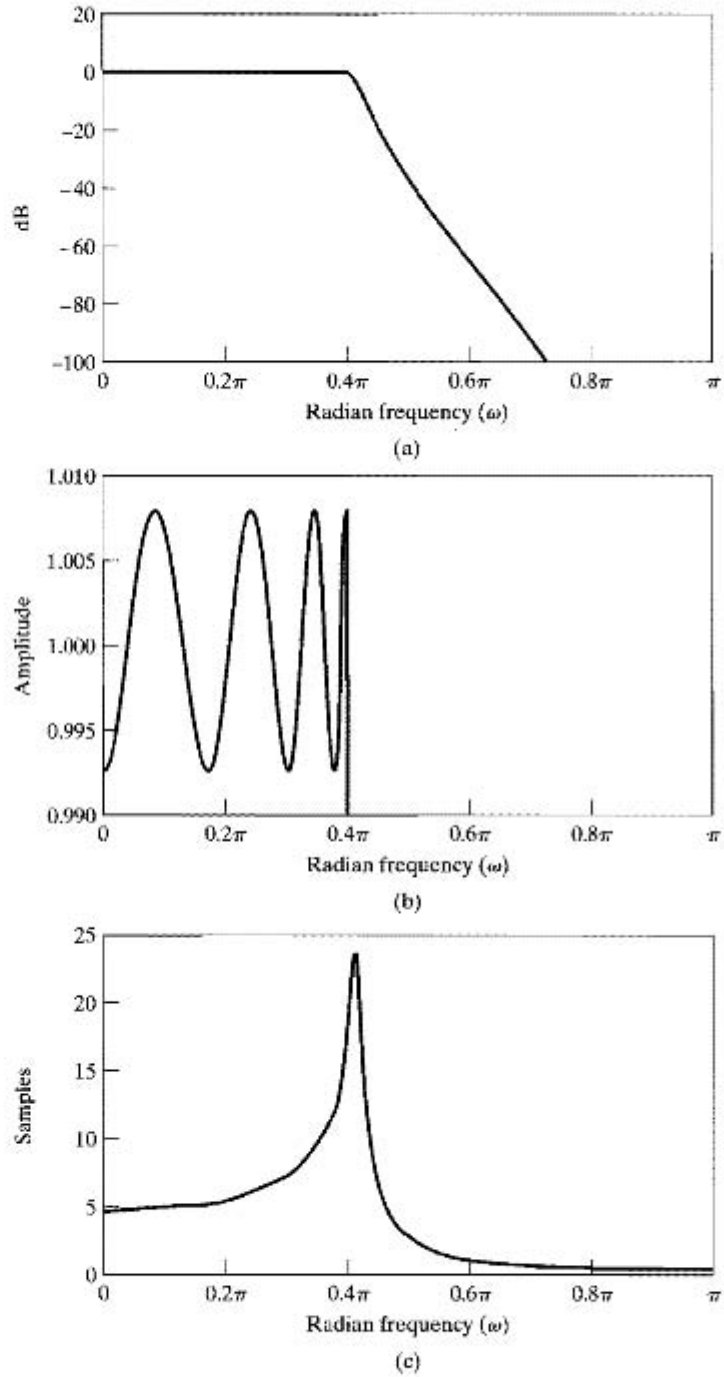

Figure 7.18 Frequency response of 8th-order Chebyshev type I filter in Example 7.5. (a) Log magnitude in dB. (b) Detailed plot of magnitude in passband. (c) Group delay.

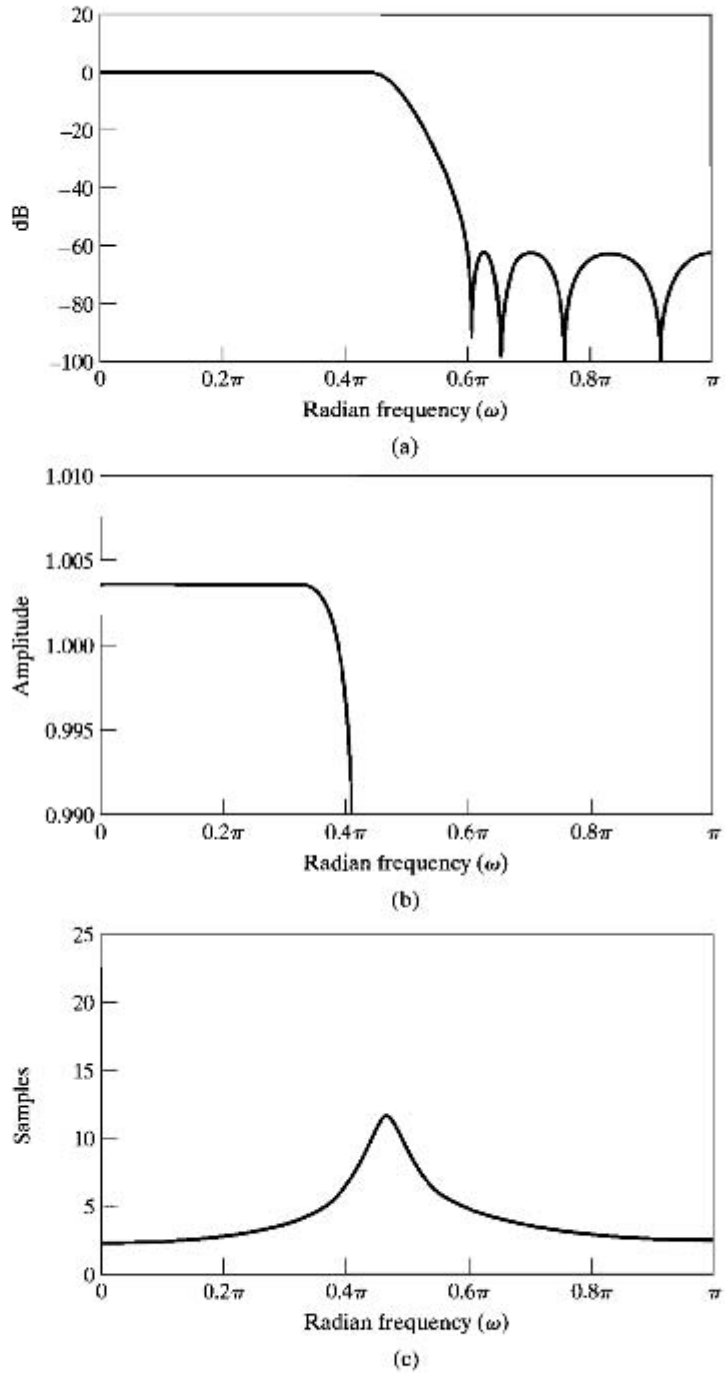

Figure 7.19 Frequency response of 8^{th}-order Chebyshev type II filter in Example 7.5. (a) Log magnitude in dB. (b) Detailed plot of magnitude in passband. (c) Group delay.

For the specifications in this example, the Butterworth approximation method requires a system of 14^{th}-order. The frequency response of the discrete-time filter that results from the bilinear transformation of the appropriate prewarped Butterworth filter is shown in Figure 7.17. Figure 7.17(a) shows the log magnitude in dB, Figure 7.17(b) shows the magnitude of $H(e^{j\omega})$ in the passband only, and Figure 7.17(c) shows the group delay of the filter. From these plots, we see that as expected, the Butterworth frequency response decreases monotonically with frequency, and the gain of the filter becomes very small above about $\omega = 0.7\pi$.

Both Chebyshev designs I and II lead to the same order for a given set of specifications. For our specifications the required order is 8 rather than 14, as was required for the Butterworth approximation. Figure 7.18 shows the log magnitude, passband magnitude, and group delay for the type I approximation to the specifications of Eqs. (7.37a) and (7.37b). Note that as expected, the frequency response oscillates with equal maximum error on either side of the desired gain of unity in the passband.

Figure 7.19 shows the frequency-response functions for the Chebyshev type II approximation. In this case, the equiripple approximation behavior is in the stopband. The pole–zero plots for the Chebyshev filters are shown in Figure 7.20. Note that the Chebyshev type I filter is similar to the Butterworth filter in that it has all eight of its zeros at $z = -1$. On the other hand, the type II filter has its zeros arrayed on the unit circle. These zeros are naturally positioned by the design equations so as to achieve the equiripple behavior in the stopband.

The specifications of Eqs. (7.37a) and (7.37b) are met by an elliptic filter of order six. This is the lowest order rational function approximation to the specifications. Figure 7.21 clearly shows the equiripple behavior in both approximation bands. Figure 7.22 shows that the elliptic filter, like the Chebyshev type II, has its zeros arrayed in the stopband region of the unit circle.

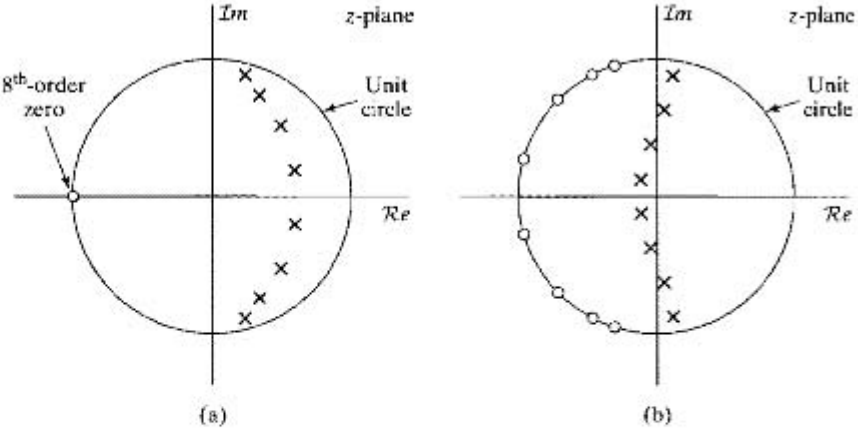

Figure 7.20 Pole–zero plot of 8^{th}-order Chebyshev filters in Example 7.5. (a) Type I. (b) Type II.

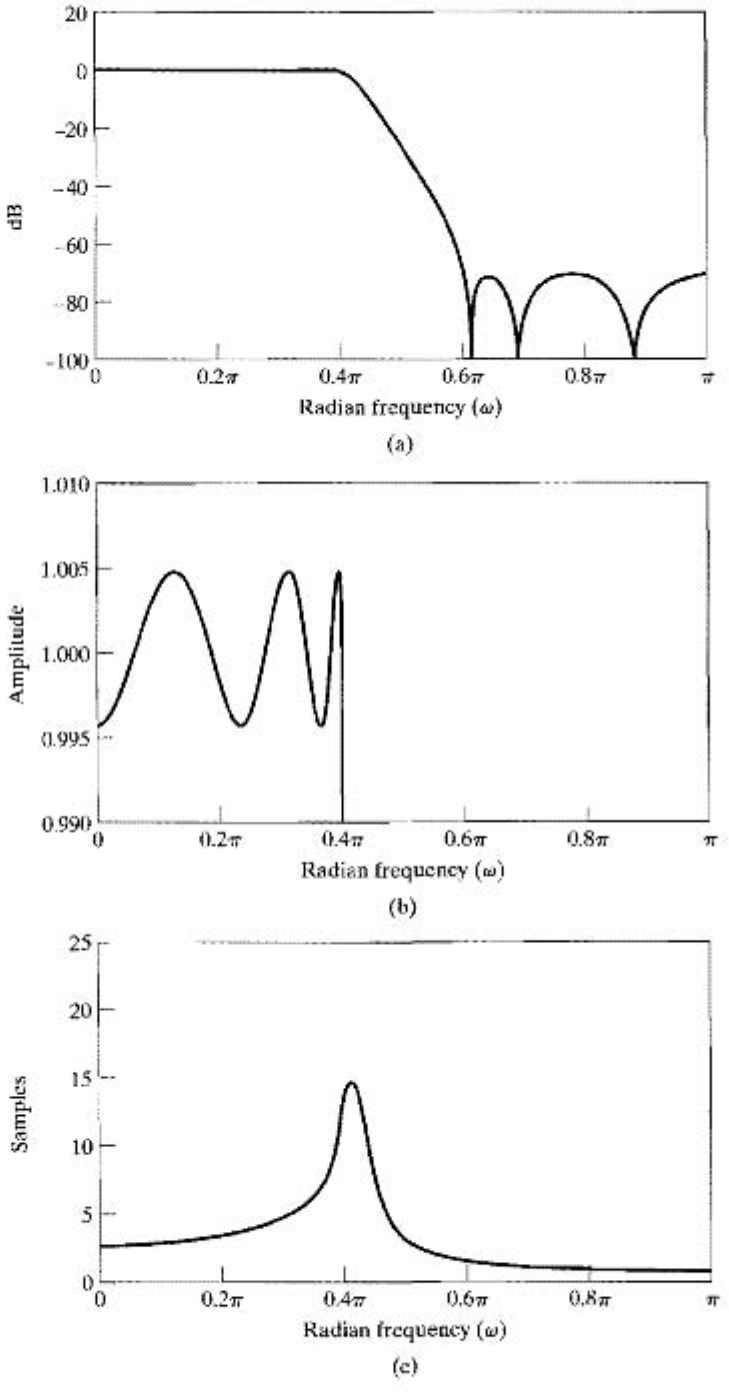

Figure 7.21 Frequency response of 6th-order elliptic filter in Example 7.5. (a) Log magnitude in dB. (b) Detailed plot of magnitude in passband. (c) Group delay.

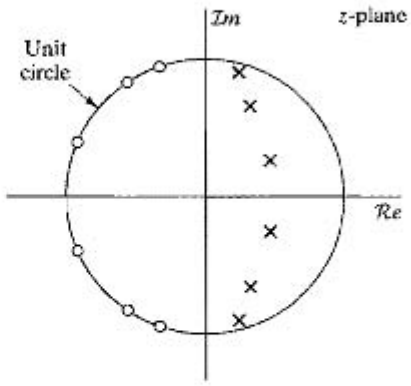

Figure 7.22 Pole–zero plot of 6th-order elliptic filter in Example 7.5.

7.4 FREQUENCY TRANSFORMATIONS OF LOWPASS IIR FILTERS

Our discussion and examples of IIR filter design have focused on the design of frequency-selective lowpass filters. Other types of frequency-selective filters such as highpass, bandpass, bandstop, and multiband filters are equally important. As with lowpass filters, these other classes are characterized by one or several passbands and stopbands, each specified by passband and stopband edge frequencies. Generally the desired filter gain is unity in the passbands and zero in the stopbands, but as with lowpass filters, the filter design specifications include tolerance limits by which the ideal gains or attenuation in the pass- and stopbands can be exceeded. A typical tolerance scheme for a multiband filter with two passbands and one stopband is shown in Figure 7.23.

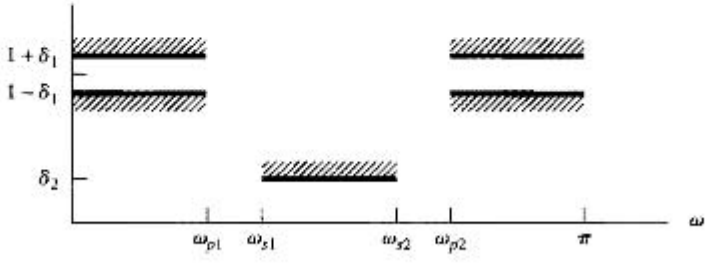

Figure 7.23 Tolerance scheme for a multiband filter.

The traditional approach to the design of many continuous-time frequency-selective filters is to first design a frequency-normalized prototype lowpass filter and then, using an algebraic transformation, derive the desired filter from the prototype lowpass filter (see Guillemin, 1957 and Daniels, 1974). In the case of discrete-time frequency-selective filters, we could design a continuous-time frequency-selective filter of the desired type and then transform it to a discrete-time filter. This procedure would be acceptable with the bilinear transformation, but impulse invariance clearly could not be used to transform highpass and bandstop continuous-time filters into corresponding discrete-time filters because of the aliasing that results from sampling. An alternative procedure that works with either the bilinear transformation or impulse invariance is to design a discrete-time prototype lowpass filter and then perform an algebraic transformation on it to obtain the desired frequency-selective discrete-time filter.

Frequency-selective filters of the lowpass, highpass, bandpass, and bandstop types can be obtained from a lowpass discrete-time filter by use of transformations very similar to the bilinear transformation used to transform continuous-time system functions into discrete-time system functions. To see how this is done, assume that we are given a lowpass system function $H_{lp}(Z)$ that we wish to transform to a new system function $H(z)$, which has either lowpass, highpass, bandpass, or bandstop characteristics when evaluated on the unit circle. Note that we associate the complex variable Z with the prototype lowpass filter and the complex variable z with the transformed filter. Then, we define a mapping from the Z-plane to the z-plane of the form

$$Z^{-1} = G(z^{-1}) \tag{7.38}$$

such that

$$H(z) = H_{lp}(Z)\big|_{Z^{-1}=G(z^{-1})} \tag{7.39}$$

Instead of expressing Z as a function of z, we have assumed in Eq. (7.38) that Z^{-1} is expressed as a function of z^{-1}. Thus, according to Eq. (7.39), in obtaining $H(z)$ from $H_{lp}(z)$ we replace Z^{-1} everywhere in $H_{lp}(Z)$ by the function $G(z^{-1})$. This is a convenient representation, because $H_{lp}(Z)$ is normally expressed as a rational function of Z^{-1}.

If $H_{lp}(Z)$ is the rational system function of a causal and stable system, we naturally require that the transformed system function $H(z)$ be a rational function of z^{-1} and that the system also be causal and stable. This places the following constraints on the transformation $Z^{-1} = G(z^{-1})$:

1. $G(z^{-1})$ must be a rational function of z^{-1}.
2. The inside of the unit circle of the Z-plane must map to the inside of the unit circle of the z-plane.
3. The unit circle of the Z-plane must map onto the unit circle of the z-plane.

Let θ and ω be the frequency variables (angles) in the Z-plane and z-plane, respectively, i.e., on the respective unit circles $Z = e^{j\theta}$ and $z = e^{j\omega}$. Then, for condition 3 to hold, it must be true that

$$e^{-j\theta} = |G(e^{-j\omega})|e^{j\angle G(e^{-j\omega})}, \tag{7.40}$$

and thus,

$$|G(e^{-j\omega})| = 1. \tag{7.41}$$

Therefore, the relationship between the frequency variables is

$$-\theta = \angle G(e^{-j\omega}). \tag{7.42}$$

Constantinides (1970) showed that the most general form of the function $G(z^{-1})$ that satisfies all the above requirements is

$$Z^{-1} = G(z^{-1}) = \pm \prod_{k=1}^{N} \frac{z^{-1} - \alpha_k}{1 - \alpha_k z^{-1}}. \tag{7.43}$$

From our discussion of allpass systems in Chapter 5, it should be clear that $G(z^{-1})$ as given in Eq. (7.43) satisfies Eq. (7.41), and it is easily shown that Eq. (7.43) maps the inside of the unit circle of the Z-plane to the inside of the unit circle of the z-plane if and only if $|\alpha_k| < 1$. By choosing appropriate values for N and the constants α_k, a variety of mappings can be obtained. The simplest is the one that transforms a lowpass filter into another lowpass filter with different passband and stopband edge frequencies. For this case,

$$Z^{-1} = G(z^{-1}) = \frac{z^{-1} - \alpha}{1 - \alpha z^{-1}}. \tag{7.44}$$

If we substitute $Z = e^{j\theta}$ and $z = e^{j\omega}$, we obtain

$$e^{-j\theta} = \frac{e^{-j\omega} - \alpha}{1 - \alpha e^{-j\omega}}, \tag{7.45}$$

from which it follows that

$$\omega = \arctan\left[\frac{(1 - \alpha^2)\sin\theta}{2\alpha + (1 + \alpha^2)\cos\theta}\right]. \tag{7.46}$$

This relationship is plotted in Figure 7.24 for different values of α. Although a warping of the frequency scale is evident in Figure 7.24 (except in the case $\alpha = 0$, which corresponds to $Z^{-1} = z^{-1}$), if the original system has a piecewise-constant lowpass frequency response with cutoff frequency θ_p, then the transformed system will likewise have a similar lowpass response with cutoff frequency ω_p determined by the choice of α.

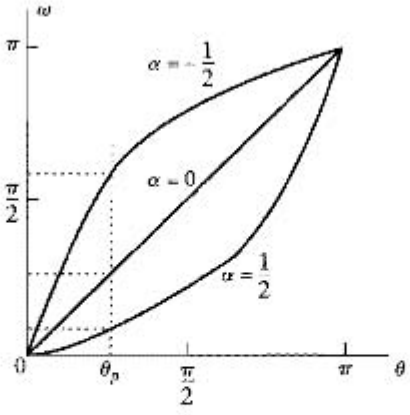

Figure 7.24 Warping of the frequency scale in lowpass-to-lowpass transformation.

TABLE 7.1 TRANSFORMATIONS FROM A LOWPASS DIGITAL FILTER PROTOTYPE OF CUTOFF FREQUENCY θ_p TO HIGHPASS, BANDPASS, AND BANDSTOP FILTERS

Filter Type	Transformations	Associated Design Formulas
Lowpass	$Z^{-1} = \dfrac{z^{-1} - \alpha}{1 - \alpha z^{-1}}$	$\alpha = \dfrac{\sin\left(\frac{\theta_p - \omega_p}{2}\right)}{\sin\left(\frac{\theta_p + \omega_p}{2}\right)}$ ω_p = desired cutoff frequency
Highpass	$Z^{-1} = -\dfrac{z^{-1} + \alpha}{1 + \alpha z^{-1}}$	$\alpha = -\dfrac{\cos\left(\frac{\theta_p + \omega_p}{2}\right)}{\cos\left(\frac{\theta_p - \omega_p}{2}\right)}$ ω_p = desired cutoff frequency
Bandpass	$Z^{-1} = -\dfrac{z^{-2} - \frac{2\alpha k}{k+1} z^{-1} + \frac{k-1}{k+1}}{\frac{k-1}{k+1} z^{-2} - \frac{2\alpha k}{k+1} z^{-1} + 1}$	$\alpha = \dfrac{\cos\left(\frac{\omega_{p2} + \omega_{p1}}{2}\right)}{\cos\left(\frac{\omega_{p2} - \omega_{p1}}{2}\right)}$ $k = \cot\left(\dfrac{\omega_{p2} - \omega_{p1}}{2}\right) \tan\left(\dfrac{\theta_p}{2}\right)$ ω_{p1} = desired lower cutoff frequency ω_{p2} = desired upper cutoff frequency
Bandstop	$Z^{-1} = \dfrac{z^{-2} - \frac{2\alpha}{1+k} z^{-1} + \frac{1-k}{1+k}}{\frac{1-k}{1+k} z^{-2} - \frac{2\alpha}{1+k} z^{-1} + 1}$	$\alpha = \dfrac{\cos\left(\frac{\omega_{p2} + \omega_{p1}}{2}\right)}{\cos\left(\frac{\omega_{p2} - \omega_{p1}}{2}\right)}$ $k = \tan\left(\dfrac{\omega_{p2} - \omega_{p1}}{2}\right) \tan\left(\dfrac{\theta_p}{2}\right)$ ω_{p1} = desired lower cutoff frequency ω_{p2} = desired upper cutoff frequency

Solving for α in terms of θ_p and ω_p, we obtain

$$\alpha = \frac{\sin[(\theta_p - \omega_p)/2]}{\sin[(\theta_p + \omega_p)/2]}. \tag{7.47}$$

Thus, to use these results to obtain a lowpass filter $H(z)$ with cutoff frequency ω_p from an already available lowpass filter $H_{lp}(Z)$ with cutoff frequency θ_p, we would use Eq. (7.47) to determine α in the expression

$$H(z) = H_{lp}(Z)\Big|_{Z^{-1}=(z^{-1}-\alpha)/(1-\alpha z^{-1})}. \tag{7.48}$$

(Problem 7.51 explores how the lowpass–lowpass transformation can be used to obtain a network structure for a variable cutoff frequency filter where the cutoff frequency is determined by a single parameter α.)

Transformations from a lowpass filter to highpass, bandpass, and bandstop filters can be derived in a similar manner. These transformations are summarized in Table 7.1. In the design formulas, all of the cutoff frequencies are assumed to be between zero and π radians. The following example illustrates the use of such transformations.

Example 7.6 Transformation of a Lowpass Filter to a Highpass Filter

Consider a Type I Chebyshev lowpass filter with system function

$$H_{lp}(Z) = \frac{0.001836(1 + Z^{-1})^4}{(1 - 1.5548Z^{-1} + 0.6493Z^{-2})(1 - 1.4996Z^{-1} + 0.8482Z^{-2})}. \tag{7.49}$$

This 4th-order system was designed to meet the specifications

$$0.89125 \le |H_{lp}(e^{j\theta})| \le 1, \quad 0 \le \theta \le 0.2\pi, \tag{7.50a}$$

$$|H_{lp}(e^{j\theta})| \le 0.17783, \quad 0.3\pi \le \theta \le \pi. \tag{7.50b}$$

The frequency response of this filter is shown in Figure 7.25.

To transform this filter to a highpass filter with passband cutoff frequency $\omega_p = 0.6\pi$, we obtain from Table 7.1

$$\alpha = -\frac{\cos[(0.2\pi + 0.6\pi)/2]}{\cos[(0.2\pi - 0.6\pi)/2]} = -0.38197. \tag{7.51}$$

Thus, using the lowpass–highpass transformation indicated in Table 7.1, we obtain

$$H(z) = H_{lp}(Z)\Big|_{Z^{-1}=-[(z^{-1}-0.38197)/(1-0.38197z^{-1})]}$$

$$= \frac{0.02426(1 - z^{-1})^4}{(1 + 1.0416z^{-1} + 0.4019z^{-2})(1 + 0.5661z^{-1} + 0.7657z^{-2})}. \tag{7.52}$$

The frequency response of this system is shown in Figure 7.26. Note that except for some distortion of the frequency scale, the highpass frequency response appears very much as if the lowpass frequency response were shifted in frequency by π. Also note that the 4th-order zero at $Z = -1$ for the lowpass filter now appears at $z = 1$ for the highpass filter. This example also verifies that the equiripple passband and stopband behavior is preserved by frequency transformations of this type. Also note that the group delay in Figure 7.26(c) is not simply a stretched and shifted version of Figure 7.25(c). This is because the phase variations are stretched and shifted, so that the derivative of the phase is smaller for the highpass filter.

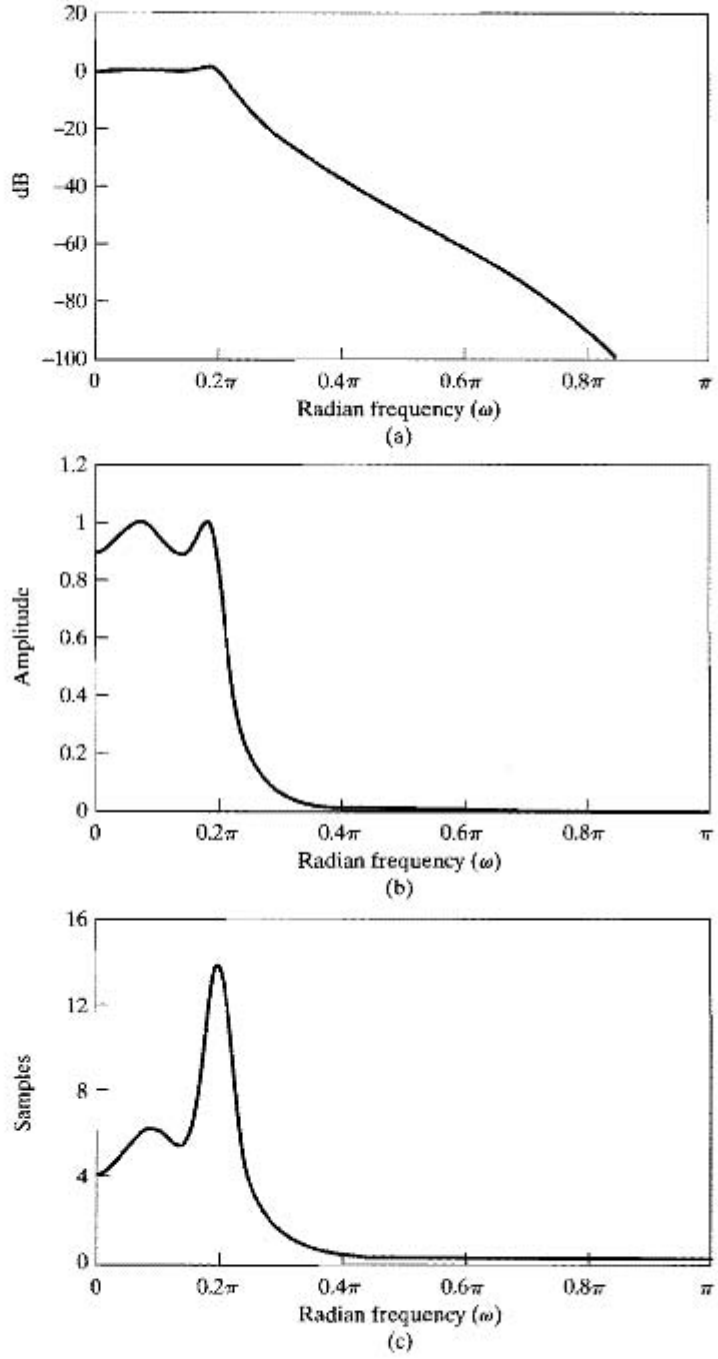

Figure 7.25 Frequency response of 4th-order Chebyshev lowpass filter. (a) Log magnitude in dB. (b) Magnitude. (c) Group delay.

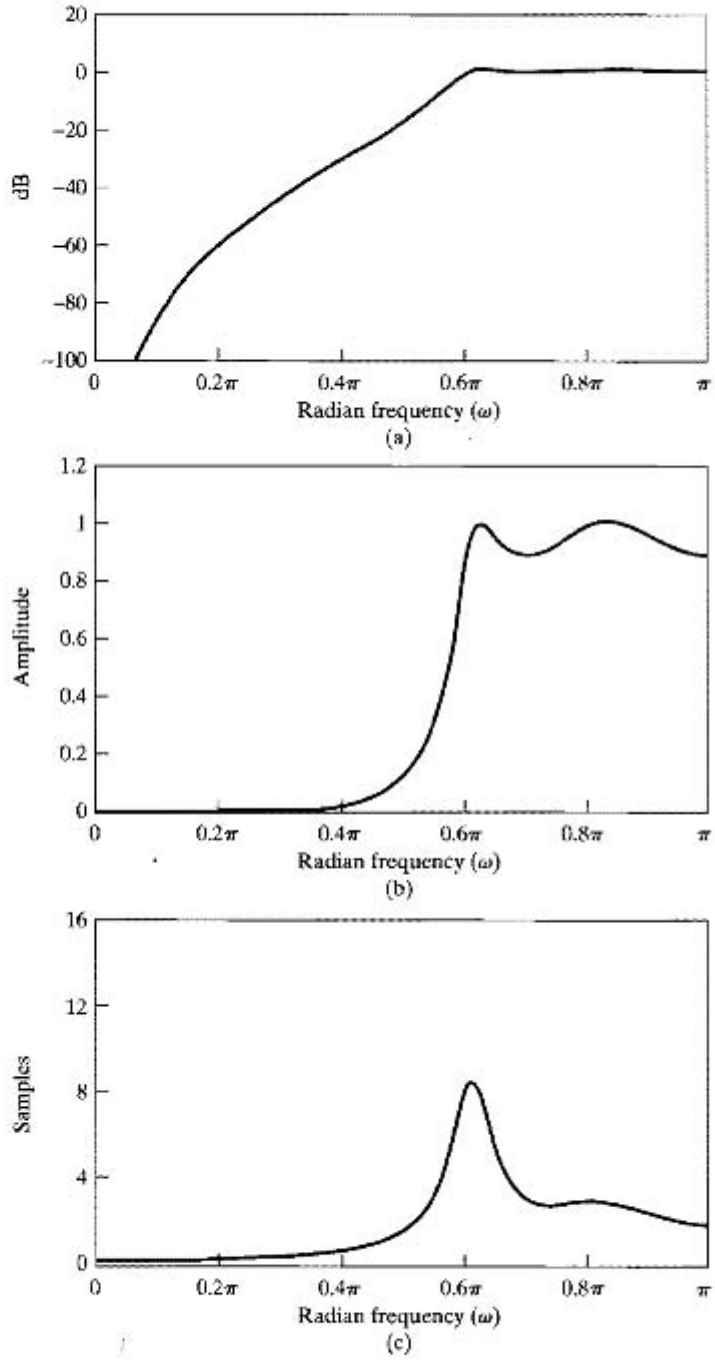

Figure 7.26 Frequency response of 4th-order Chebyshev highpass filter obtained by frequency transformation. (a) Log magnitude in dB. (b) Magnitude. (c) Group delay.

7.5 DESIGN OF FIR FILTERS BY WINDOWING

As discussed in Section 7.2, commonly used techniques for the design of IIR filters have evolved from applying transformations of continuous-time IIR systems into discrete-time IIR systems. In contrast, the design techniques for FIR filters are based on directly approximating the desired frequency response or impulse response of the discrete-time system.

The simplest method of FIR filter design is called the *window method*. This method generally begins with an ideal desired frequency response that can be represented as

$$H_d(e^{j\omega}) = \sum_{n=-\infty}^{\infty} h_d[n]e^{-j\omega n}, \tag{7.53}$$

where $h_d[n]$ is the corresponding impulse response sequence, which can be expressed in terms of $H_d(e^{j\omega})$ as

$$h_d[n] = \frac{1}{2\pi}\int_{-\pi}^{\pi} H_d(e^{j\omega})e^{j\omega n}d\omega. \tag{7.54}$$

Many idealized systems are defined by piecewise-constant or piecewise-smooth frequency responses with discontinuities at the boundaries between bands. As a result, these systems have impulse responses that are noncausal and infinitely long. The most straightforward approach to obtaining an FIR approximation to such systems is to truncate the ideal impulse response through the process referred to as windowing. Equation (7.53) can be thought of as a Fourier series representation of the periodic frequency response $H_d(e^{j\omega})$, with the sequence $h_d[n]$ playing the role of the Fourier coefficients. Thus, the approximation of an ideal filter by truncation of the ideal impulse response is identical to the issue of the convergence of Fourier series, a subject that has received a great deal of study. A particularly important concept from this theory is the Gibbs phenomenon, which was discussed in Example 2.18. In the following discussion, we will see how this effect of nonuniform convergence manifests itself in the design of FIR filters.

A particularly simple way to obtain a causal FIR filter from $h_d[n]$ is to truncate $h_d[n]$, i.e., to define a new system with impulse response $h[n]$ given by[4]

$$h[n] = \begin{cases} h_d[n], & 0 \le n \le M, \\ 0, & \text{otherwise.} \end{cases} \tag{7.55}$$

More generally, we can represent $h[n]$ as the product of the desired impulse response and a finite-duration "window" $w[n]$; i.e.,

$$h[n] = h_d[n]w[n], \tag{7.56}$$

[4]The notation for FIR systems was established in Chapter 5. That is, M is the order of the system function polynomial. Thus, $(M+1)$ is the length, or duration, of the impulse response. Often in the literature, N is used for the length of the impulse response of an FIR filter; however, we have used N to denote the order of the denominator polynomial in the system function of an IIR filter. Thus, to avoid confusion and maintain consistency throughout this book, we will consider the length of the impulse response of an FIR filter to be $(M+1)$.

where, for simple truncation as in Eq. (7.55), the window is the *rectangular window*

$$w[n] = \begin{cases} 1, & 0 \le n \le M, \\ 0, & \text{otherwise.} \end{cases} \tag{7.57}$$

It follows from the modulation, or windowing, theorem (Section 2.9.7) that

$$H(e^{j\omega}) = \frac{1}{2\pi}\int_{-\pi}^{\pi} H_d(e^{j\theta})W(e^{j(\omega-\theta)})d\theta. \tag{7.58}$$

That is, $H(e^{j\omega})$ is the periodic convolution of the desired ideal frequency response with the Fourier transform of the window. Thus, the frequency response $H(e^{j\omega})$ will be a "smeared" version of the desired response $H_d(e^{j\omega})$. Figure 7.27(a) depicts typical functions $H_d(e^{j\theta})$ and $W(e^{j(\omega-\theta)})$ as a function of θ, as required in Eq. (7.58).

If $w[n] = 1$ for all n (i.e., if we do not truncate at all), $W(e^{j\omega})$ is a periodic impulse train with period 2π, and therefore, $H(e^{j\omega}) = H_d(e^{j\omega})$. This interpretation suggests that if $w[n]$ is chosen so that $W(e^{j\omega})$ is concentrated in a narrow band of frequencies around $\omega = 0$, i.e., it approximates an impulse, then $H(e^{j\omega})$ will "look like" $H_d(e^{j\omega})$, except where $H_d(e^{j\omega})$ changes very abruptly. Consequently, the choice of window is governed by the desire to have $w[n]$ as short as possible in duration, so as to minimize computation in the implementation of the filter, while having $W(e^{j\omega})$ approximate an impulse; that is, we want $W(e^{j\omega})$ to be highly concentrated in frequency so that the convolution of Eq. (7.58) faithfully reproduces the desired frequency response. These are conflicting requirements, as can be seen in the case of the rectangular window of Eq. (7.57), where

$$W(e^{j\omega}) = \sum_{n=0}^{M} e^{-j\omega n} = \frac{1 - e^{-j\omega(M+1)}}{1 - e^{-j\omega}} = e^{-j\omega M/2}\frac{\sin[\omega(M+1)/2]}{\sin(\omega/2)}. \tag{7.59}$$

The magnitude of the function $\sin[\omega(M+1)/2]/\sin(\omega/2)$ is plotted in Figure 7.28 for the case $M = 7$. Note that $W(e^{j\omega})$ for the rectangular window has a generalized linear phase. As M increases, the width of the "main lobe" decreases. The main lobe is usually defined as the region between the first zero-crossings on either side of the origin. For the rectangular window, the width of the main lobe is $\Delta\omega_m = 4\pi/(M+1)$. However, for the rectangular window, the side lobes are large, and in fact, as M increases, the peak amplitudes of the main lobe and the side lobes grow in a manner such that the area under each lobe is a constant while the width of each lobe decreases with M. Consequently, as $W(e^{j(\omega-\theta)})$ "slides by" a discontinuity of $H_d(e^{j\theta})$ as ω varies, the integral of $W(e^{j(\omega-\theta)})H_d(e^{j\theta})$ will oscillate as each side lobe of $W(e^{j(\omega-\theta)})$ moves past the discontinuity. This result is depicted in Figure 7.27(b). Since the area under each lobe remains constant with increasing M, the oscillations occur more rapidly, but do not decrease in amplitude as M increases.

In the theory of Fourier series, it is well known that this nonuniform convergence, the *Gibbs phenomenon*, can be moderated through the use of a less abrupt truncation of the Fourier series. By tapering the window smoothly to zero at each end, the height of the side lobes can be diminished; however, this is achieved at the expense of a wider main lobe and thus a wider transition at the discontinuity.

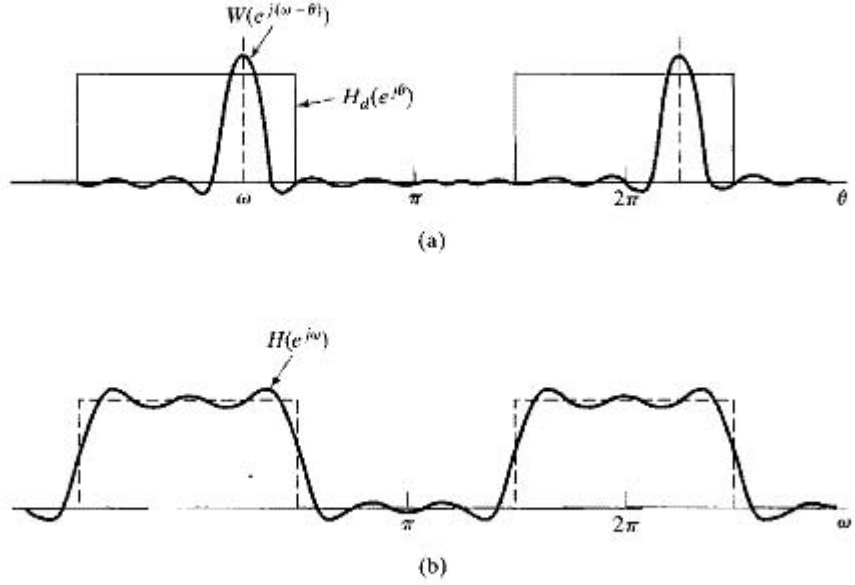

Figure 7.27 (a) Convolution process implied by truncation of the ideal impulse response. (b) Typical approximation resulting from windowing the ideal impulse response.

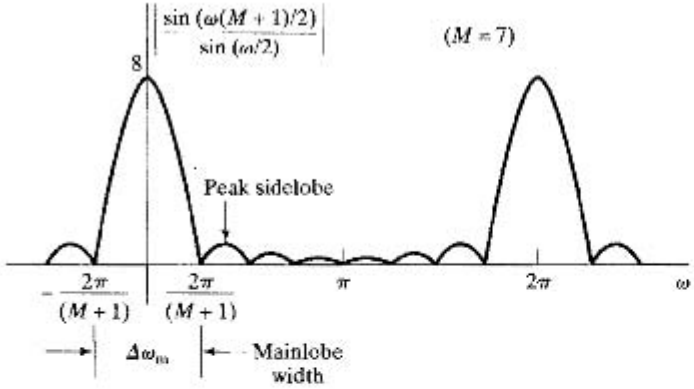

Figure 7.28 Magnitude of the Fourier transform of a rectangular window $(M = 7)$.

7.5.1 Properties of Commonly Used Windows

Some commonly used windows are shown in Figure 7.29. These windows are defined by the following equations:

Rectangular

$$w[n] = \begin{cases} 1, & 0 \le n \le M, \\ 0, & \text{otherwise} \end{cases} \tag{7.60a}$$

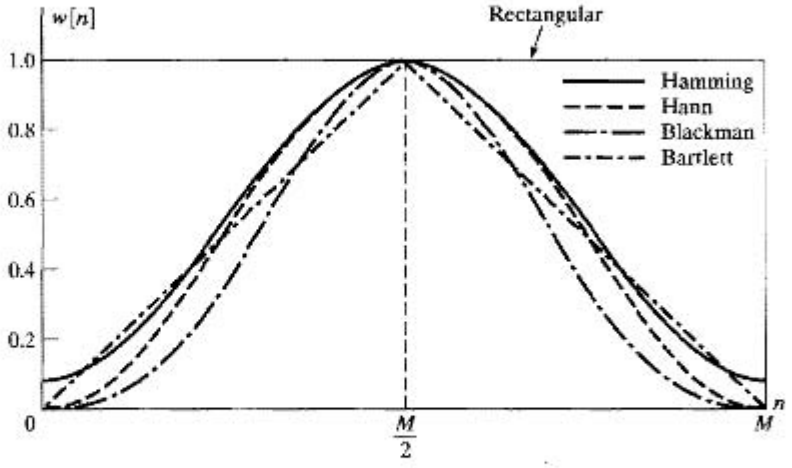

Figure 7.29 Commonly used windows.

Bartlett (triangular)

$$w[n] = \begin{cases} 2n/M, & 0 \le n \le M/2, \ M \text{ even} \\ 2 - 2n/M, & M/2 < n \le M, \\ 0, & \text{otherwise} \end{cases} \tag{7.60b}$$

Hann

$$w[n] = \begin{cases} 0.5 - 0.5\cos(2\pi n/M), & 0 \le n \le M, \\ 0, & \text{otherwise} \end{cases} \tag{7.60c}$$

Hamming

$$w[n] = \begin{cases} 0.54 - 0.46\cos(2\pi n/M), & 0 \le n \le M, \\ 0, & \text{otherwise} \end{cases} \tag{7.60d}$$

Blackman

$$w[n] = \begin{cases} 0.42 - 0.5\cos(2\pi n/M) + 0.08\cos(4\pi n/M), & 0 \le n \le M, \\ 0, & \text{otherwise} \end{cases} \tag{7.60e}$$

(For convenience, Figure 7.29 shows these windows plotted as functions of a continuous variable; however, as specified in Eq. (7.60), the window sequence is defined only at integer values of n.)

The Bartlett, Hann, Hamming, and Blackman windows are all named after their originators. The Hann window is associated with Julius von Hann, an Austrian meteorologist. The term "hanning" was used by Blackman and Tukey (1958) to describe the operation of applying this window to a signal and has since become the most widely used name for the window, with varying preferences for the choice of "Hanning" or "hanning." There is some slight variation in the definition of the Bartlett and Hann windows. As we have defined them, $w[0] = w[M] = 0$, so that it would be reasonable to assert that with this definition, the window length is really only $M - 1$ samples. Other

definitions of the Bartlett and Hann windows are related to our definitions by a shift of one sample and redefinition of the window length.

As will be discussed in Chapter 10, the windows defined in Eq. (7.60) are commonly used for spectrum analysis as well as for FIR filter design. They have the desirable property that their Fourier transforms are concentrated around $\omega = 0$, and they have a simple functional form that allows them to be computed easily. The Fourier transform of the Bartlett window can be expressed as a product of Fourier transforms of rectangular windows, and the Fourier transforms of the other windows can be expressed as sums of frequency-shifted Fourier transforms of the rectangular window, as given by Eq. (7.59). (See Problem 7.43.)

The function $20\log_{10}|W(e^{j\omega})|$ is plotted in Figure 7.30 for each of these windows with $M = 50$. The rectangular window clearly has the narrowest main lobe, and thus, for a given length, it should yield the sharpest transitions of $H(e^{j\omega})$ at a discontinuity of $H_d(e^{j\omega})$. However, the first side lobe is only about 13 dB below the main peak, resulting in oscillations of $H(e^{j\omega})$ of considerable size around discontinuities of $H_d(e^{j\omega})$. Table 7.2, which compares the windows of Eq. (7.60), shows that, by tapering the window smoothly to zero, as with the Bartlett, Hamming, Hann, and Blackman windows, the side lobes (second column) are greatly reduced in amplitude; however, the price paid is a much wider main lobe (third column) and thus wider transitions at discontinuities of $H_d(e^{j\omega})$. The other columns of Table 7.2 will be discussed later.

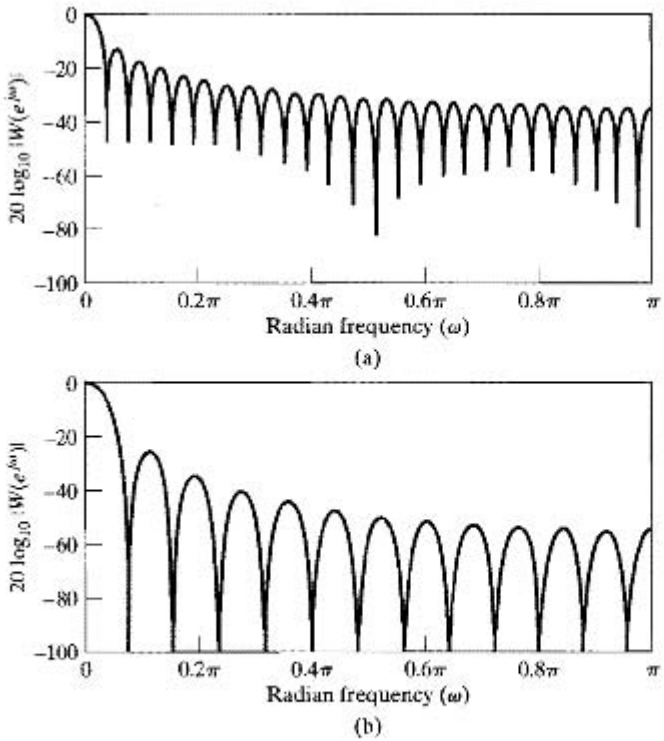

Figure 7.30 Fourier transforms (log magnitude) of windows of Figure 7.29 with $M = 50$. (a) Rectangular. (b) Bartlett.

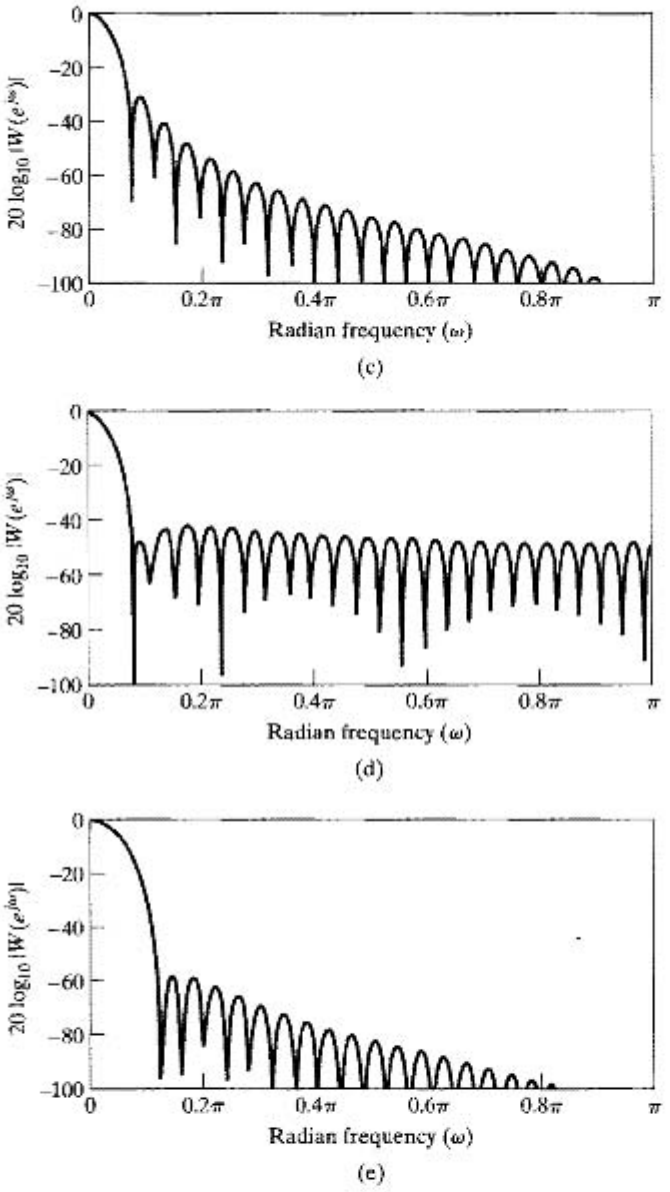

Figure 7.30 (*continued*) (c) Hann. (d) Hamming. (e) Blackman.

7.5.2 Incorporation of Generalized Linear Phase

In designing many types of FIR filters, it is desirable to obtain causal systems with a generalized linear-phase response. All the windows of Eq. (7.60) have been defined in anticipation of this need. Specifically, note that all the windows have the property that

$$w[n] = \begin{cases} w[M-n], & 0 \le n \le M, \\ 0, & \text{otherwise;} \end{cases} \tag{7.61}$$

TABLE 7.2 COMPARISON OF COMMONLY USED WINDOWS

Type of Window	Peak Side-Lobe Amplitude (Relative)	Approximate Width of Main Lobe	Peak Approximation Error, $20\log_{10}\delta$ (dB)	Equivalent Kaiser Window, β	Transition Width of Equivalent Kaiser Window
Rectangular	−13	$4\pi/(M+1)$	−21	0	$1.81\pi/M$
Bartlett	−25	$8\pi/M$	−25	1.33	$2.37\pi/M$
Hann	−31	$8\pi/M$	−44	3.86	$5.01\pi/M$
Hamming	−41	$8\pi/M$	−53	4.86	$6.27\pi/M$
Blackman	−57	$12\pi/M$	−74	7.04	$9.19\pi/M$

i.e., they are symmetric about the point $M/2$. As a result, their Fourier transforms are of the form

$$W(e^{j\omega}) = W_e(e^{j\omega})e^{-j\omega M/2}, \tag{7.62}$$

where $W_e(e^{j\omega})$ is a real, even function of ω. This is illustrated by Eq. (7.59). The convention of Eq. (7.61) leads to causal filters in general, and if the desired impulse response is also symmetric about $M/2$, i.e., if $h_d[M-n] = h_d[n]$, then the windowed impulse response will also have that symmetry, and the resulting frequency response will have a generalized linear phase; that is,

$$H(e^{j\omega}) = A_e(e^{j\omega})e^{-j\omega M/2}, \tag{7.63}$$

where $A_e(e^{j\omega})$ is real and is an even function of ω. Similarly, if the desired impulse response is antisymmetric about $M/2$, i.e., if $h_d[M-n] = -h_d[n]$, then the windowed impulse response will also be antisymmetric about $M/2$, and the resulting frequency response will have a generalized linear phase with a constant phase shift of ninety degrees; i.e.,

$$H(e^{j\omega}) = jA_o(e^{j\omega})e^{-j\omega M/2}, \tag{7.64}$$

where $A_o(e^{j\omega})$ is real and is an odd function of ω.

Although the preceding statements are straightforward if we consider the product of the symmetric window with the symmetric (or antisymmetric) desired impulse response, it is useful to consider the frequency-domain representation. Suppose $h_d[M-n] = h_d[n]$. Then,

$$H_d(e^{j\omega}) = H_e(e^{j\omega})e^{-j\omega M/2}, \tag{7.65}$$

where $H_e(e^{j\omega})$ is real and even.

If the window is symmetric, we can substitute Eqs. (7.62) and (7.65) into Eq. (7.58) to obtain

$$H(e^{j\omega}) = \frac{1}{2\pi}\int_{-\pi}^{\pi} H_e(e^{j\theta})e^{-j\theta M/2}W_e(e^{j(\omega-\theta)})e^{-j(\omega-\theta)M/2}d\theta. \tag{7.66}$$

A simple manipulation of the phase factors leads to

$$H(e^{j\omega}) = A_e(e^{j\omega})e^{-j\omega M/2}, \tag{7.67}$$

where

$$A_e(e^{j\omega}) = \frac{1}{2\pi}\int_{-\pi}^{\pi} H_e(e^{j\theta})W_e(e^{j(\omega-\theta)})d\theta. \tag{7.68}$$

Thus, we see that the resulting system has a generalized linear phase and, moreover, the real function $A_e(e^{j\omega})$ is the result of the periodic convolution of the real functions $H_e(e^{j\omega})$ and $W_e(e^{j\omega})$.

The detailed behavior of the convolution of Eq. (7.68) determines the magnitude response of the filter that results from windowing. The following example illustrates this for a linear-phase lowpass filter.

Example 7.7 Linear-Phase Lowpass Filter

The desired frequency response is defined as

$$H_{lp}(e^{j\omega}) = \begin{cases} e^{-j\omega M/2}, & |\omega| < \omega_c, \\ 0, & \omega_c < |\omega| \le \pi. \end{cases} \tag{7.69}$$

where the generalized linear-phase factor has been incorporated into the definition of the ideal lowpass filter. The corresponding ideal impulse response is

$$h_{lp}[n] = \frac{1}{2\pi}\int_{-\omega_c}^{\omega_c} e^{-j\omega M/2}e^{j\omega n}d\omega = \frac{\sin[\omega_c(n-M/2)]}{\pi(n-M/2)} \tag{7.70}$$

for $-\infty < n < \infty$. It is easily shown that $h_{lp}[M-n] = h_{lp}[n]$, so if we use a symmetric window in the equation

$$h[n] = \frac{\sin[\omega_c(n-M/2)]}{\pi(n-M/2)}w[n], \tag{7.71}$$

then a linear-phase system will result.

The upper part of Figure 7.31 depicts the character of the amplitude response that would result for all the windows of Eq. (7.60), except the Bartlett window, which is rarely used for filter design. (For M even, the Bartlett window would produce a monotonic function $A_e(e^{j\omega})$, because $W_e(e^{j\omega})$ is a positive function.) The figure displays the important properties of window method approximations to desired frequency responses that have step discontinuities. It applies accurately when ω_c is not close to zero or to π and when the width of the main lobe is smaller than $2\omega_c$. At the bottom of the figure is a typical Fourier transform for a symmetric window (except for the linear phase). This function should be visualized in different positions as an aid in understanding the shape of the approximation $A_e(e^{j\omega})$ in the vicinity of ω_c.

When $\omega = \omega_c$, the symmetric function $W_e(e^{j(\omega-\theta)})$ is centered on the discontinuity, and about one-half its area contributes to $A_e(e^{j\omega})$. Similarly, we can see that the peak overshoot occurs when $W_e(e^{j(\omega-\theta)})$ is shifted such that the first negative side lobe on the right is just to the right of ω_c. Similarly, the peak negative undershoot occurs when the first negative side lobe on the left is just to the left of ω_c. This means that the distance between the peak ripples on either side of the discontinuity is approximately the main-lobe width $\Delta\omega_m$, as shown in Figure 7.31. The transition width $\Delta\omega$ as defined in the figure is therefore somewhat less than the main-lobe width. Finally, owing to the symmetry of $W_e(e^{j(\omega-\theta)})$, the approximation tends to be symmetric around ω_c; i.e., the approximation overshoots by an amount δ in the passband and undershoots by the same amount in the stopband.

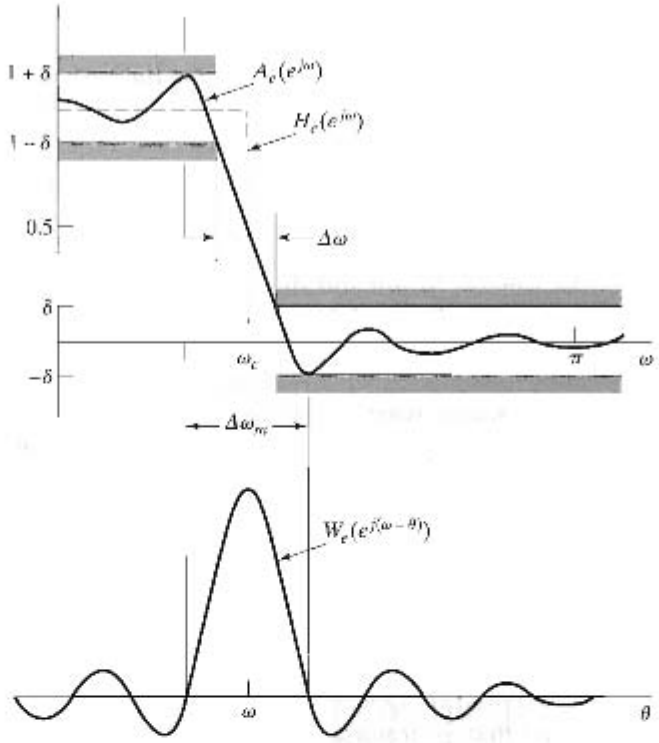

Figure 7.31 Illustration of type of approximation obtained at a discontinuity of the ideal frequency response.

The fourth column of Table 7.2 shows the peak approximation error at a discontinuity (in dB) for the windows of Eq. (7.60). Clearly, the windows with the smaller side lobes yield better approximations of the ideal response at a discontinuity. Also, the third column, which shows the width of the main lobe, suggests that narrower transition regions can be achieved by increasing M. Thus, through the choice of the shape and duration of the window, we can control the properties of the resulting FIR filter. However, trying different windows and adjusting lengths by trial and error is not a very satisfactory way to design filters. Fortunately, a simple formalization of the window method has been developed by Kaiser (1974).

7.5.3 The Kaiser Window Filter Design Method

The trade-off between the main-lobe width and side-lobe area can be quantified by seeking the window function that is maximally concentrated around $\omega = 0$ in the frequency domain. The issue was considered in depth in a series of classic papers by Slepian et al. (1961). The solution found in this work involves prolate spheroidal wave functions, which are difficult to compute and therefore unattractive for filter design. However, Kaiser (1966, 1974) found that a near-optimal window could be formed using the zeroth-order modified Bessel function of the first kind, a function that is much easier to

compute. The Kaiser window is defined as

$$w[n] = \begin{cases} \dfrac{I_0[\beta(1-[(n-\alpha)/\alpha]^2)^{1/2}]}{I_0(\beta)}, & 0 \le n \le M, \\ 0, & \text{otherwise}, \end{cases} \tag{7.72}$$

where $\alpha = M/2$, and $I_0(\cdot)$ represents the zero$^{\text{th}}$-order modified Bessel function of the first kind. In contrast to the other windows in Eqs. (7.60), the Kaiser window has two parameters: the length $(M+1)$ and a shape parameter β. By varying $(M+1)$ and β, the window length and shape can be adjusted to trade side-lobe amplitude for main-lobe width. Figure 7.32(a) shows continuous envelopes of Kaiser windows of length $M+1 = 21$ for $\beta = 0, 3$, and 6. Notice from Eq. (7.72) that the case $\beta = 0$ reduces to the rectangular window. Figure 7.32(b) shows the corresponding Fourier transforms of the Kaiser windows in Figure 7.32(a). Figure 7.32(c) shows Fourier transforms of Kaiser windows with $\beta = 6$ and $M = 10, 20$, and 40. The plots in Figures 7.32(b) and (c) clearly show that the desired trade-off can be achieved. If the window is tapered more, the side lobes of the Fourier transform become smaller, but the main lobe becomes wider. Figure 7.32(c) shows that increasing M while holding β constant causes the main lobe to decrease in width, but it does not affect the peak amplitude of the side lobes. In fact, through extensive numerical experimentation, Kaiser obtained a pair of formulas that permit the filter designer to predict in advance the values of M and β needed to meet a given frequency-selective filter specification. The upper plot of Figure 7.31 is also typical of approximations obtained using the Kaiser window, and Kaiser (1974) found that, over a usefully wide range of conditions, the peak approximation error (δ in Figure 7.31) is determined by the choice of β. Given that δ is fixed, the passband cutoff frequency ω_p of the lowpass filter is defined to be the highest frequency such that $|H(e^{j\omega})| \ge 1 - \delta$. The stopband cutoff frequency ω_s is defined to be the lowest frequency such that $|H(e^{j\omega})| \le \delta$. Therefore, the transition region has width

$$\Delta\omega = \omega_s - \omega_p \tag{7.73}$$

for the lowpass filter approximation. Defining

$$A = -20\log_{10}\delta, \tag{7.74}$$

Kaiser determined empirically that the value of β needed to achieve a specified value of A is given by

$$\beta = \begin{cases} 0.1102(A-8.7), & A > 50, \\ 0.5842(A-21)^{0.4} + 0.07886(A-21), & 21 \le A \le 50, \\ 0.0, & A < 21. \end{cases} \tag{7.75}$$

(Recall that the case $\beta = 0$ is the rectangular window for which $A = 21$.) Furthermore, Kaiser found that to achieve prescribed values of A and $\Delta\omega$, M must satisfy

$$M = \frac{A-8}{2.285\Delta\omega}. \tag{7.76}$$

Equation (7.76) predicts M to within ± 2 over a wide range of values of $\Delta\omega$ and A. Thus, with these formulas, the Kaiser window design method requires almost no iteration or trial and error. The examples in Section 7.6 outline and illustrate the procedure.

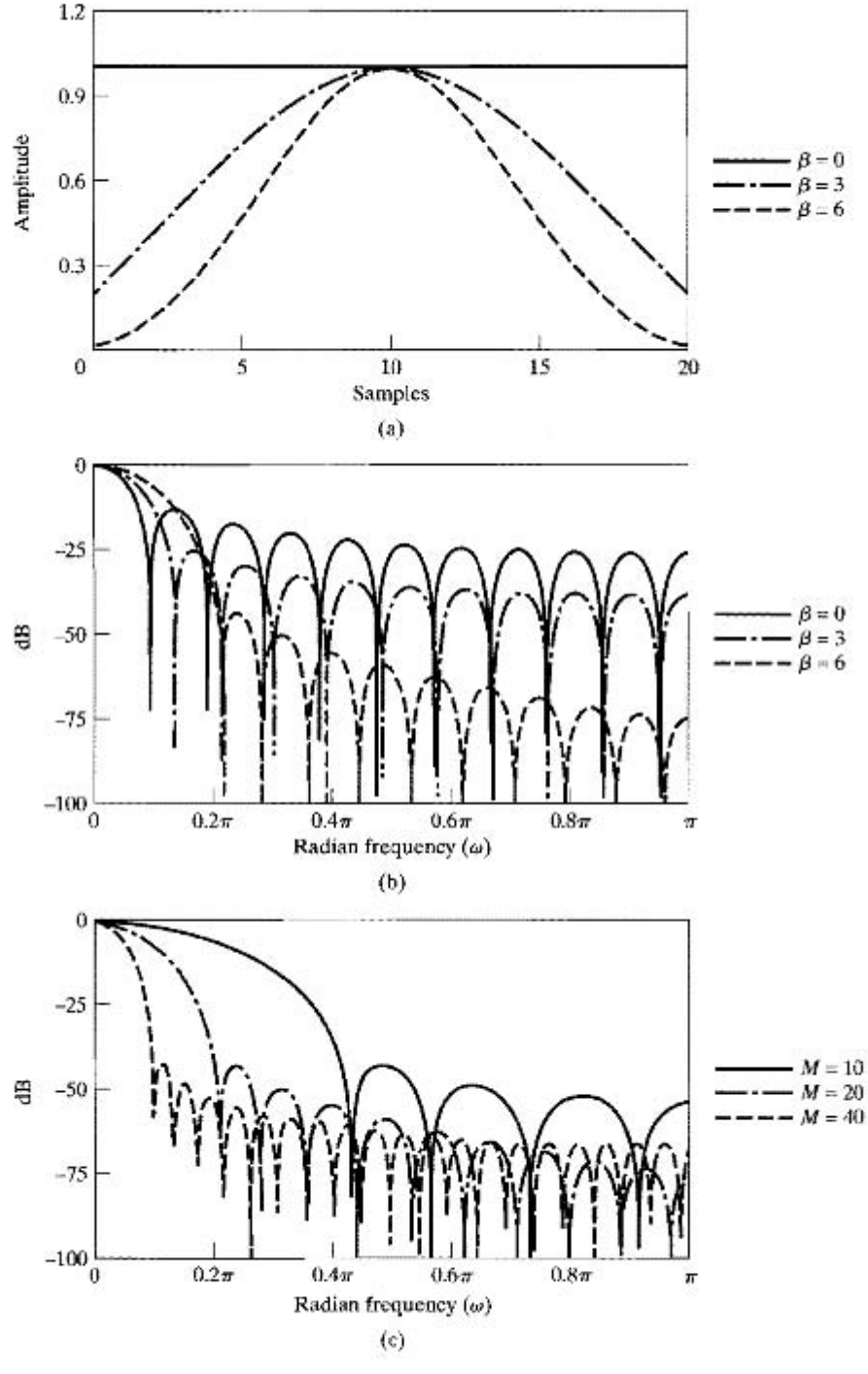

Figure 7.32 (a) Kaiser windows for $\beta = 0$, 3, and 6 and $M = 20$. (b) Fourier transforms corresponding to windows in (a). (c) Fourier transforms of Kaiser windows with $\beta = 6$ and $M = 10$, 20, and 40.

Relationship of the Kaiser Window to Other Windows

The basic principle of the window design method is to truncate the ideal impulse response with a finite-length window such as one of those discussed in this section. The corresponding effect in the frequency domain is that the ideal frequency response is convolved with the Fourier transform of the window. If the ideal filter is a lowpass filter, the discontinuity in its frequency response is smeared as the main lobe of the Fourier transform of the window moves across the discontinuity in the convolution process. To a first approximation, the width of the resulting transition band is determined by the width of the main lobe of the Fourier transform of the window, and the passband and stopband ripples are determined by the side lobes of the Fourier transform of the window. Because the passband and stopband ripples are produced by integration of the symmetric window side lobes, the ripples in the passband and the stopband are approximately the same. Furthermore, to a very good approximation, the maximum passband and stopband deviations are not dependent on M and can be changed only by changing the shape of the window used. This is illustrated by Kaiser's formula, Eq. (7.75), for the window shape parameter, which is independent of M. The last two columns of Table 7.2 compare the Kaiser window with the windows of Eqs. (7.60). The fifth column gives the Kaiser window shape parameter (β) that yields the same peak approximation error (δ) as the window indicated in the first column. The sixth column shows the corresponding transition width [from Eq. (7.76)] for filters designed with the Kaiser window. This formula would be a much better predictor of the transition width for the other windows than would the main-lobe width given in the third column of the table.

In Figure 7.33 is shown a comparison of maximum approximation error versus transition width for the various fixed windows and the Kaiser window for different

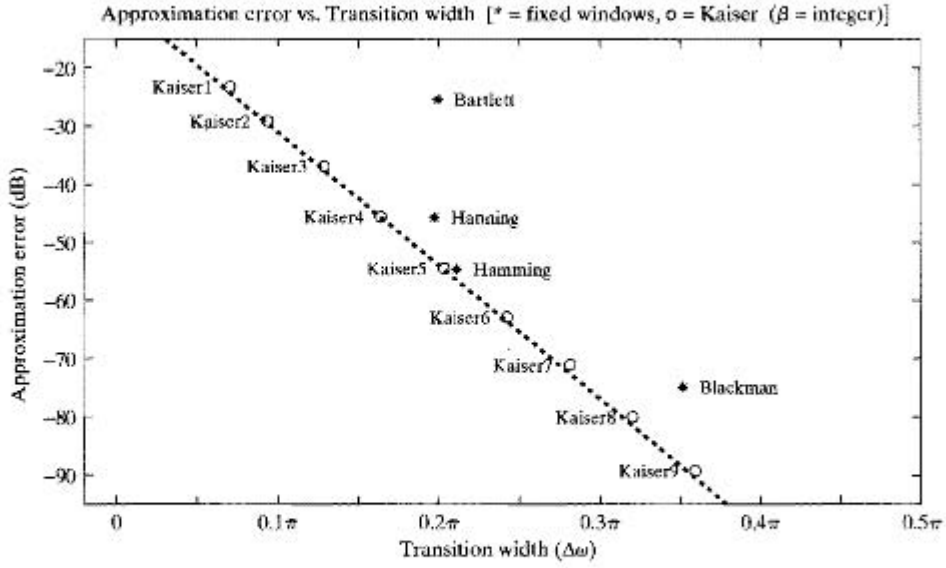

Figure 7.33 Comparison of fixed windows with Kaiser windows in a lowpass filter design application ($M = 32$ and $\omega_c = \pi/2$). (Note that the designation "Kaiser 6" means Kaiser window with $\beta = 6$, etc.)

values of β. The dashed line obtained from Eq. (7.76), shows that Kaiser's formula is an accurate representation of approximation error as a function of transition width for the Kaiser window.

7.6 EXAMPLES OF FIR FILTER DESIGN BY THE KAISER WINDOW METHOD

In this section, we give several examples that illustrate the use of the Kaiser window to obtain FIR approximations to several filter types including lowpass filters. These examples also serve to point out some important properties of FIR systems.

7.6.1 Lowpass Filter

With the use of the design formulas for the Kaiser window, it is straightforward to design an FIR lowpass filter to meet prescribed specifications. The procedure is as follows:

1. First, the specifications must be established. This means selecting the desired ω_p and ω_s and the maximum tolerable approximation error. For window design, the resulting filter will have the same peak error δ in both the passband and the stopband. For this example, we use the same specifications as in Example 7.5, $\omega_p = 0.4\pi$, $\omega_s = 0.6\pi$, $\delta_1 = 0.01$, and $\delta_2 = 0.001$. Since filters designed by the window method inherently have $\delta_1 = \delta_2$, we must set $\delta = 0.001$.
2. The cutoff frequency of the underlying ideal lowpass filter must be found. Owing to the symmetry of the approximation at the discontinuity of $H_d(e^{j\omega})$, we would set
$$\omega_c = \frac{\omega_p + \omega_s}{2} = 0.5\pi.$$
3. To determine the parameters of the Kaiser window, we first compute
$$\Delta\omega = \omega_s - \omega_p = 0.2\pi, \qquad A = -20\log_{10}\delta = 60.$$
We substitute these two quantities into Eqs. (7.75) and (7.76) to obtain the required values of β and M. For this example the formulas predict
$$\beta = 5.653, \qquad M = 37.$$
4. The impulse response of the filter is computed using Eqs. (7.71) and (7.72). We obtain
$$h[n] = \begin{cases} \dfrac{\sin\omega_c(n-\alpha)}{\pi(n-\alpha)} \cdot \dfrac{I_0[\beta(1-[(n-\alpha)/\alpha]^2)^{1/2}]}{I_0(\beta)}, & 0 \le n \le M, \\ 0, & \text{otherwise,} \end{cases}$$
where $\alpha = M/2 = 37/2 = 18.5$. Since $M = 37$ is an odd integer, the resulting linear-phase system would be of type II. (See Section 5.7.3 for the definitions of the four types of FIR systems with generalized linear phase.) The response characteristics of the filter are shown in Figure 7.34. Figure 7.34(a), which shows the impulse response, displays the characteristic symmetry of a type II system.

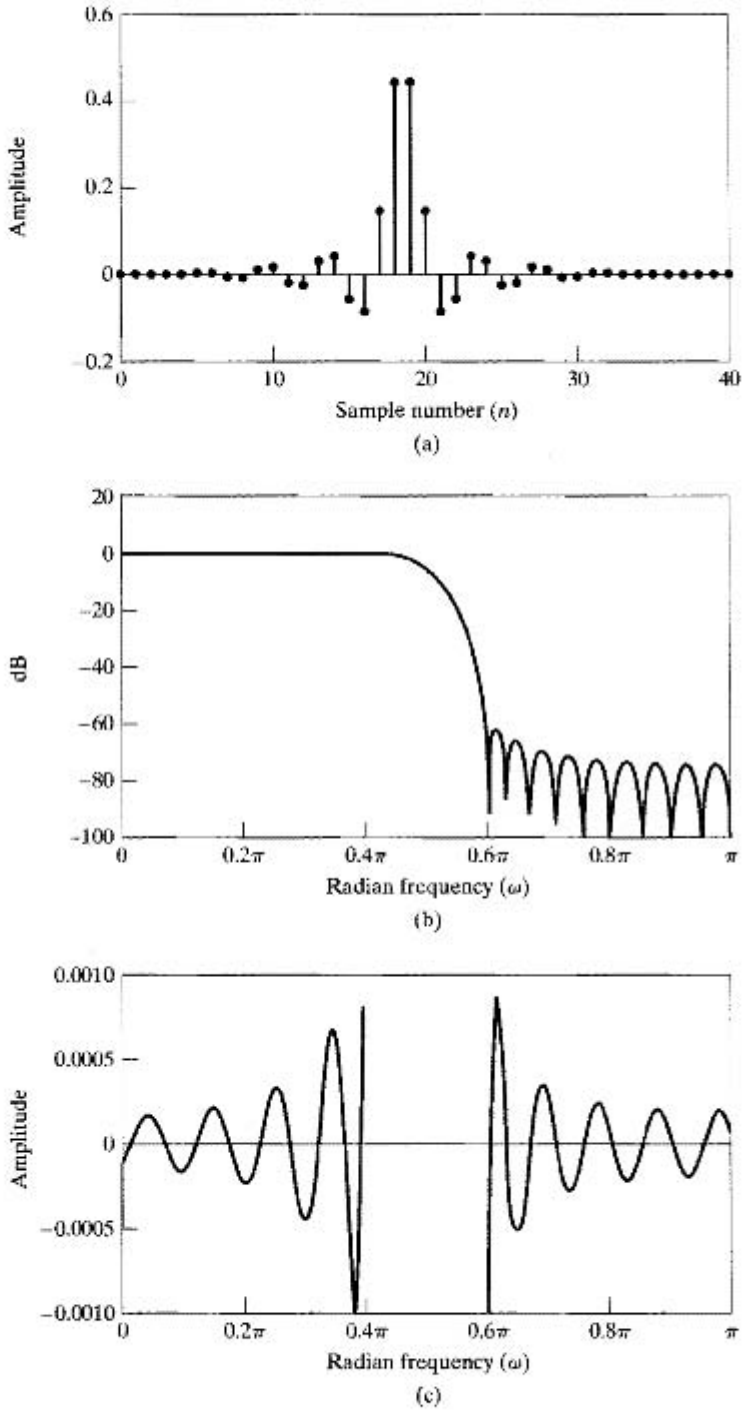

Figure 7.34 Response functions for the lowpass filter designed with a Kaiser window. (a) Impulse response ($M = 37$). (b) Log magnitude. (c) Approximation error for $A_e(e^{j\omega})$.

Figure 7.34(b), which shows the log magnitude response in dB, indicates that $H(e^{j\omega})$ is zero at $\omega = \pi$ or, equivalently, that $H(z)$ has a zero at $z = -1$, as required for a type II FIR system. Figure 7.34(c) shows the approximation error in the passband and stopbands. This error function is defined as

$$E_A(\omega) = \begin{cases} 1 - A_e(e^{j\omega}), & 0 \le \omega \le \omega_p, \\ 0 - A_e(e^{j\omega}), & \omega_s \le \omega \le \pi. \end{cases} \tag{7.77}$$

(The error is not defined in the transition region, $0.4\pi < \omega < 0.6\pi$.) Note the slight asymmetry of the approximation error, and note also that the peak approximation error is $\delta = 0.00113$ instead of the desired value of 0.001. In this case it is necessary to increase M to 40 in order to meet the specifications.

5. Finally, observe that it is not necessary to plot either the phase or the group delay, since we know that the phase is precisely linear and the delay is $M/2 = 18.5$ samples.

7.6.2 Highpass Filter

The ideal highpass filter with generalized linear phase has the frequency response

$$H_{\text{hp}}(e^{j\omega}) = \begin{cases} 0, & |\omega| < \omega_c, \\ e^{-j\omega M/2}, & \omega_c < |\omega| \le \pi. \end{cases} \tag{7.78}$$

The corresponding impulse response can be found by evaluating the inverse transform of $H_{\text{hp}}(e^{j\omega})$, or we can observe that

$$H_{\text{hp}}(e^{j\omega}) = e^{-j\omega M/2} - H_{\text{lp}}(e^{j\omega}), \tag{7.79}$$

where $H_{\text{lp}}(e^{j\omega})$ is given by Eq. (7.69). Thus, $h_{\text{hp}}[n]$ is

$$h_{\text{hp}}[n] = \frac{\sin \pi(n - M/2)}{\pi(n - M/2)} - \frac{\sin \omega_c(n - M/2)}{\pi(n - M/2)}, \qquad -\infty < n < \infty. \tag{7.80}$$

To design an FIR approximation to the highpass filter, we can proceed in a manner similar to that in Section 7.6.1.

Suppose that we wish to design a filter to meet the highpass specifications

$$|H(e^{j\omega})| \le \delta_2, \qquad |\omega| \le \omega_s$$

$$1 - \delta_1 \le |H(e^{j\omega})| \le 1 + \delta_1, \qquad \omega_p \le |\omega| \le \pi$$

where $\omega_s = 0.35\pi$, $\omega_p = 0.5\pi$, and $\delta_1 = \delta_2 = \delta = 0.02$. Since the ideal response also has a discontinuity, we can apply Kaiser's formulas in Eqs. (7.75) and (7.76) with $A = 33.98$ and $\Delta\omega = 0.15\pi$ to estimate the required values of $\beta = 2.65$ and $M = 24$. Figure 7.35 shows the response characteristics that result when a Kaiser window with these parameters is applied to $h_{\text{hp}}[n]$ with $\omega_c = (0.35\pi + 0.5\pi)/2$. Note that, since M is an even integer, the filter is a type I FIR system with linear phase, and the delay is precisely $M/2 = 12$ samples. In this case, the actual peak approximation error is $\delta = 0.0209$ rather than 0.02, as specified. Since the error is less than 0.02 everywhere except at the stopband edge, it is tempting to simply increase M to 25, keeping β the same, thereby narrowing the transition region. This type II filter, which is shown in Figure 7.36, is highly unsatisfactory, owing to the zero of $H(z)$ that is forced by the

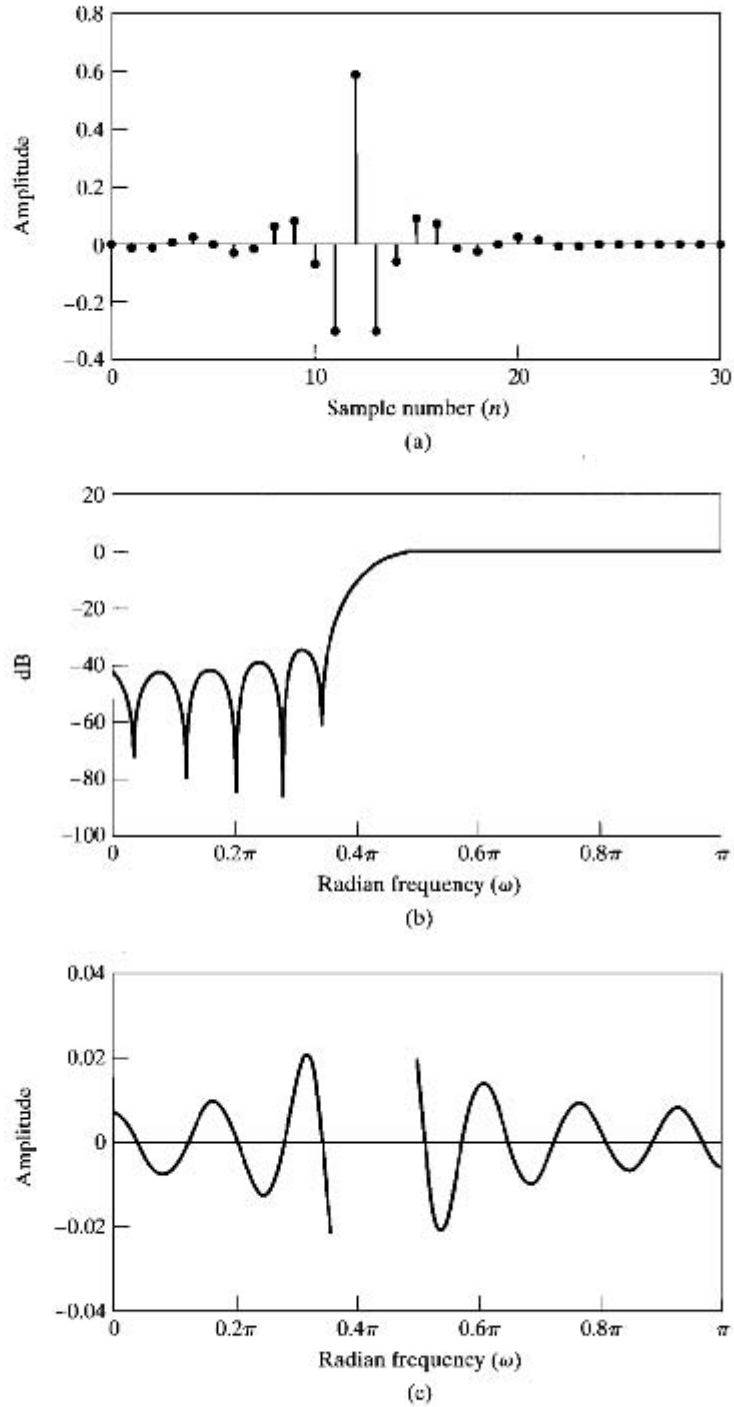

Figure 7.35 Response functions for type I FIR highpass filter. (a) Impulse response ($M = 24$). (b) Log magnitude. (c) Approximation error for $A_e(e^{j\omega})$.

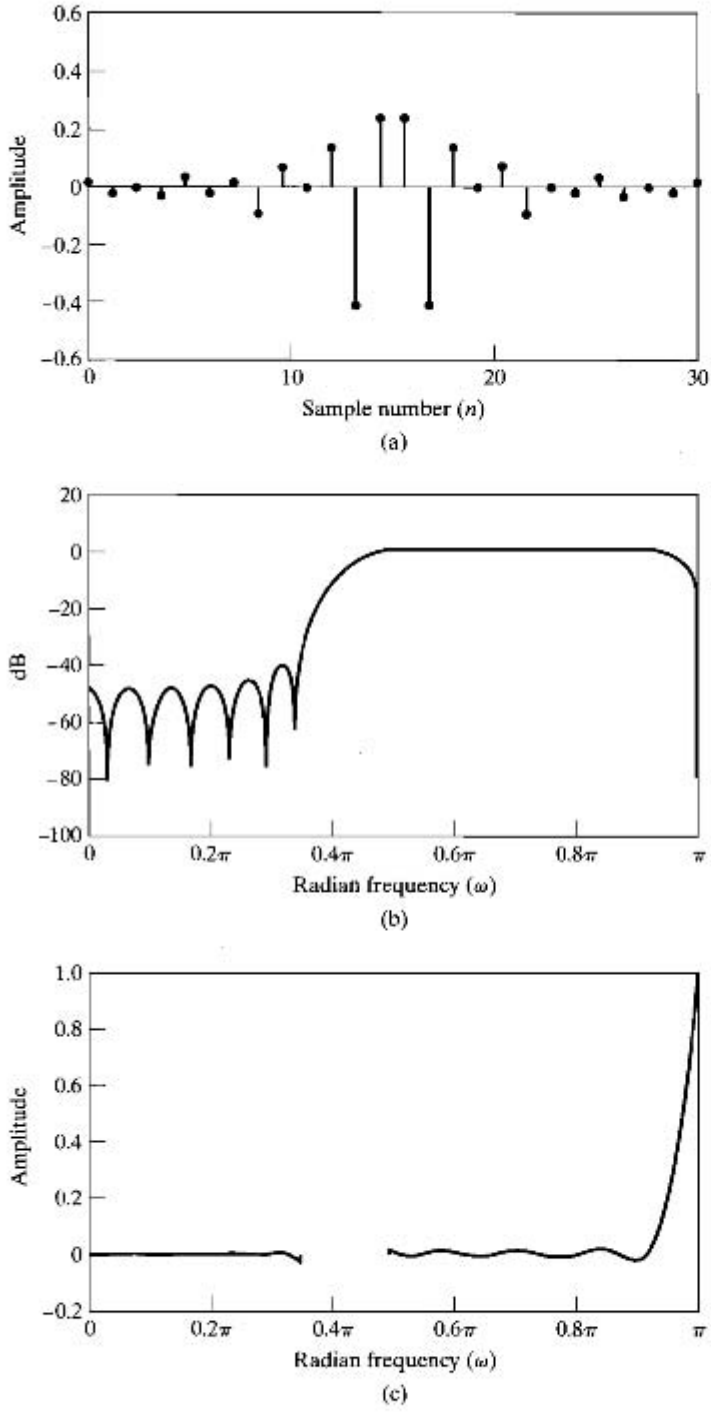

Figure 7.36 Response functions for type II FIR highpass filter. (a) Impulse response ($M = 25$). (b) Log magnitude of Fourier transform. (c) Approximation error for $A_e(e^{j\hat{\omega}})$.

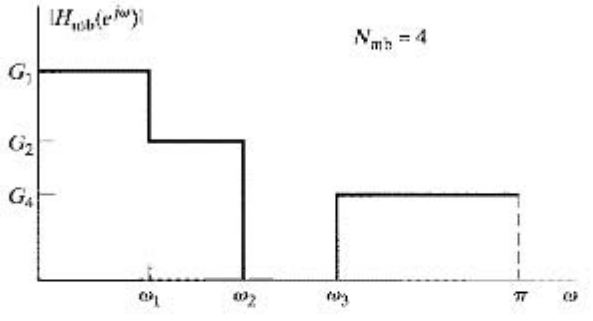

Figure 7.37 Ideal frequency response for multiband filter.

linear-phase constraint to be at $z = -1$, i.e., $\omega = \pi$. Although increasing the order by 1 leads to a worse result, increasing M to 26 would, of course, lead to a type I system that would exceed the specifications. Clearly, type II FIR linear-phase systems are generally not appropriate approximations for either highpass or bandstop filters.

The previous discussion of highpass filter design can be generalized to the case of multiple passbands and stopbands. Figure 7.37 shows an ideal multiband frequency-selective frequency response. This generalized multiband filter includes lowpass, highpass, bandpass, and bandstop filters as special cases. If such a magnitude function is multiplied by a linear-phase factor $e^{-j\omega M/2}$, the corresponding ideal impulse response is

$$h_{mb}[n] = \sum_{k=1}^{N_{mb}} (G_k - G_{k+1}) \frac{\sin \omega_k (n - M/2)}{\pi (n - M/2)}, \tag{7.81}$$

where N_{mb} is the number of bands and $G_{N_{mb}+1} = 0$. If $h_{mb}[n]$ is multiplied by a Kaiser window, the type of approximations that we have observed at the single discontinuity of the lowpass and highpass systems will occur at *each* of the discontinuities. The behavior will be the same at each discontinuity, provided that the discontinuities are far enough apart. Thus, Kaiser's formulas for the window parameters can be applied to this case to predict approximation errors and transition widths. Note that the approximation errors will be scaled by the size of the jump that produces them. That is, if a discontinuity of unity produces a peak error of δ, then a discontinuity of one-half will have a peak error of $\delta/2$.

7.6.3 Discrete-Time Differentiators

As illustrated in Example 4.4, sometimes it is of interest to obtain samples of the derivative of a bandlimited signal from samples of the signal itself. Since the Fourier transform of the derivative of a continuous-time signal is $j\Omega$ times the Fourier transform of the signal, it follows that, for bandlimited signals, a discrete-time system with frequency response $(j\omega/T)$ for $-\pi < \omega < \pi$ (and that is periodic, with period 2π) will yield output samples that are equal to samples of the derivative of the continuous-time signal. A system with this property is referred to as a discrete-time differentiator.

For an ideal discrete-time differentiator with linear phase, the appropriate frequency response is

$$H_{\text{diff}}(e^{j\omega}) = (j\omega)e^{-j\omega M/2}, \qquad -\pi < \omega < \pi. \tag{7.82}$$

(We have omitted the factor $1/T$.) The corresponding ideal impulse response is

$$h_{\text{diff}}[n] = \frac{\cos\pi(n - M/2)}{(n - M/2)} - \frac{\sin\pi(n - M/2)}{\pi(n - M/2)^2}, \qquad -\infty < n < \infty. \tag{7.83}$$

If $h_{\text{diff}}[n]$ is multiplied by a symmetric window of length $(M + 1)$, then it is easily shown that $h[n] = -h[M - n]$. Thus, the resulting system is either a type III or a type IV generalized linear-phase system.

Since Kaiser's formulas were developed for frequency responses with simple magnitude discontinuities, it is not straightforward to apply them to differentiators, wherein the discontinuity in the ideal frequency response is introduced by the phase. Nevertheless, as we show in the next example, the window method is very effective in designing such systems.

Kaiser Window Design of a Differentiator

To illustrate the window design of a differentiator, suppose $M = 10$ and $\beta = 2.4$. The resulting response characteristics are shown in Figure 7.38. Figure 7.38(a) shows the antisymmetric impulse response. Since M is even, the system is a type III linear-phase system, which implies that $H(z)$ has zeros at *both* $z = +1$ ($\omega = 0$) and $z = -1$ ($\omega = \pi$). This is clearly displayed in the magnitude response shown in Figure 7.38(b). The phase is exact, since type III systems have a $\pi/2$-radian constant phase shift plus a linear phase corresponding in this case to $M/2 = 5$ samples delay. Figure 7.38(c) shows the amplitude approximation error

$$E_{\text{diff}}(\omega) = \omega - A_e(e^{j\omega}), \qquad 0 \le \omega \le 0.8\pi, \tag{7.84}$$

where $A_e(e^{j\omega})$ is the amplitude of the approximation. (Note that the error is large around $\omega = \pi$ and is not plotted for frequencies above $\omega = 0.8\pi$.) Clearly, the linearly increasing magnitude is not achieved over the whole band, and, obviously, the relative error (i.e., $E_{\text{diff}}(\omega)/\omega$) is very large for low frequencies or high frequencies (around $\omega = \pi$).

Type IV linear-phase systems do not constrain $H(z)$ to have a zero at $z = -1$. This type of system leads to much better approximations to the amplitude function, as shown in Figure 7.39, for $M = 5$ and $\beta = 2.4$. In this case, the amplitude approximation error is very small up to and beyond $\omega = 0.8\pi$. The phase for this system is again a $\pi/2$-radian constant phase shift plus a linear phase corresponding to a delay of $M/2 = 2.5$ samples. This noninteger delay is the price paid for the exceedingly good amplitude approximation. Instead of obtaining samples of the derivative of the continuous-time signal at the original sampling times $t = nT$, we obtain samples of the derivative at times $t = (n - 2.5)T$. However, in many applications, this noninteger delay may not cause a problem, or it could be compensated for by other noninteger delays in a more complex system involving other linear-phase filters.

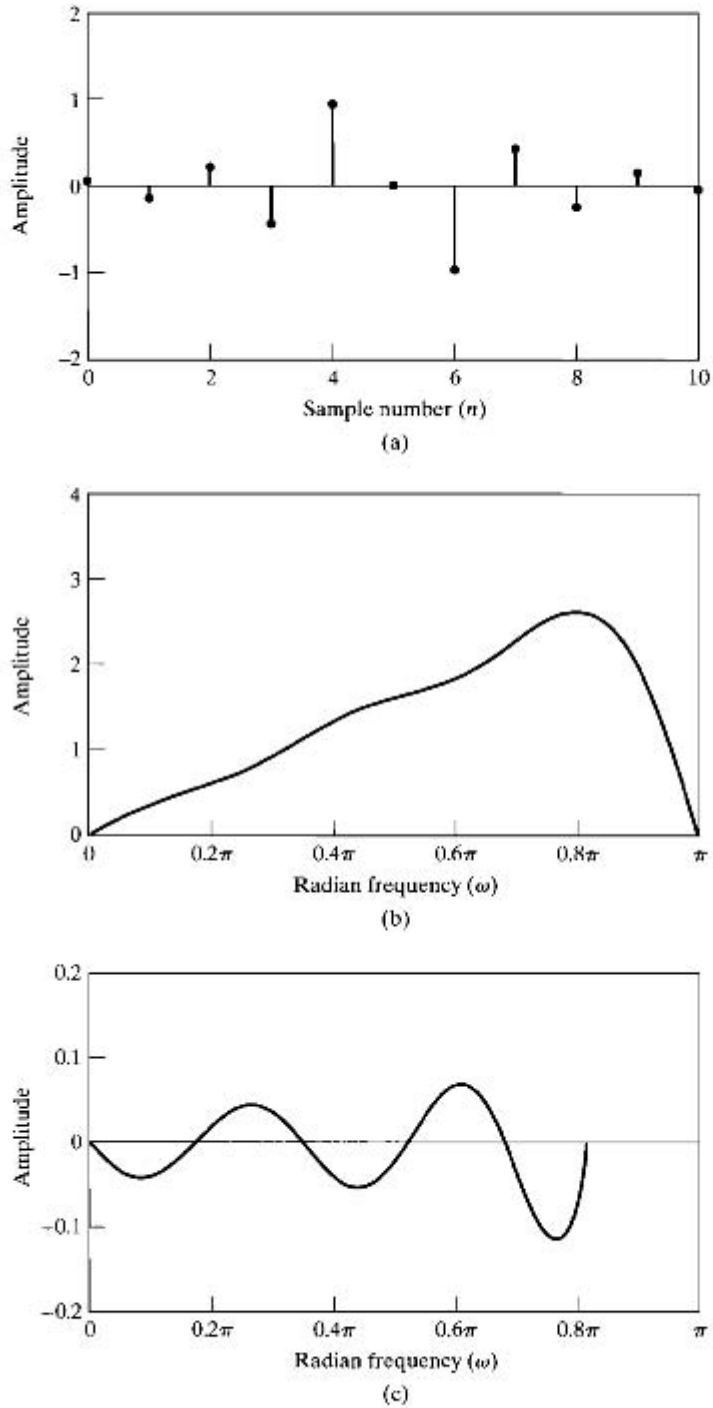

Figure 7.38 Response functions for type III FIR discrete-time differentiator. (a) Impulse response ($M = 10$). (b) Magnitude. (c) Approximation error for $A_0(e^{j\omega})$.

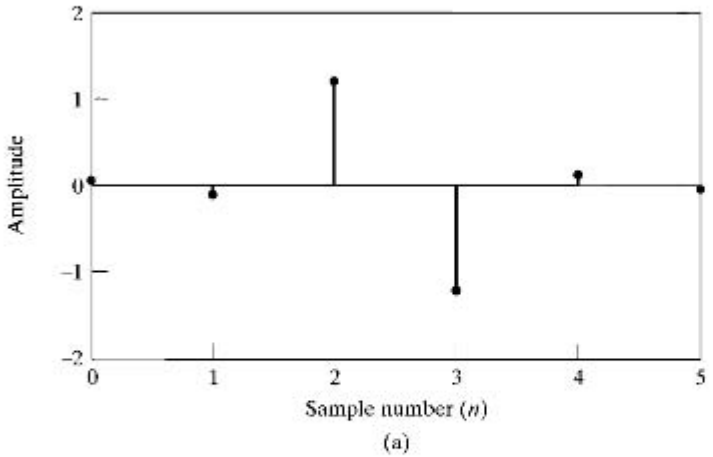

(a)

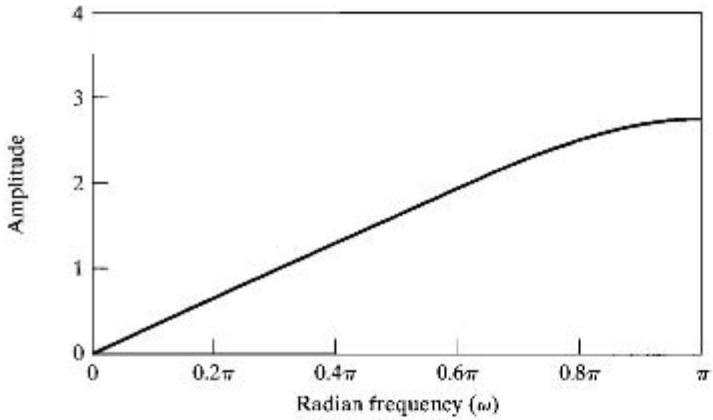

(b)

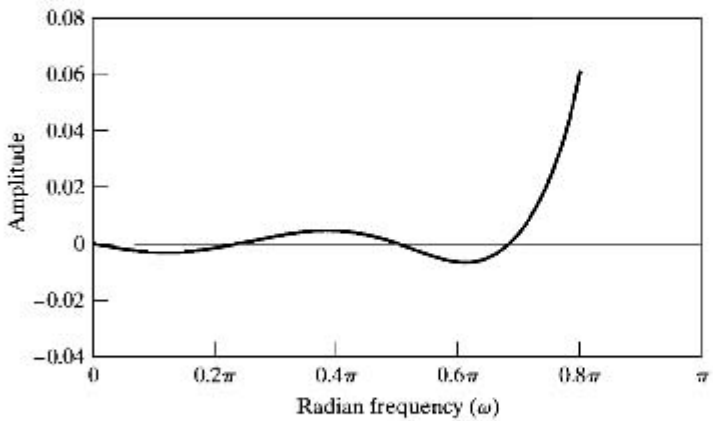

(c)

Figure 7.39 Response functions for type IV FIR discrete-time differentiator. (a) Impulse response ($M = 5$). (b) Magnitude. (c) Approximation error for $A_0(e^{j\omega})$.

7.7 OPTIMUM APPROXIMATIONS OF FIR FILTERS

The design of FIR filters by windowing is straightforward and is quite general, even though it has a number of limitations as discussed below. However, we often wish to design a filter that is the "best" that can be achieved for a given value of M. It is meaningless to discuss this question in the absence of an approximation criterion. For example, in the case of the window design method, it follows from the theory of Fourier series that the rectangular window provides the best mean-square approximation to a desired frequency response for a given value of M. That is,

$$h[n] = \begin{cases} h_d[n], & 0 \le n \le M, \\ 0, & \text{otherwise}, \end{cases} \tag{7.85}$$

minimizes the expression

$$\varepsilon^2 = \frac{1}{2\pi} \int_{-\pi}^{\pi} |H_d(e^{j\omega}) - H(e^{j\omega})|^2 d\omega. \tag{7.86}$$

(See Problem 7.25.) However, as we have seen, this approximation criterion leads to adverse behavior at discontinuities of $H_d(e^{j\omega})$. Furthermore, the window method does not permit individual control over the approximation errors in different bands. For many applications, better filters result from a minimax strategy (minimization of the maximum errors) or a frequency-weighted error criterion. Such designs can be achieved using algorithmic techniques.

As the previous examples show, frequency-selective filters designed by windowing often have the property that the error is greatest on either side of a discontinuity of the ideal frequency response, and the error becomes smaller for frequencies away from the discontinuity. Furthermore, as suggested by Figure 7.31, such filters typically result in approximately equal errors in the passband and stopband. (See Figures 7.34(c) and 7.35(c), for example.) We have already seen that, for IIR filters, if the approximation error is spread out uniformly in frequency and if the passband and stopband ripples are adjusted separately, a given design specification can be met with a lower-order filter than if the approximation just meets the specification at one frequency and far exceeds it at others. This intuitive notion is confirmed for FIR systems by a theorem to be discussed later in the section.

In the following discussion, we consider a particularly effective and widely used algorithmic procedure for the design of FIR filters with a generalized linear phase. Although we consider only type I filters in detail, we indicate where appropriate, how the results apply to types II, III, and IV generalized linear-phase filters.

In designing a causal type I linear-phase FIR filter, it is convenient first to consider the design of a zero-phase filter, i.e., one for which

$$h_e[n] = h_e[-n], \tag{7.87}$$

and then to insert a delay sufficient to make it causal. Consequently, we consider $h_e[n]$ satisfying the condition of Eq. (7.87). The corresponding frequency response is given by

$$A_e(e^{j\omega}) = \sum_{n=-L}^{L} h_e[n] e^{-j\omega n}, \tag{7.88}$$

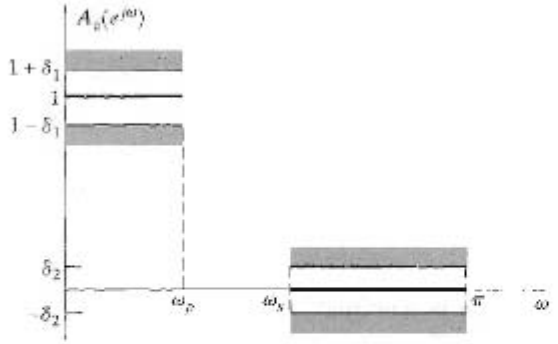

Figure 7.40 Tolerance scheme and ideal response for lowpass filter.

with $L = M/2$ an integer, or, because of Eq. (7.87),

$$A_e(e^{j\omega}) = h_e[0] + \sum_{n=1}^{L} 2h_e[n]\cos(\omega n). \tag{7.89}$$

Note that $A_e(e^{j\omega})$ is a real, even, and periodic function of ω. A causal system can be obtained from $h_e[n]$ by delaying it by $L = M/2$ samples. The resulting system has impulse response

$$h[n] = h_e[n - M/2] = h[M - n] \tag{7.90}$$

and frequency response

$$H(e^{j\omega}) = A_e(e^{j\omega})e^{-j\omega M/2}. \tag{7.91}$$

Figure 7.40 shows a tolerance scheme for an approximation to a lowpass filter with a real function such as $A_e(e^{j\omega})$. Unity is to be approximated in the band $0 \le |\omega| \le \omega_p$ with maximum absolute error δ_1, and zero is to be approximated in the band $\omega_s \le |\omega| \le \pi$ with maximum absolute error δ_2. An algorithmic technique for designing a filter to meet these specifications must, in effect, systematically vary the $(L + 1)$ unconstrained impulse response values $h_e[n]$, where $0 \le n \le L$. Design algorithms have been developed in which some of the parameters L, δ_1, δ_2, ω_p, and ω_s are fixed and an iterative procedure is used to obtain optimum adjustments of the remaining parameters. Two distinct approaches have been developed. Herrmann (1970), Herrmann and Schüssler (1970a), and Hofstetter, Oppenheim and Siegel (1971) developed procedures in which L, δ_1, and δ_2 are fixed, and ω_p and ω_s are variable. Parks and McClellan (1972a, 1972b), McClellan and Parks (1973), and Rabiner (1972a, 1972b) developed procedures in which L, ω_p, ω_s, and the ratio δ_1/δ_2 are fixed and δ_1 (or δ_2) is variable. Since the time when these different approaches were developed, the Parks–McClellan algorithm has become the dominant method for optimum design of FIR filters. This is because it is the most flexible and the most computationally efficient. Thus, we will discuss only that algorithm here.

The Parks–McClellan algorithm is based on reformulating the filter design problem as a problem in polynomial approximation. Specifically, the terms $\cos(\omega n)$ in Eq. (7.89) can be expressed as a sum of powers of $\cos\omega$ in the form

$$\cos(\omega n) = T_n(\cos\omega), \tag{7.92}$$

where $T_n(x)$ is an n^{th}-order polynomial.[5] Consequently, Eq. (7.89) can be rewritten as an L^{th}-order polynomial in $\cos\omega$, namely,

$$A_e(e^{j\omega}) = \sum_{k=0}^{L} a_k(\cos\omega)^k, \tag{7.93}$$

where the a_ks are constants that are related to $h_e[n]$, the values of the impulse response. With the substitution $x = \cos\omega$, we can express Eq. (7.93) as

$$A_e(e^{j\omega}) = P(x)|_{x=\cos\omega}, \tag{7.94}$$

where $P(x)$ is the L^{th}-order polynomial

$$P(x) = \sum_{k=0}^{L} a_k x^k. \tag{7.95}$$

We will see that it is not necessary to know the relationship between the a_ks and $h_e[n]$ (although a formula can be obtained); it is enough to know that $A_e(e^{j\omega})$ can be expressed as the L^{th}-order trigonometric polynomial of Eq. (7.93).

The key to gaining control over ω_p and ω_s is to fix them at their desired values and let δ_1 and δ_2 vary. Parks and McClellan (1972a, 1972b) showed that with L, ω_p, and ω_s fixed, the frequency-selective filter design problem becomes a problem in Chebyshev approximation over disjoint sets, an important problem in approximation theory and one for which several useful theorems and procedures have been developed. (See Cheney, 1982.) To formalize the approximation problem in this case, let us define an approximation error function

$$E(\omega) = W(\omega)[H_d(e^{j\omega}) - A_e(e^{j\omega})], \tag{7.96}$$

where the weighting function $W(\omega)$ incorporates the approximation error parameters into the design process. In this design method, the error function $E(\omega)$, the weighting function $W(\omega)$, and the desired frequency response $H_d(e^{j\omega})$ are defined only over closed subintervals of $0 \le \omega \le \pi$. For example, to approximate a lowpass filter, these functions are defined for $0 \le \omega \le \omega_p$ and $\omega_s \le \omega \le \pi$. The approximating function $A_e(e^{j\omega})$ is not constrained in the transition region(s) (e.g., $\omega_p < \omega < \omega_s$), and it may take any shape necessary to achieve the desired response in the other subintervals.

For example, suppose that we wish to obtain an approximation as in Figure 7.40, where L, ω_p, and ω_s are fixed design parameters. For this case,

$$H_d(e^{j\omega}) = \begin{cases} 1, & 0 \le \omega \le \omega_p, \\ 0, & \omega_s \le \omega \le \pi. \end{cases} \tag{7.97}$$

The weighting function $W(\omega)$ allows us to weight the approximation errors differently in the different approximation intervals. For the lowpass filter approximation problem, the weighting function is

$$W(\omega) = \begin{cases} \dfrac{1}{K}, & 0 \le \omega \le \omega_p, \\ 1, & \omega_s \le \omega \le \pi, \end{cases} \tag{7.98}$$

[5] More specifically, $T_n(x)$ is the n^{th}-order Chebyshev polynomial, defined as $T_n(x) = \cos(n\cos^{-1}x)$.

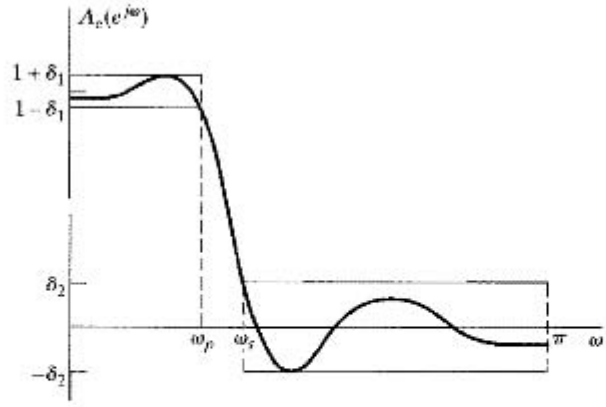

Figure 7.41 Typical frequency response meeting the specifications of Figure 7.40.

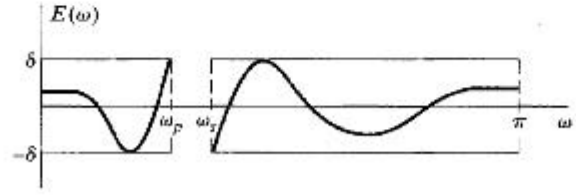

Figure 7.42 Weighted error for the approximation of Figure 7.41.

where $K = \delta_1/\delta_2$. If $A_e(e^{j\omega})$ is as shown in Figure 7.41, the weighted approximation error, $E(\omega)$ in Eq. (7.96), would be as indicated in Figure 7.42. Note that with this weighting, the maximum weighted absolute approximation error is $\delta = \delta_2$ in both bands.

The particular criterion used in this design procedure is the so-called minimax or Chebyshev criterion, where, within the frequency intervals of interest (the passband and stopband for a lowpass filter), we seek a frequency response $A_e(e^{j\omega})$ that *minimizes* the *maximum* weighted approximation error of Eq. (7.96). Stated more compactly, the best approximation is to be found in the sense of

$$\min_{\{h_e[n]:0\le n\le L\}} \left(\max_{\omega\in F} |E(\omega)| \right),$$

where F is the closed subset of $0 \le \omega \le \pi$ such that $0 \le \omega \le \omega_p$ or $\omega_s \le \omega \le \pi$. Thus, we seek the set of impulse response values that minimizes δ in Figure 7.42.

Parks and McClellan (1972a, 1972b) applied the following theorem of approximation theory to this filter design problem.

Alternation Theorem: Let F_P denote the closed subset consisting of the disjoint union of closed subsets of the real axis x. Furthermore,

$$P(x) = \sum_{k=0}^{r} a_k x^k$$

is an r^{th}-order polynomial, and $D_P(x)$ denotes a given desired function of x that is continuous on F_P; $W_P(x)$ is a positive function, continuous on F_P, and

$$E_P(x) = W_P(x)[D_P(x) - P(x)]$$

is the weighted error. The maximum error is defined as

$$\|E\| = \max_{x\in F_P} |E_P(x)|.$$

A necessary and sufficient condition that $P(x)$ be the unique r^{th}-order polynomial that minimizes $\|E\|$ is that $E_P(x)$ exhibit *at least* $(r+2)$ alternations; i.e., there must exist at least $(r+2)$ values x_i in F_p such that $x_1 < x_2 < \cdots < x_{r+2}$ and such that $E_P(x_i) = -E_P(x_{i+1}) = \pm\|E\|$ for $i = 1, 2, \ldots, (r+1)$.

At first glance, it may seem to be difficult to relate this formal theorem to the problem of filter design. However, in the discussion that follows, all of the elements of the theorem will be shown to be important in developing the design algorithm. To aid in understanding the alternation theorem, in Section 7.7.1 we will interpret it specifically for the design of a type I lowpass filter. Before proceeding to apply the alternation theorem to filter design, however, we illustrate in Example 7.8 how the theorem is applied to polynomials.

Example 7.8 Alternation Theorem and Polynomials

The alternation theorem provides a necessary and sufficient condition that a polynomial must satisfy in order that it be the polynomial that minimizes the maximum weighted error for a given order. To illustrate how the theorem is applied, suppose we want to examine polynomials $P(x)$ that approximate unity for $-1 \le x \le -0.1$ and zero for $0.1 \le x \le 1$. Consider three such polynomials, as shown in Figure 7.43. Each of these polynomials is of 5^{th}-order, and we would like to determine which, if any, satisfy the alternation theorem. The closed subsets of the real axis x referred to in the theorem are the regions $-1 \le x \le -0.1$ and $0.1 \le x \le 1$. We will weight errors equally in both regions, i.e., $W_p(x) = 1$. To begin, it will be useful for the reader to carefully construct sketches of the approximation error function for each polynomial in Figure 7.43.

According to the alternation theorem, the optimal 5^{th}-order polynomial must exhibit *at least* seven alternations of the error in the regions corresponding to the closed subset F_P. $P_1(x)$ has only five alternations—three in the region $-1 \le x \le -0.1$ and two in the region $0.1 \le x \le 1$. The points x at which the polynomial attains the maximum approximation error $\|E\|$ within the set F_P are called extremal points (or simply extremals). All alternations occur at extremals, but not all extremal points are alternations, as we will see. For example, the point with zero slope close to $x = 1$ that does not touch the dotted line is a local maximum, but is not an alternation, because the corresponding error function does not reach the negative extreme value.[6] The alternation theorem specifies that adjacent alternations must alternate sign, so the extremal value at $x = 1$ cannot be an alternation either, since the previous alternation was a positive extremal value at the first point with zero slope in $0.1 \le x \le 1$. The locations of the alterations are indicated by the symbol o on the polynomials in Figure 7.43.

$P_2(x)$ also has only five alternations and thus is not optimal. Specifically, $P_2(x)$ has three alternations in $-1 \le x \le -0.1$, but again, only two alternations in $0.1 \le x \le 1$. The difficulty occurs because $x = 0.1$ is not a negative extremal value. The previous alternation at $x = -0.1$ is a positive extremal value, so we need a negative extremal value for the next alternation. The first point with zero slope inside $0.1 \le x \le 1$ also cannot be counted, since it is a positive extremal value, like $x = -0.1$, and does not alternate sign. We can count the second point with zero slope in this region and $x = 1$, giving two alternations in $0.1 \le x \le 1$ and a total of five.

[6] In this discussion, we refer to positive and negative extremals of the error function. Since the polynomial is subtracted from a constant to form the error, the extremal points are easily located on the polynomial curves in Figure 7.43, but the sign is opposite of the variation above and below the desired constant values.

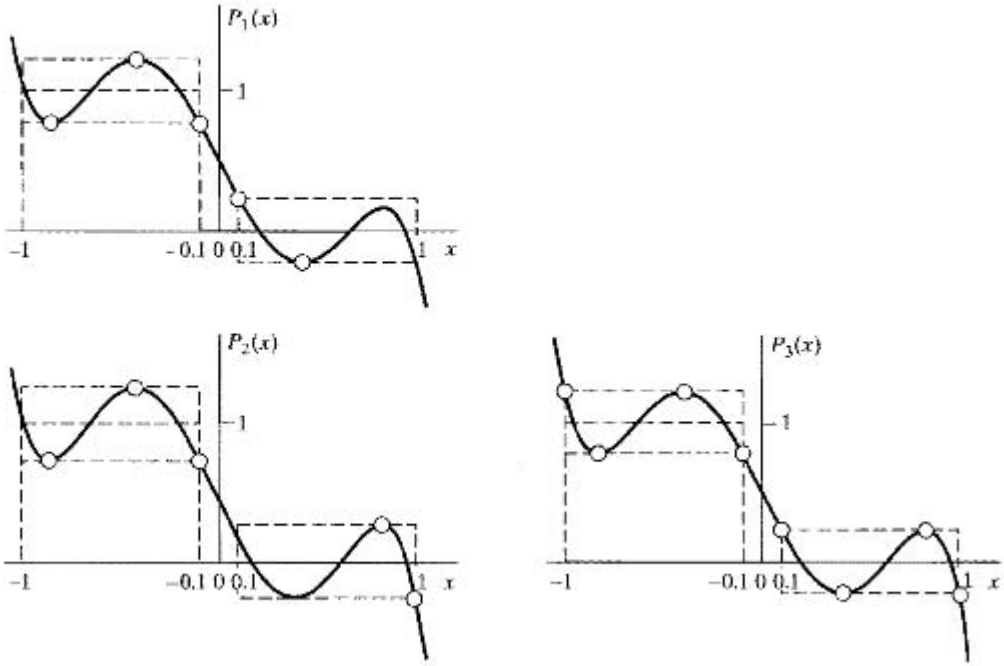

Figure 7.43 5th-order polynomials for Example 7.8. Alternation points are indicated by ○.

$P_3(x)$ has eight alternations; all points of zero slope, $x = -1$, $x = -0.1$, $x = 0.1$ and $x = 1$. Since eight alternations satisfies the alternation theorem, which specifies a minimum of seven, $P_3(x)$ is the unique optimal 5th-order polynomial approximation for this region.

7.7.1 Optimal Type I Lowpass Filters

For type I filters, the polynomial $P(x)$ is the cosine polynomial $A_e(e^{j\omega})$ in Eq. (7.93), with the transformation of variable $x = \cos\omega$ and $r = L$:

$$P(\cos\omega) = \sum_{k=0}^{L} a_k(\cos\omega)^k. \tag{7.99}$$

$D_P(x)$ is the desired lowpass filter frequency response in Eq. (7.97), with $x = \cos\omega$:

$$D_P(\cos\omega) = \begin{cases} 1, & \cos\omega_p \le \cos\omega \le 1, \\ 0, & -1 \le \cos\omega \le \cos\omega_s. \end{cases} \tag{7.100}$$

$W_P(\cos\omega)$ is given by Eq. (7.98), rephrased in terms of $\cos\omega$:

$$W_P(\cos\omega) = \begin{cases} \dfrac{1}{K}, & \cos\omega_p \le \cos\omega \le 1, \\ 1, & -1 \le \cos\omega \le \cos\omega_s. \end{cases} \tag{7.101}$$

And the weighted approximation error is

$$E_P(\cos\omega) = W_P(\cos\omega)[D_P(\cos\omega) - P(\cos\omega)]. \tag{7.102}$$

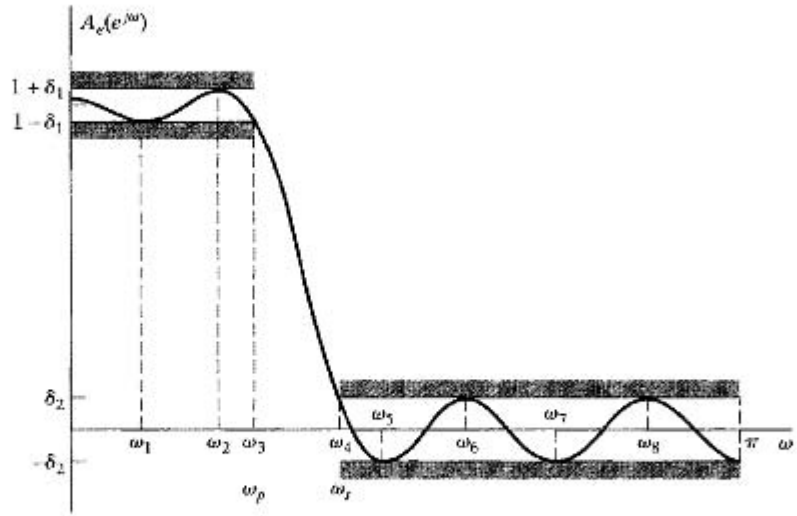

Figure 7.44 Typical example of a lowpass filter approximation that is optimal according to the alternation theorem for $L = 7$.

The closed subset F_P is made up of the union of the intervals $0 \leq \omega \leq \omega_p$ and $\omega_s \leq \omega \leq \pi$, or, in terms of $\cos\omega$, of the corresponding intervals $\cos\omega_p \leq \cos\omega \leq 1$ and $-1 \leq \cos\omega \leq \cos\omega_s$. The alternation theorem then states that a set of coefficients a_k in Eq. (7.99) will correspond to the filter representing the unique best approximation to the ideal lowpass filter, with the ratio δ_1/δ_2 fixed at K and with passband and stopband edges ω_p and ω_s, if and only if $E_P(\cos\omega)$ exhibits at least $(L+2)$ alternations on F_P, i.e., if and only if $E_P(\cos\omega)$ alternately equals plus and minus its maximum value at least $(L+2)$ times. We have previously seen such *equiripple approximations* in the case of elliptic IIR filters.

Figure 7.44 shows a filter frequency response that is optimal according to the alternation theorem for $L = 7$. In this figure, $A_e(e^{j\omega})$ is plotted against ω. To formally test the alternation theorem, we should first redraw $A_e(e^{j\omega})$ as a function of $x = \cos\omega$. Furthermore, we want to explicitly examine the alternations of $E_P(x)$. Consequently, in Figure 7.45(a), (b), and (c), we show $P(x)$, $W_P(x)$, and $E_P(x)$, respectively, as a function of $x = \cos\omega$. In this example, where $L = 7$, we see that there are nine alternations of the error. Consequently, the alternation theorem is satisfied. An important point is that, in counting alternations, we include the points $\cos\omega_p$ and $\cos\omega_s$, since, according to the alternation theorem, the subsets (or subintervals) included in F_P are closed, i.e., the endpoints of the intervals are counted. Although this might seem to be a small issue, it is in fact very significant, as we will see.

Comparing Figures 7.44 and 7.45 suggests that when the desired filter is a lowpass filter (or any piecewise-constant filter) we could easily count the alternations by direct examination of the frequency response, keeping in mind that the maximum error is different (in the ratio $K = \delta_1/\delta_2$) in the passband and stopband.

The alternation theorem states that the optimum filter must have a minimum of $(L+2)$ alternations, but it does not exclude the possibility of more than $(L+2)$ alternations. In fact, we will show that for a lowpass filter, the maximum possible number of alternations is $(L+3)$. First, however, we illustrate this in Figure 7.46 for $L = 7$.

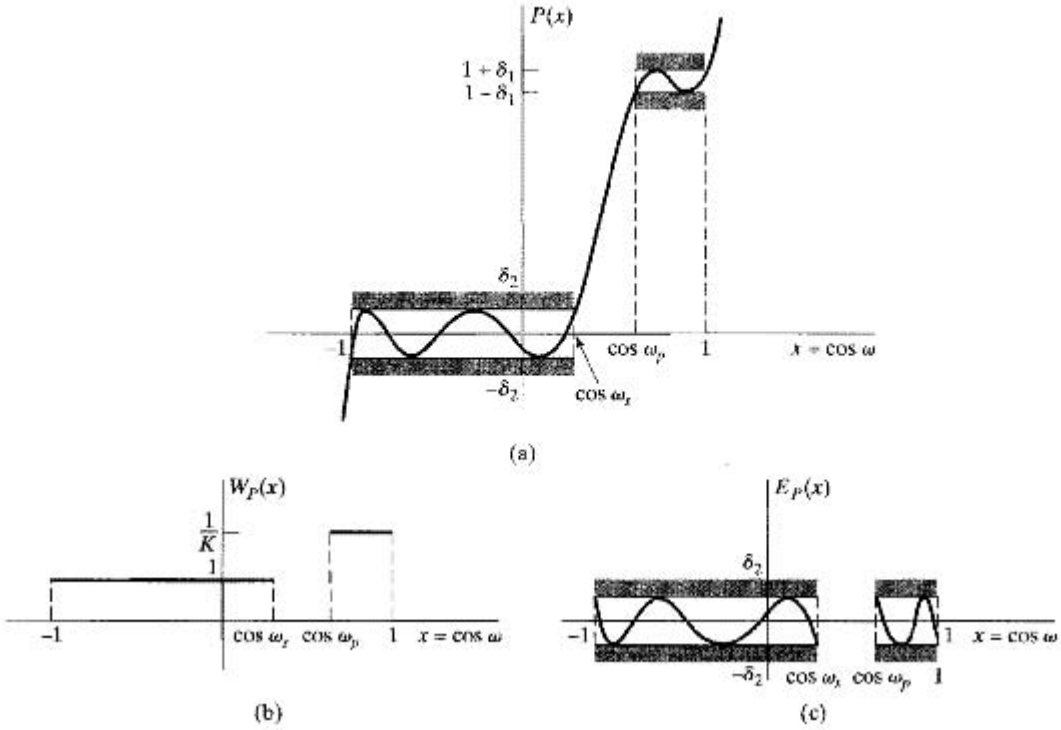

Figure 7.45 Equivalent polynomial approximation functions as a function of $x = \cos\omega$. (a) Approximating polynomial. (b) Weighting function. (c) Approximation error.

Figure 7.46(a) has $L + 3 = 10$ alternations, whereas Figures 7.46(b), (c), and (d) each have $L+2 = 9$ alternations. The case of $L+3$ alternations (Figure 7.46a) is often referred to as the *extraripple case*. Note that for the extraripple filter, there are alternations at $\omega = 0$ and π, as well as at $\omega = \omega_p$ and $\omega = \omega_s$, i.e., at all the band edges. For Figures 7.46(b) and (c), there are again alternations at ω_p and ω_s, but not at both $\omega = 0$ and $\omega = \pi$. In Figure 7.46(d), there are alternations at $0, \pi, \omega_p$, and ω_s, but there is one less point of zero slope inside the stopband. We also observe that all of these cases are equiripple inside the passband and stopband; i.e., all points of zero slope inside the interval $0 < \omega < \pi$ are frequencies at which the magnitude of the weighted error is maximal. Finally, because all of the filters in Figure 7.46 satisfy the alternation theorem for $L = 7$ and for the same value of $K = \delta_1/\delta_2$, it follows that ω_p and/or ω_s must be different for each, since the alternation theorem states that the optimum filter under the conditions of the theorem is unique.

The properties referred to in the preceding paragraph for the filters in Figure 7.46 result from the alternation theorem. Specifically, we will show that for type I lowpass filters:

- The maximum possible number of alternations of the error is $(L + 3)$.
- Alternations will always occur at ω_p and ω_s.
- All points with zero slope inside the passband and all points with zero slope inside the stopband (for $0 < \omega < \omega_p$ and $\omega_s < \omega < \pi$) will correspond to alternations; i.e., the filter will be equiripple, except possibly at $\omega = 0$ and $\omega = \pi$.

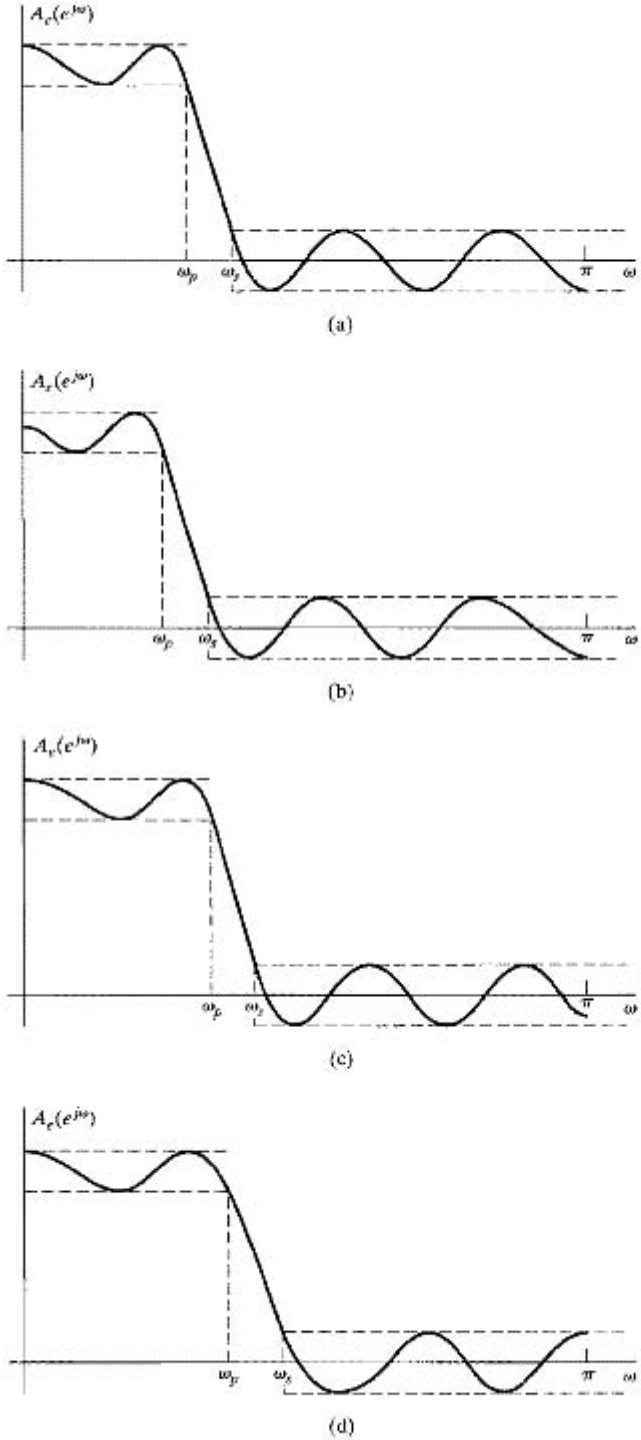

Figure 7.46 Possible optimum lowpass filter approximations for $L = 7$. (a) $L + 3$ alternations (extraripple case). (b) $L + 2$ alternations (extremum at $\omega = \pi$). (c) $L + 2$ alternations (extremum at $\omega = 0$). (d) $L + 2$ alternations (extremum at both $\omega = 0$ and $\omega = \pi$).

The maximum possible number of alternations is (L + 3)

Reference to Figure 7.44 or Figure 7.46 suggests that the maximum possible number of locations for alternations, are the four band edges ($\omega = 0, \pi, \omega_p, \omega_s$) and the frequencies at which $A_e(e^{j\omega})$ has zero slope. Since an L^{th}-order polynomial can have at most $(L-1)$ points with zero slope in an open interval, the maximum possible number of locations for alternations are the $(L-1)$ local maxima or minima of the polynomial plus the four band edges, a total of $(L+3)$. In considering points with zero slope for trigonometric polynomials, it is important to observe that the trigonometric polynomial

$$P(\cos\omega) = \sum_{k=0}^{L} a_k(\cos\omega)^k, \tag{7.103}$$

when considered as a function of ω, will always have zero slope at $\omega = 0$ and $\omega = \pi$, even though $P(x)$ considered as a function of x may not have zero slope at the corresponding points $x = 1$ and $x = -1$. This is because

$$\begin{aligned}\frac{dP(\cos\omega)}{d\omega} &= -\sin\omega\left(\sum_{k=0}^{L} k a_k(\cos\omega)^{k-1}\right)\\ &= -\sin\omega\left(\sum_{k=0}^{L-1}(k+1)a_{k+1}(\cos\omega)^k\right),\end{aligned} \tag{7.104}$$

which is always zero at $\omega = 0$ and $\omega = \pi$, as well as at the $(L-1)$ roots of the $(L-1)$st-order polynomial represented by the sum. This behavior at $\omega = 0$ and $\omega = \pi$ is evident in Figure 7.46. In Figure 7.46(d), it happens that the polynomial $P(x)$ also has zero slope at $x = -1 = \cos\pi$.

Alternations always occur at ω_p and ω_s

For all of the frequency responses in Figure 7.46, $A_e(e^{j\omega})$ is exactly equal to $1-\delta_1$ at the passband edge ω_p and exactly equal to $+\delta_2$ at the stopband edge ω_s. To suggest why this must always be the case, let us consider whether the filter in Figure 7.46(a) could also be optimal if we redefined ω_p as indicated in Figure 7.47 leaving the polynomial unchanged. The frequencies at which the magnitude of the maximum weighted error are equal are the frequencies $\omega = 0, \omega_1, \omega_2, \omega_s, \omega_3, \omega_4, \omega_5, \omega_6$, and $\omega = \pi$, for a total of $(L+2) = 9$. However, not all of the frequencies are alternations, since, to be counted in the alternation theorem, the error must *alternate* between $\delta = \pm\|E\|$ at these frequencies. Therefore, because the error is negative at both ω_2 and ω_s, the frequencies counted in the alternation theorem are $\omega = 0, \omega_1, \omega_2, \omega_3, \omega_4, \omega_5, \omega_6$, and π, for a total of 8. Since $(L+2) = 9$, the conditions of the alternation theorem are not

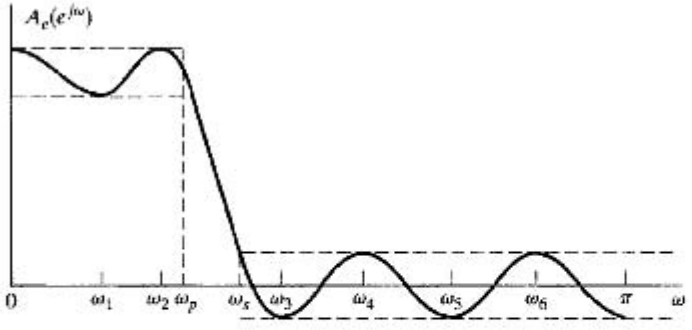

Figure 7.47 Illustration that the passband edge ω_p must be an alternation frequency.

satisfied, and the frequency response of Figure 7.47 is not optimal with ω_p and ω_s as indicated. In other words, the removal of ω_p as an alternation frequency removes two alternations. Since the maximum number is $(L + 3)$, this leaves at most $(L + 1)$, which is not a sufficient number. An identical argument would hold if ω_s were removed as an alternation frequency. A similar argument can be constructed for highpass filters, but this is not necessarily the case for bandpass or multiband filters. (See Problem 7.63.)

The filter will be equiripple except possibly at $\omega = 0$ or $\omega = \pi$

The argument here is very similar to the one used to show that both ω_p and ω_s must be alternations. Suppose, for example, that the filter in Figure 7.46(a) was modified as indicated in Figure 7.48, so that one point with zero slope did not achieve the maximum error. Although the maximum error occurs at nine frequencies, only eight of these can be counted as alternations. Consequently, eliminating one ripple as a point of maximum error reduces the number of alternations by two, leaving $(L+1)$ as the maximum possible number.

The foregoing represent only a few of many properties that can be inferred from the alternation theorem. A variety of others are discussed in Rabiner and Gold (1975). Furthermore, we have considered only type I lowpass filters. While a much broader and detailed discussion of type II, III, and IV filters or filters with more general desired frequency responses is beyond the scope of this book, we briefly consider type II lowpass filters to further emphasize a number of aspects of the alternation theorem.

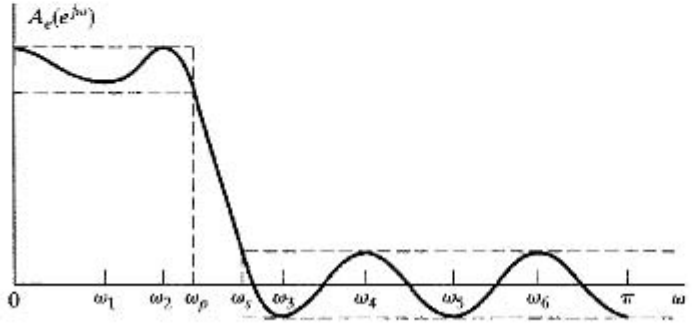

Figure 7.48 Illustration that the frequency response must be equiripple in the approximation bands.

7.7.2 Optimal Type II Lowpass Filters

A type II causal filter is a filter for which $h[n] = 0$ outside the range $0 \le n \le M$, with the filter length $(M + 1)$ even, i.e., M odd, and with the symmetry property

$$h[n] = h[M - n]. \tag{7.105}$$

Consequently, the frequency response $H(e^{j\omega})$ can be expressed in the form

$$H(e^{j\omega}) = e^{-j\omega M/2} \sum_{n=0}^{(M-1)/2} 2h[n] \cos\left[\omega\left(\frac{M}{2} - n\right)\right]. \tag{7.106}$$

Letting $b[n] = 2h[(M + 1)/2 - n]$, $n = 1, 2, \ldots, (M + 1)/2$, we can rewrite Eq. (7.106) as

$$H(e^{j\omega}) = e^{-j\omega M/2} \left\{ \sum_{n=1}^{(M+1)/2} b[n] \cos\left[\omega\left(n - \frac{1}{2}\right)\right] \right\}. \tag{7.107}$$

To apply the alternation theorem to the design of type II filters, we must be able to identify the problem as one of polynomial approximation. To accomplish this, we express the summation in Eq. (7.107) in the form

$$\sum_{n=1}^{(M+1)/2} b[n] \cos\left[\omega\left(n - \frac{1}{2}\right)\right] = \cos(\omega/2) \left[\sum_{n=0}^{(M-1)/2} \tilde{b}[n] \cos(\omega n) \right]. \tag{7.108}$$

(See Problem 7.58.) The summation on the right-hand side of Eq. (7.108) can now be represented as a trigonometric polynomial $P(\cos\omega)$ so that

$$H(e^{j\omega}) = e^{-j\omega M/2} \cos(\omega/2) P(\cos\omega), \tag{7.109a}$$

where

$$P(\cos\omega) = \sum_{k=0}^{L} a_k (\cos\omega)^k \tag{7.109b}$$

and $L = (M - 1)/2$. The coefficients a_k in Eq. (7.109b) are related to the coefficients $\tilde{b}[n]$ in Eq. (7.108), which in turn are related to the coefficients $b[n] = 2h[(M + 1)/2 - n]$ in Eq. (7.107). As in the type I case, it is not necessary to obtain an explicit relationship between the impulse response and the a_ks. We now can apply the alternation theorem to the weighted error between $P(\cos\omega)$ and the desired frequency response. For a type I lowpass filter with a specified ratio K of passband to stopband ripple, the desired function is given by Eq. (7.97), and the weighting function for the error is given by Eq. (7.98). For type II lowpass filters, because of the presence of the factor $\cos(\omega/2)$ in Eq. (7.109a), the function to be approximated by the polynomial $P(\cos\omega)$ is defined as

$$H_d(e^{j\omega}) = D_P(\cos\omega) = \begin{cases} \dfrac{1}{\cos(\omega/2)}, & 0 \le \omega \le \omega_p, \\ 0, & \omega_s \le \omega \le \pi, \end{cases} \tag{7.110}$$

and the weighting function to be applied to the error is

$$W(\omega) = W_P(\cos\omega) = \begin{cases} \dfrac{\cos(\omega/2)}{K}, & 0 \le \omega \le \omega_p, \\ \cos(\omega/2), & \omega_s \le \omega \le \pi. \end{cases} \tag{7.111}$$

Consequently, type II filter design is a different polynomial approximation problem than type I filter design.

In this section, we have only outlined the design of type II filters, principally to highlight the requirement that the design problem first be formulated as a polynomial approximation problem. A similar set of issues arises in the design of type III and type IV linear-phase FIR filters. Specifically, these classes also can be formulated as polynomial approximation problems, but in each class, the weighting function applied to the error has a trigonometric form, just as it does for type II filters. (See Problem 7.58.) A detailed discussion of the design and properties of these classes of filters can be found in Rabiner and Gold (1975).

The details of the formulation of the problem for type I and type II linear-phase systems have been illustrated for the case of the lowpass filter. However, the discussion of type II systems in particular should suggest that there is great flexibility in the choice of both the desired response function $H_d(e^{j\omega})$ and the weighting function $W(\omega)$. For example, the weighting function can be defined in terms of the desired function so as to yield equiripple percentage error approximation. This approach is valuable in designing type III and type IV differentiator systems.

7.7.3 The Parks–McClellan Algorithm

The alternation theorem gives necessary and sufficient conditions on the error for optimality in the Chebyshev or minimax sense. Although the theorem does not state explicitly how to find the optimum filter, the conditions that are presented serve as the basis for an efficient algorithm for finding it. While our discussion is phrased in terms of type I lowpass filters, the algorithm easily generalizes.

From the alternation theorem, we know that the optimum filter $A_e(e^{j\omega})$ will satisfy the set of equations

$$W(\omega_i)[H_d(e^{j\omega_i}) - A_e(e^{j\omega_i})] = (-1)^{i+1}\delta, \qquad i = 1, 2, \ldots, (L+2), \tag{7.112}$$

where δ is the optimum error and $A_e(e^{j\omega})$ is given by either Eq. (7.89) or Eq. (7.93). Using Eq. (7.93) for $A_e(e^{j\omega})$, we can write these equations as

$$\begin{bmatrix} 1 & x_1 & x_1^2 & \cdots & x_1^L & \dfrac{1}{W(\omega_1)} \\ 1 & x_2 & x_2^2 & \cdots & x_2^L & \dfrac{-1}{W(\omega_2)} \\ \vdots & \vdots & \vdots & & \vdots & \vdots \\ 1 & x_{L+2} & x_{L+2}^2 & \cdots & x_{L+2}^L & \dfrac{(-1)^{L+1}}{W(\omega_{L+2})} \end{bmatrix} \begin{bmatrix} a_0 \\ a_1 \\ \vdots \\ \delta \end{bmatrix} = \begin{bmatrix} H_d(e^{j\omega_1}) \\ H_d(e^{j\omega_2}) \\ \vdots \\ H_d(e^{j\omega_{L+2}}) \end{bmatrix}, \tag{7.113}$$

where $x_i = \cos\omega_i$. This set of equations serves as the basis for an iterative algorithm for finding the optimum $A_e(e^{j\omega})$. The procedure begins by guessing a set of alternation frequencies ω_i for $i = 1, 2, \ldots, (L+2)$. Note that ω_p and ω_s are fixed and, based on our discussion in Section 7.7.1, are necessarily members of the set of alternation frequencies. Specifically, if $\omega_\ell = \omega_p$, then $\omega_{\ell+1} = \omega_s$. The set of Eqs. (7.113) could be solved for the set of coefficients a_k and δ. However, a more efficient alternative is to use polynomial

interpolation. In particular, Parks and McClellan (1972a, 1972b) found that, for the given set of the extremal frequencies,

$$\delta = \frac{\sum_{k=1}^{L+2} b_k H_d(e^{j\omega_k})}{\sum_{k=1}^{L+2} \frac{b_k(-1)^{k+1}}{W(\omega_k)}}, \tag{7.114}$$

where

$$b_k = \prod_{\substack{i=1 \\ i \neq k}}^{L+2} \frac{1}{(x_k - x_i)} \tag{7.115}$$

and, as before, $x_i = \cos \omega_i$. That is, if $A_e(e^{j\omega})$ is determined by the set of coefficients a_k that satisfy Eq. (7.113), with δ given by Eq. (7.114), then the error function goes through $\pm\delta$ at the $(L+2)$ frequencies ω_i, or, equivalently, $A_e(e^{j\omega})$ has values $1 \pm K\delta$ if $0 \leq \omega_i \leq \omega_p$ and $\pm\delta$ if $\omega_s \leq \omega_i \leq \pi$. Now, since $A_e(e^{j\omega})$ is known to be an L^{th}-order trigonometric polynomial, we can interpolate a trigonometric polynomial through $(L+1)$ of the $(L+2)$ known values $E(\omega_i)$ (or equivalently, $A_e(e^{j\omega_i})$). Parks and McClellan used the Lagrange interpolation formula to obtain

$$A_e(e^{j\omega}) = P(\cos\omega) = \frac{\sum_{k=1}^{L+1} [d_k/(x - x_k)]C_k}{\sum_{k=1}^{L+1} [d_k/(x - x_k)]}, \tag{7.116a}$$

where $x = \cos\omega$, $x_i = \cos\omega_i$,

$$C_k = H_d(e^{j\omega_k}) - \frac{(-1)^{k+1}\delta}{W(\omega_k)}, \tag{7.116b}$$

and

$$d_k = \prod_{\substack{i=1 \\ i \neq k}}^{L+1} \frac{1}{(x_k - x_i)} = b_k(x_k - x_{L+2}). \tag{7.116c}$$

Although only the frequencies $\omega_1, \omega_2, \ldots, \omega_{L+1}$ are used in fitting the L^{th}-order polynomial, we can be assured that the polynomial also takes on the correct value at ω_{L+2} because Eqs. (7.113) are satisfied by the resulting $A_e(e^{j\omega})$.

Now $A_e(e^{j\omega})$ is available at any desired frequency, without the need to solve the set of equations (7.113) for the coefficients a_k. The polynomial of Eq. (7.116a) can be used to evaluate $A_e(e^{j\omega})$ and also $E(\omega)$ on a dense set of frequencies in the passband and stopband. If $|E(\omega)| \leq \delta$ for all ω in the passband and stopband, then the optimum approximation has been found. Otherwise, we must find a new set of extremal frequencies.

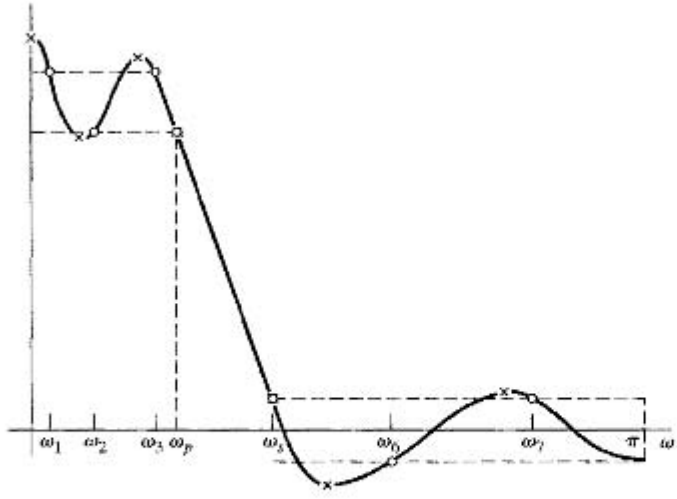

Figure 7.49 Illustration of the Parks–McClellan algorithm for equiripple approximation.

Figure 7.49 shows a typical example for a type I lowpass filter before the optimum has been found. Clearly, the set of frequencies ω_i used to find δ (as represented by open circles in the figure) was such that δ was too small. Adopting the philosophy of the Remez exchange method (see Cheney, 2000), the extremal frequencies are exchanged for a completely new set defined by the $(L + 2)$ largest peaks of the error curve. The points marked with $\times$ would be the new set of frequencies for the example shown in the figure. As before, ω_p and ω_s must be selected as extremal frequencies. Recall that there are at most $(L - 1)$ local minima and maxima in the open intervals $0 < \omega < \omega_p$ and $\omega_s < \omega < \pi$. The remaining extremal frequency can be at either $\omega = 0$ or $\omega = \pi$. If there is a maximum of the error function at both 0 and π, then the frequency at which the greatest error occurs is taken as the new estimate of the frequency of the remaining extremum. The cycle—computing the value of δ, fitting a polynomial to the assumed error peaks, and then locating the actual error peaks—is repeated until δ does not change from its previous value by more than a prescribed small amount. This value of δ is then the desired minimum maximum weighted approximation error.

A flowchart for the Parks–McClellan algorithm is shown in Figure 7.50. In this algorithm, all the impulse response values $h_e[n]$ are implicitly varied on each iteration to obtain the desired optimal approximation, but the values of $h_e[n]$ are never explicitly computed. After the algorithm has converged, the impulse response can be computed from samples of the polynomial representation using the discrete Fourier transform, as will be discussed in Chapter 8.

7.7.4 Characteristics of Optimum FIR Filters

Optimum lowpass FIR filters have the smallest maximum weighted approximation error δ for prescribed passband and stopband edge frequencies ω_p and ω_s. For the weighting function of Eq. (7.98), the resulting maximum stopband approximation error is $\delta_2 = \delta$, and the maximum passband approximation error is $\delta_1 = K\delta$. In Figure 7.51, we illustrate how δ varies with the order of the filter and the passband cutoff frequency. For this

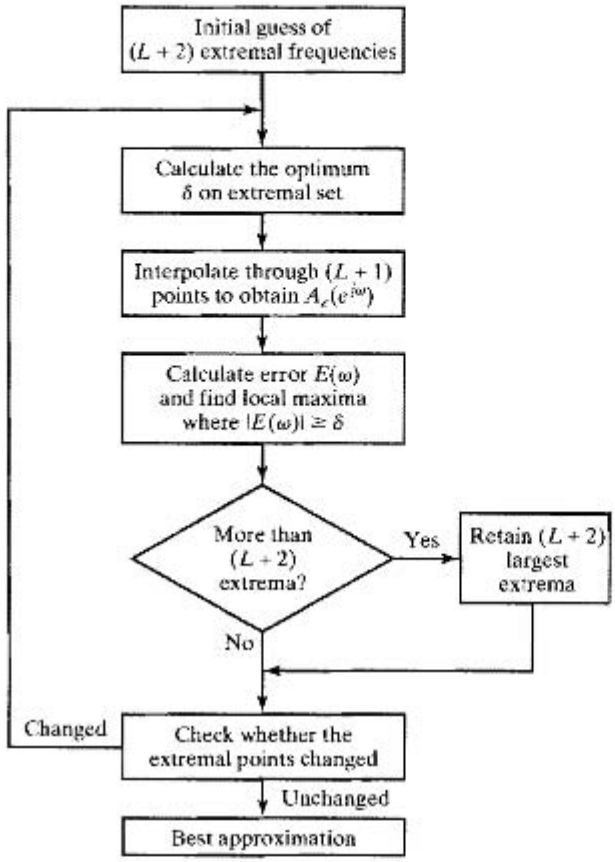

Figure 7.50 Flowchart of Parks–McClellan algorithm.

example, $K = 1$ and the transition width is fixed at $(\omega_s - \omega_p) = 0.2\pi$. The curves show that as ω_p increases, the error δ attains local minima. These minima on the curves correspond to the extraripple ($L + 3$ extrema) filters. All points between the minima correspond to filters that are optimal according to the alternation theorem. The filters for $M = 8$ and $M = 10$ are type I filters, while $M = 9$ and $M = 11$ correspond to a type II filter. It is interesting to note that, for some choices of parameters, a shorter filter ($M = 9$) may be better (i.e., it yields a smaller error) than a longer filter ($M = 10$). This may at first seem surprising and even contradictory. However, the cases $M = 9$ and $M = 10$ represent fundamentally different types of filters. Interpreted another way, filters for $M = 9$ cannot be considered to be special cases of $M = 10$ with one point set to zero, since this would violate the linear-phase symmetry requirement. On the other hand, $M = 8$ could always be thought of as a special case of $M = 10$ with the first and last samples set to zero. For that reason, an optimal filter for $M = 8$ cannot be better than one for $M = 10$. This restriction can be seen in Figure 7.51, where the curve for $M = 8$ is always above or equal to the one for $M = 10$. The points at which the two curves touch correspond to identical impulse responses, with the $M = 10$ filter having the first and last points equal to zero.

Herrmann et al. (1973) did an extensive computational study of the relationships

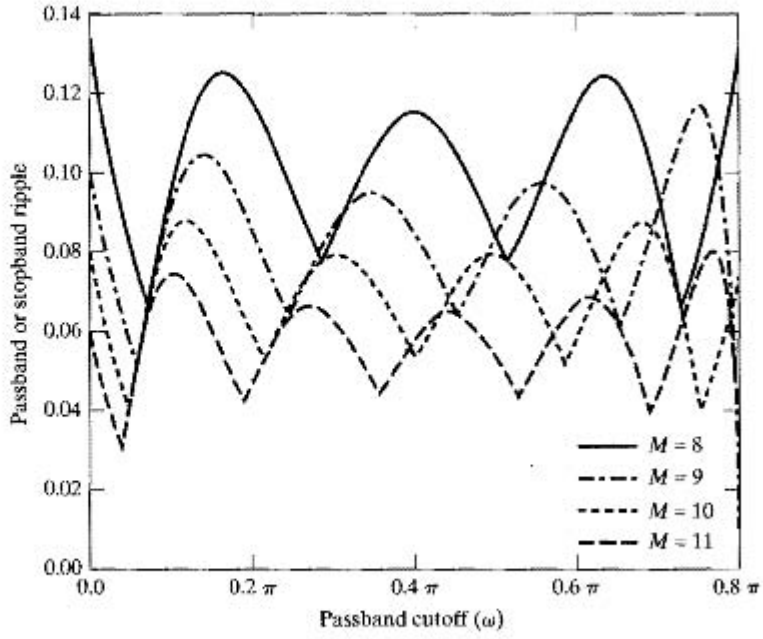

Figure 7.51 Illustration of the dependence of passband and stopband error on cutoff frequency for optimal approximations of a lowpass filter. For this example, $K = 1$ and $(\omega_S - \omega_P) = 0.2\pi$. (After Herrmann, Rabiner and Chan, 1973.)

among the parameters $M, \delta_1, \delta_2, \omega_p$, and ω_s for equiripple lowpass approximations, and Kaiser (1974) subsequently obtained the simplified formula

$$M = \frac{-10\log_{10}(\delta_1\delta_2) - 13}{2.324\Delta\omega}, \tag{7.117}$$

where $\Delta\omega = \omega_s - \omega_p$, as a fit to their data. By comparing Eq. (7.117) with the design formula of Eq. (7.76) for the Kaiser window method, we can see that, for the comparable case ($\delta_1 = \delta_2 = \delta$), the optimal approximations provide about 5 dB better approximation error for a given value of M. Another important advantage of the equiripple filters is that δ_1 and δ_2 need not be equal, as must be the case for the window method.

7.8 EXAMPLES OF FIR EQUIRIPPLE APPROXIMATION

The Parks–McClellan algorithm for optimum equiripple approximation of FIR filters can be used to design a wide variety of such filters. In this section, we give several examples that illustrate some of the properties of the optimum approximation and suggest the great flexibility that is afforded by the design method.

7.8.1 Lowpass Filter

For the lowpass filter case, we again approximate the set of specifications used in Example 7.5 and Section 7.6.1 so that we can compare all the major design methods on the

same lowpass filter specifications. These specifications call for $\omega_p = 0.4\pi$, $\omega_s = 0.6\pi$, $\delta_1 = 0.01$, and $\delta_2 = 0.001$. In contrast to the window method, the Parks–McClellan algorithm can accommodate the different approximation error in the passband versus that in the stopband by fixing the weighting function parameter at $K = \delta_1/\delta_2 = 10$.

Substituting the foregoing specifications into Eq. (7.117) and rounding up yields the estimate $M = 26$ for the value of M that is necessary to achieve the specifications. Figures 7.52(a), (b), and (c) show the impulse response, log magnitude, and approximation error, respectively, for the optimum filter with $M = 26$, $\omega_p = 0.4\pi$, and $\omega_s = 0.6\pi$. Figure 7.52(c) shows the *unweighted* approximation error

$$E_A(\omega) = \frac{E(\omega)}{W(\omega)} = \begin{cases} 1 - A_e(e^{j\omega}), & 0 \le \omega \le \omega_p, \\ 0 - A_e(e^{j\omega}), & \omega_s \le \omega \le \pi, \end{cases} \tag{7.118}$$

rather than the weighted error used in the formulation of the design algorithm. The weighted error would be identical to Figure 7.52(c), except that the error would be divided by 10 in the passband.[7] The alternations of the approximation error are clearly in evidence in Figure 7.52(c). There are seven alternations in the passband and eight in the stopband, for a total of fifteen alternations. Since $L = M/2$ for type I (M even) systems, and $M = 26$, the minimum number of alternations is $(L + 2) = (26/2 + 2) = 15$. Thus, the filter of Figure 7.52 is the optimum filter for $M = 26$, $\omega_p = 0.4\pi$, and $\omega_s = 0.6\pi$. However, Figure 7.52(c) shows that the filter fails to meet the original specifications on passband and stopband error. (The maximum errors in the passband and stopband are 0.0116 and 0.00116, respectively.) To meet or exceed the specifications, we must increase M.

The filter response functions for the case $M = 27$ are shown in Figure 7.53. Now the passband and stopband approximation errors are slightly less than the specified values. (The maximum errors in the passband and stopband are 0.0092 and 0.00092, respectively.) In this case, there are again seven alternations in the passband and eight alternations in the stopband, for a total of fifteen. Note that, since $M = 27$, this is a type II system, and for type II systems, the order of the implicit approximating polynomial is $L = (M - 1)/2 = (27 - 1)/2 = 13$. Thus, the minimum number of alternations is still 15. Note also that in the type II case, the system is constrained to have a zero of its system function at $z = -1$ or $\omega = \pi$. This is clearly shown in Figures 7.53(b) and (c).

If we compare the results of this example with the results of Section 7.6.1, we find that the Kaiser window method requires a value $M = 40$ to meet or exceed the specifications, whereas the Parks–McClellan method requires $M = 27$. This disparity is accentuated because the window method produces approximately equal maximum errors in the passband and stopband, while the Parks–McClellan method can weight the errors differently.

7.8.2 Compensation for Zero-Order Hold

In many cases, a discrete-time filter is designed to be used in a system such as that depicted in Figure 7.54; i.e., the filter is used to process a sequence of samples $x[n]$ to obtain

[7] For frequency-selective filters, the unweighted approximation error also conveniently displays the passband and stopband behavior, since $A_e(e^{j\omega}) = 1 - E(\omega)$ in the passband and $A_e(e^{j\omega}) = -E(\omega)$ in the stopband.

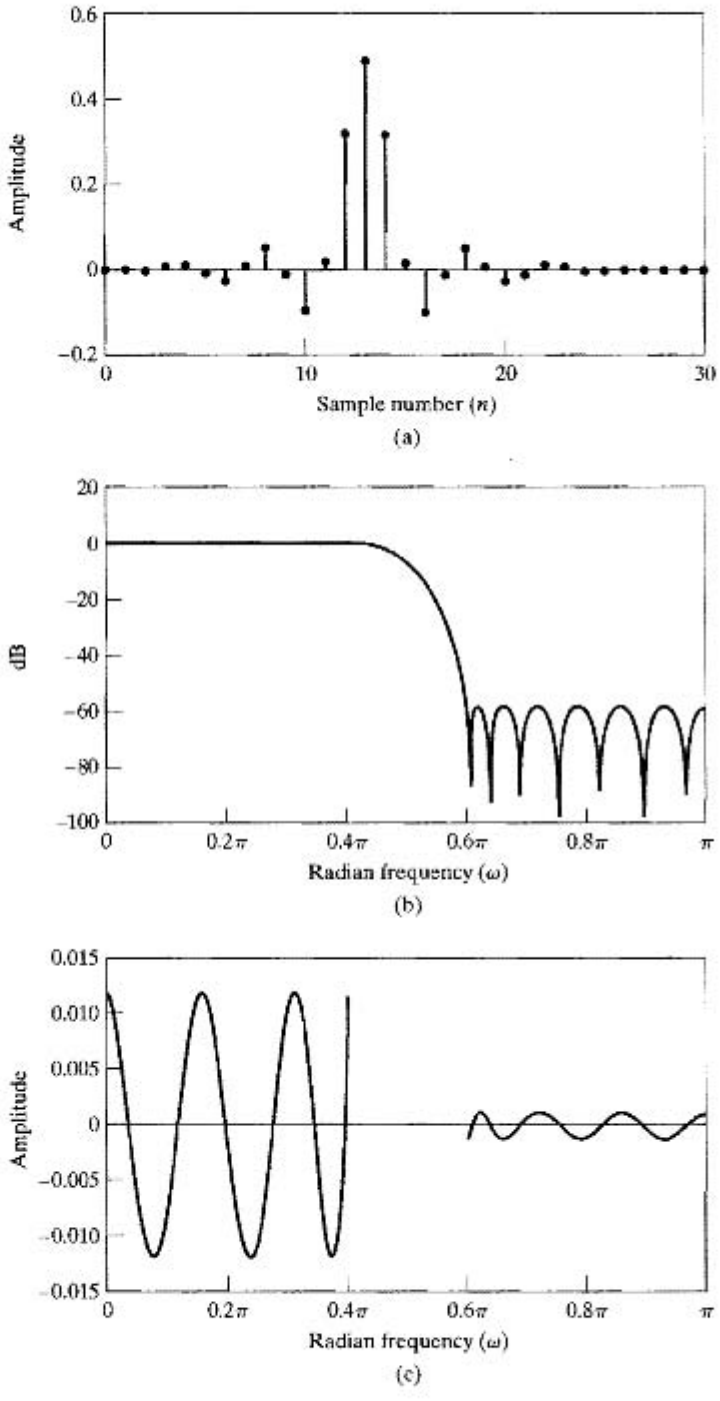

Figure 7.52 Optimum type I FIR lowpass filter for $\omega_p = 0.4\pi$, $\omega_S = 0.6\pi$, $K = 10$, and $M = 26$. (a) Impulse response. (b) Log magnitude of the frequency response. (c) Approximation error (unweighted).

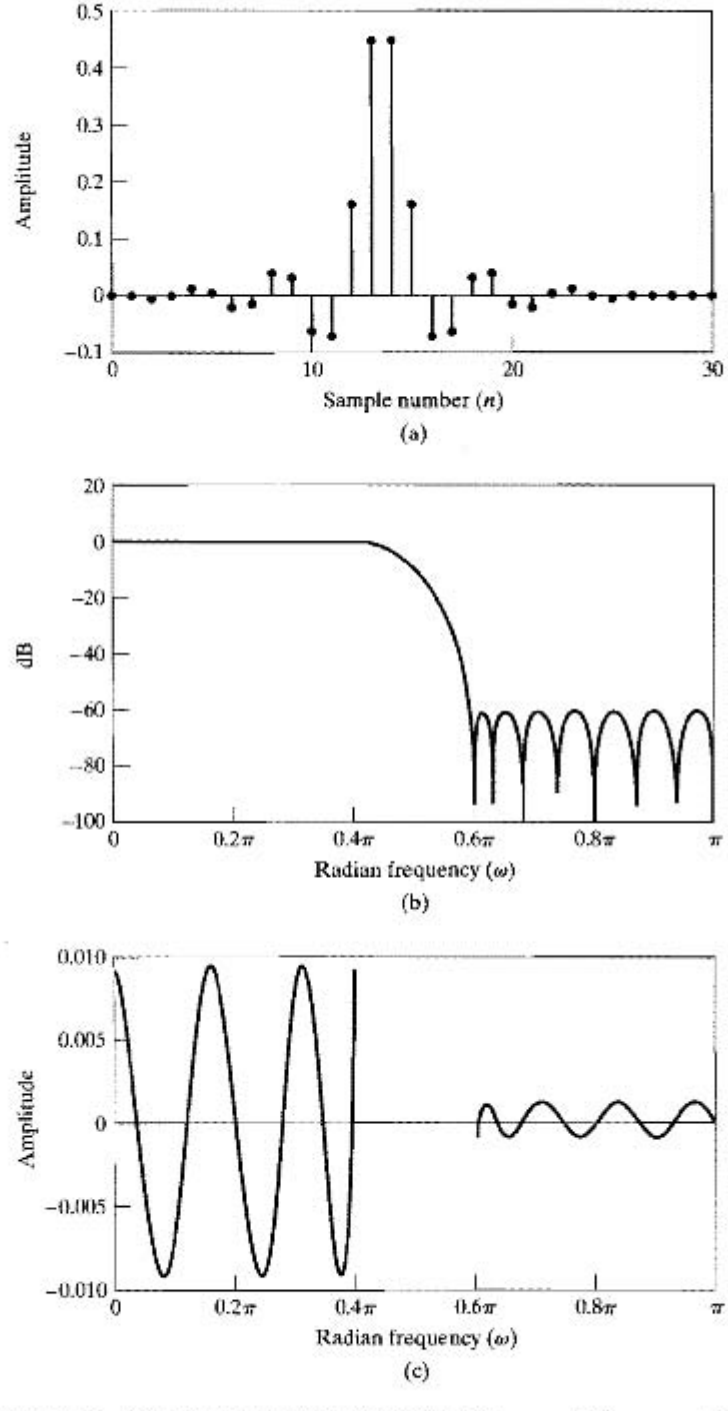

Figure 7.53 Optimum type II FIR lowpass filter for $\omega_p = 0.4\pi$, $\omega_s = 0.6\pi$, $K = 10$, and $M = 27$. (a) Impulse response. (b) Log magnitude of frequency response. (c) Approximation error (unweighted).

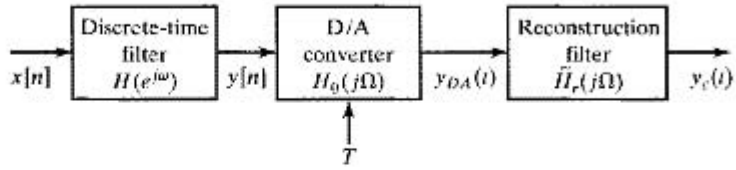

Figure 7.54 Precompensation of a discrete-time filter for the effects of a D/A converter.

a sequence $y[n]$, which is then the input to a D/A converter and continuous-time lowpass filter (as an approximation to the ideal D/C converter) used for the reconstruction of a continuous-time signal $y_c(t)$. Such a system arises as part of a system for discrete-time filtering of a continuous-time signal, as discussed in Section 4.8. If the D/A converter holds its output constant for the entire sampling period T, the Fourier transform of the output $y_c(t)$ is

$$Y_c(j\Omega) = \tilde{H}_r(j\Omega)H_o(j\Omega)H(e^{j\Omega T})X(e^{j\Omega T}), \tag{7.119}$$

where $\tilde{H}_r(j\Omega)$ is the frequency response of an appropriate lowpass reconstruction filter and

$$H_o(j\Omega) = \frac{\sin(\Omega T/2)}{\Omega/2}e^{-j\Omega T/2} \tag{7.120}$$

is the frequency response of the zero-order hold of the D/A converter. In Section 4.8.4, we suggested that compensation for $H_o(j\Omega)$ could be incorporated into the continuous-time reconstruction filter; i.e., $\tilde{H}_r(j\Omega)$ could be chosen as

$$\tilde{H}_r(j\Omega) = \begin{cases} \dfrac{\Omega T/2}{\sin(\Omega T/2)} & |\Omega| < \dfrac{\pi}{T} \\ 0 & \text{otherwise} \end{cases} \tag{7.121}$$

so that the effect of the discrete-time filter $H(e^{j\Omega T})$ would be undistorted by the zero-order hold. Another approach is to build the compensation into the discrete-time filter by designing a filter $\tilde{H}(e^{j\Omega T})$ such that

$$\tilde{H}(e^{j\Omega T}) = \frac{\Omega T/2}{\sin(\Omega T/2)}H(e^{j\Omega T}). \tag{7.122}$$

A D/A-compensated lowpass filter can be readily designed by the Parks–McClellan algorithm if we simply define the desired response as

$$\tilde{H}_d(e^{j\omega}) = \begin{cases} \dfrac{\omega/2}{\sin(\omega/2)}, & 0 \le \omega \le \omega_p, \\ 0, & \omega_s \le \omega \le \pi. \end{cases} \tag{7.123}$$

Figure 7.55 shows the response functions for such a filter, wherein the specifications are again $\omega_p = 0.4\pi$, $\omega_s = 0.6\pi$, $\delta_1 = 0.01$, and $\delta_2 = 0.001$. In this case, the specifications are met with $M = 28$ rather than $M = 27$ as in the previous constant-gain case. Thus, for essentially no penalty, we have incorporated compensation for the D/A converter into the discrete-time filter so that the effective passband of the filter will be flat. (To emphasize the sloping nature of the passband, Figure 7.55(c) shows the magnitude response in the passband, rather than the approximation error, as in the frequency response plots for the other FIR examples.)

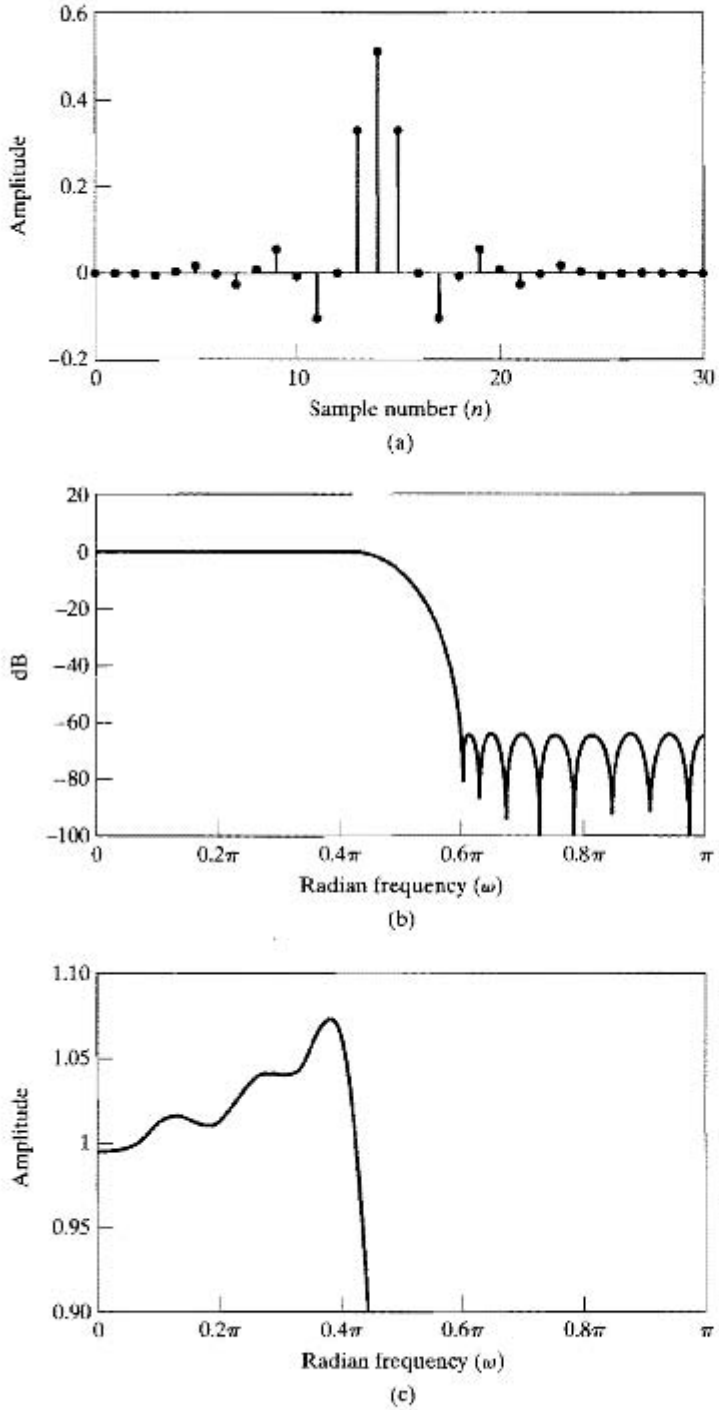

Figure 7.55 Optimum D/A-compensated lowpass filter for $\omega_p = 0.4\pi$, $\omega_S = 0.6\pi$, $K = 10$, and $M = 28$. (a) Impulse response. (b) Log magnitude of the frequency response. (c) Magnitude response in passband.

7.8.3 Bandpass Filter

Section 7.7 focused entirely on the lowpass optimal FIR, for which there are only two approximation bands. However, bandpass and bandstop filters require three approximation bands. To design such filters, it is necessary to generalize the discussion of Section 7.7 to the multiband case. This requires that we explore the implications of the alternation theorem and the properties of the approximating polynomial in the more general context. First, recall that, as stated, the alternation theorem does not assume any limit on the number of disjoint approximation intervals. Therefore, the *minimum* number of alternations for the optimum approximation is still $(L+2)$. However, multiband filters can have more than $(L+3)$ alternations, because there are more band edges. (Problem 7.63 explores this issue.) This means that some of the statements proved in Section 7.7.1 are not true in the multiband case. For example, it is *not* necessary for all the local maxima or minima of $A_e(e^{j\omega})$ to lie inside the approximation intervals. Thus, local extrema can occur in the transition regions, and the approximation need not be equiripple in the approximation regions.

To illustrate this, consider the desired response

$$H_d(e^{j\omega}) = \begin{cases} 0, & 0 \le \omega \le 0.3\pi, \\ 1, & 0.35\pi \le \omega \le 0.6\pi, \\ 0, & 0.7\pi \le \omega \le \pi, \end{cases} \tag{7.124}$$

and the error weighting function

$$W(\omega) = \begin{cases} 1, & 0 \le \omega \le 0.3\pi, \\ 1, & 0.35\pi \le \omega \le 0.6\pi, \\ 0.2, & 0.7\pi \le \omega \le \pi. \end{cases} \tag{7.125}$$

A value of $M+1 = 75$ was chosen for the length of the impulse response of the filter. Figure 7.56 shows the response functions for the resulting filter. Note that the transition region from the second approximation band to the third is no longer monotonic. However, the use of two local extrema in this unconstrained region does not violate the alternation theorem. Since $M = 74$, the filter is a type I system, and the order of the implicit approximating polynomial is $L = M/2 = 74/2 = 37$. Thus, the alternation theorem requires at least $L+2 = 39$ alternations. It can be readily seen in Figure 7.56(c), which shows the unweighted approximation error, that there are 13 alternations in each band, for a total of 39.

Such approximations as shown in Figure 7.56 are optimal in the sense of the alternation theorem, but they would probably be unacceptable in a filtering application. In general, there is no guarantee that the transition regions of a multiband filter will be monotonic, because the Parks–McClellan algorithm leaves these regions completely unconstrained. When this kind of response results for a particular choice of the filter parameters, acceptable transition regions can usually be obtained by systematically changing one or more of the band edge frequencies, the impulse-response length, or the error-weighting function and redesigning the filter.

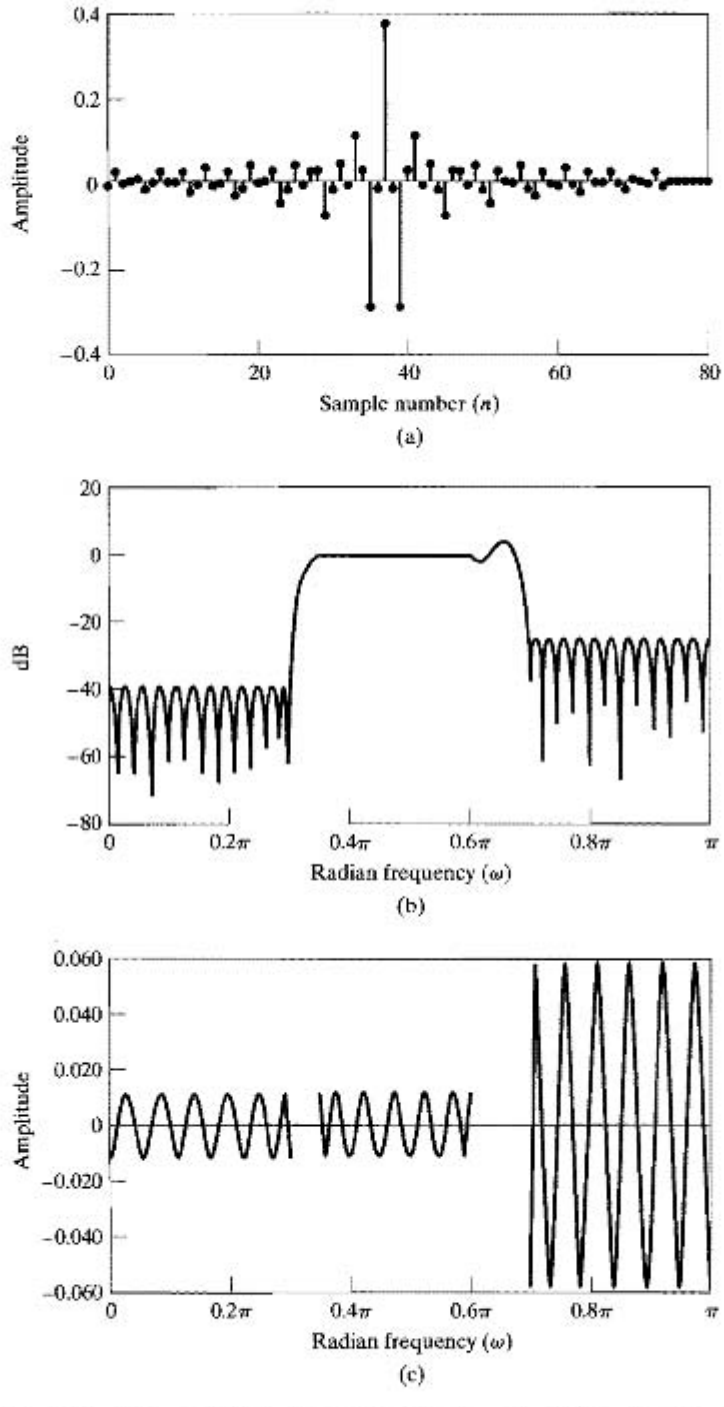

Figure 7.56 Optimum FIR bandpass filter for $M = 74$. (a) Impulse response. (b) Log magnitude of the frequency response. (c) Approximation error (unweighted).

7.9 COMMENTS ON IIR AND FIR DISCRETE-TIME FILTERS

This chapter has been concerned with design methods for LTI discrete-time systems. We have discussed a wide range of methods of designing both infinite-duration and finite-duration impulse-response filters.

The choice between an FIR filter and an IIR filter depends on the importance to the design problem of the advantages of each type. IIR filters, for example, have the advantage that a variety of frequency-selective filters can be designed using closed-form design formulas. That is, once the problem has been specified in terms appropriate for a given approximation method (e.g., Butterworth, Chebyshev, or elliptic), then the order of the filter that will meet the specifications can be computed, and the coefficients (or poles and zeros) of the discrete-time filter can be obtained by straightforward substitution into a set of design equations. This kind of simplicity of the design procedure makes it feasible to design IIR filters by manual computation if necessary, and it leads to straightforward noniterative computer programs for IIR filter design. These methods are limited to frequency-selective filters, and they permit only the magnitude response to be specified. If other magnitude shapes are desired, or if it is necessary to approximate a prescribed phase- or group-delay response, an algorithmic procedure will be required.

In contrast, FIR filters can have a precisely (generalized) linear phase. However, closed-form design equations do not exist for FIR filters. Although the window method is straightforward to apply, some iteration may be necessary to meet a prescribed specification. The Parks–McClellan algorithm leads to lower-order filters than the window method and filter design programs are readily available for both methods. Also, the window method and most of the algorithmic methods afford the possibility of approximating rather arbitrary frequency-response characteristics with little more difficulty than is encountered in the design of lowpass filters. In addition, the design problem for FIR filters is much more under control than the IIR design problem, because of the existence of an optimality theorem for FIR filters that is meaningful in a wide range of practical situations. Design techniques for FIR filters without linear phase have been given by Chen and Parks (1987), Parks and Burrus (1987), Schüssler and Steffen (1988), and Karam and McClellan (1995).

Questions of economics also arise in implementing a discrete-time filter. Economic concerns are usually measured in terms of hardware complexity, chip area, or computational speed. These factors are more or less directly related to the order of the filter required to meet a given specification. In applications where the efficiencies of polyphase implementations cannot be exploited, it is generally true that a given magnitude-response specification can be met most efficiently with an IIR filter. However, in many cases, the linear phase available with an FIR filter may be well worth the extra cost.

In any specific practical setting, the choice of class of filters and design method will be highly dependent on the context, constraints, specifications, and implementation platform. In this section, we conclude the chapter with one specific example to illustrate some of the trade offs and issues that can arise. However, it is only one of many scenarios, each of which can result in different choices and conclusions.

7.10 DESIGN OF AN UPSAMPLING FILTER

We conclude this chapter with a comparison, in the context of upsampling, of IIR and FIR filter designs. As discussed in Chapter 4, Sections 4.6.2 and 4.9.3, integer upsampling and oversampled D/A conversion employ an expander-by-L followed by a discrete-time lowpass filter. Because the sampling rate at the output of the expander is L times the rate at the input, the lowpass filter operates at a rate which is L-times the rate of the input to the upsampler or D/A converter. As we illustrate in this example, the order of the lowpass filter is very dependent on whether the filter is designed as an IIR or FIR filter and also within those classes, which filter design method is chosen. While the order of the resulting IIR filter might be significantly less than the order of the FIR filter, the FIR filter can exploit the efficiencies of a polyphase implementation. For the IIR designs, polyphase can be exploited for the implementation of the zeros of the transfer function but not for the poles.

The system to be implemented is an upsampler-by-four, i.e., $L = 4$. As discussed in Chapter 4, the ideal filter for 1:4 interpolation is an ideal lowpass filter with gain of 4 and cutoff frequency $\pi/4$. To approximate this filter we set the specifications as follows:[8]

$$\begin{aligned}
&\text{passband edge frequency } \omega_p &&= 0.22\pi \\
&\text{stopband edge frequency } \omega_s &&= 0.29\pi \\
&\text{maximum passband gain} &&= 0 \text{ dB} \\
&\text{minimum passband gain} &&= -1 \text{ dB} \\
&\text{maximum stopband gain} &&= -40 \text{ dB}.
\end{aligned}$$

Six different filters were designed to meet these specifications: the four IIR filter designs discussed in Section 7.3 (Butterworth, Chebyshev I, Chebyshev II, elliptic) and two FIR filter designs (a Kaiser window design and an optimal filter designed using the Parks–McClellan algorithm). The designs were done using the signal processing toolbox in MATLAB. Since the FIR design program used requires passband tolerance limits that are symmetric about unity, the specifications above were first scaled appropriately for the FIR designs and the resulting FIR filter was then rescaled for a maximum of 0 dB gain in the passband. (See Problem 7.3.)

The resulting filter orders for the six filters are shown in Table 7.3 and the corresponding pole–zero plots are shown in Figure 7.57(a)–(f). For the two FIR designs only the zero locations are shown in Figure 7.57. If these filters are implemented as causal

TABLE 7.3 ORDERS OF DESIGNED FILTERS.

Filter design	Order
Butterworth	18
Chebyshev I	8
Chebyshev II	8
Elliptic	5
Kaiser	63
Parks–McClellan	44

[8] The gain was normalized to unity in the passband. In all cases the filters can be scaled by 4 for use in interpolation.

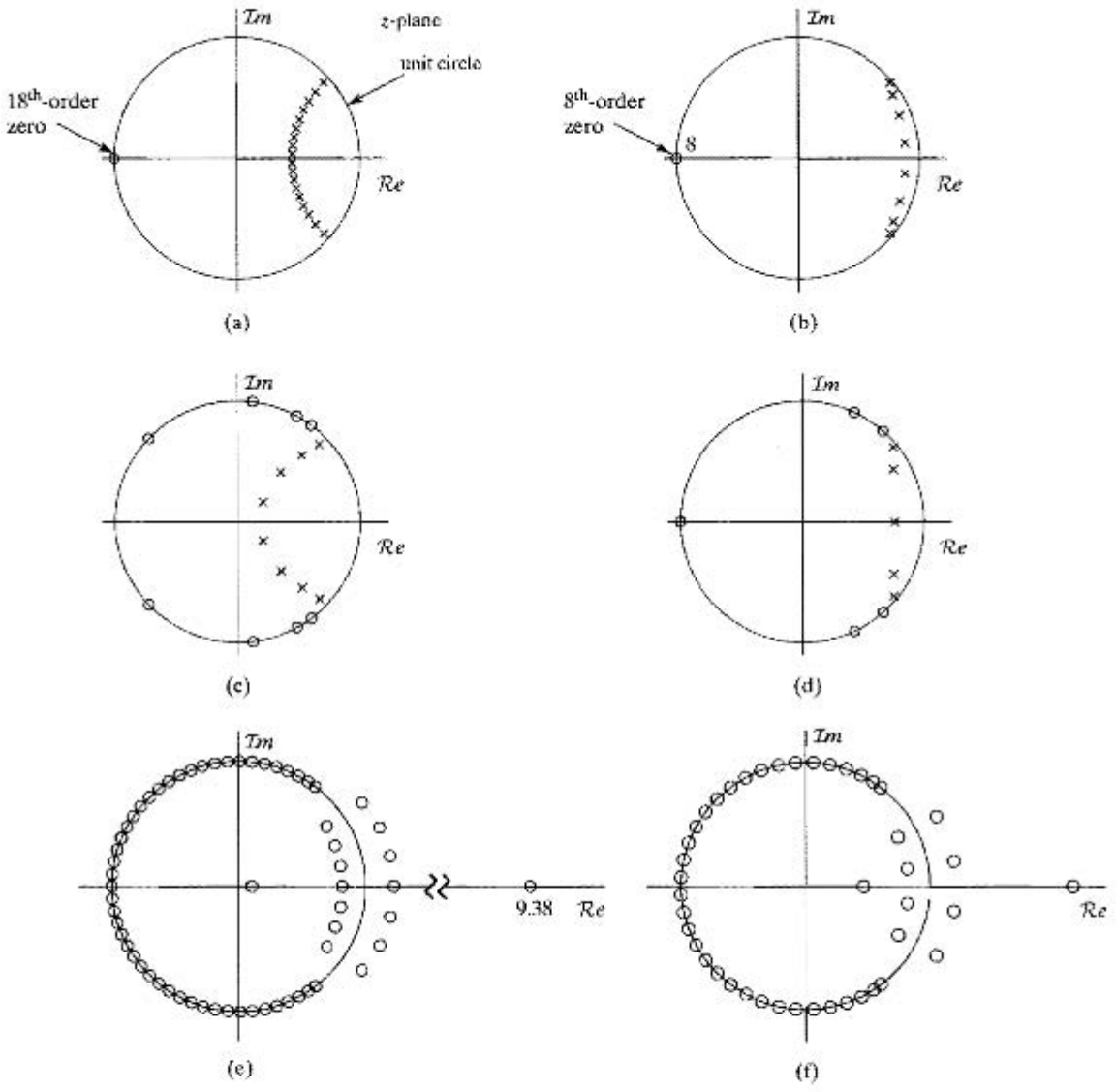

Figure 7.57 Pole–zero plots for the six designs. (a) Butterworth filter. (b) Chebyshev I filter. (c) Chebyshev II filter. (d) Elliptic filter. (e) Kaiser filter. (f) Parks–McClellan filter.

filters there will be a multiple-order pole at the origin to match the total number of zeros of the transfer function.

Without exploiting available efficiencies, such as the use of a polyphase implementation, the two FIR designs require significantly more multiplications per output sample than any of the IIR designs. In the IIR designs, the number of multiplications per output sample will be dependent on specifically how the zeros are implemented. A discussion of how to efficiently implement each of the six designs follows below with a summary in Table 7.4 comparing the required number of multiplications per output

sample. The four IIR designs can be considered as a cascade of an FIR filter (implementing the zeros of the transfer function) and an IIR filter (implementing the poles). We first discuss the two FIR designs since efficiencies that can be exploited for those can also be utilized with the FIR component of the IIR filters.

Parks–McClellan and Kaiser window designs: Without exploiting symmetry of the impulse response or a polyphase implementation, the required number of multiplications per *output* sample is equal to the length of the filter. If a polyphase implementation is used as discussed in Section 4.7.5, then the number of multiplications per *input* sample is equal to the length of the filter. Alternatively, since both filters are symmetric, the folded structure discussed in Section 6.5.3 (Figures 6.32 and 6.33) can be used to reduce the number of multiplications at the input rate by approximately a factor of 2.[9]

Butterworth design: As is characteristic of discrete-time Butterworth filters, all of the zeros occur at $z = -1$ and the poles are, of course, in complex conjugate pairs. By implementing the zeros as a cascade of 18 1st-order terms of the form $(1 + z^{-1})$ no multiplications are required for implementing the zeros. The 18 poles require a total of 18 multiplications per output sample.

Chebyshev I design: The Chebyshev I filter has order 8 with the zeros at $z = -1$ and consequently the zeros can be implemented with no multiplications. The 8 poles require 8 multiplies per output sample.

Chebyshev II design: In this design, the filter order is again 8. Since the zeros are now distributed around the unit circle, their implementation will require some multiplications. However, since all the zeros are on the unit circle, the associated FIR impulse response will be symmetric, and folding and/or polyphase efficiencies can be exploited for implementing the zeros.

Elliptic Iter design: The elliptic filter has the lowest (order 5) of the four IIR designs. From the pole–zero plot we note that it has all its zeros on the unit circle. Consequently the zeros can be implemented efficiently exploiting symmetry as well as polyphase implementation.

Table 7.4 summarizes the number of multiplications required per output sample for each of the six designs with several different implementation structures. The direct form implementation assumes that both the poles and zeros are implemented in direct form, i.e., it does not take advantage of the possibility of cascade implementation of multiple zeroes at $z = -1$. Exploiting a polyphase implementation but not also the symmetry of the impulse response, the FIR designs are slightly less efficient than the most efficient IIR designs, although they are also the only ones that have linear phase. Exploiting both symmetry and polyphase together in implementing the Parks–McClellan design, it and the elliptic filter are the most efficient.

[9]It is possible to combine both folding and polyphase efficiencies in implementing symmetric FIR filters (see Baran and Oppenheim, 2007). The resulting number of multiplications is approximately half the filter length and at the rate of the input samples rather than at the rate of the output samples. However, the resulting structure is significantly more complex.

TABLE 7.4 AVERAGE NUMBER OF REQUIRED MULTIPLICATIONS PER OUTPUT SAMPLE FOR EACH OF THE DESIGNED FILTERS.

Filter design	Direct form	Symmetric	Polyphase
Butterworth	37	18	18
Chebyshev I	17	8	8
Chebyshev II	17	13	10.25
Elliptic	11	8	6.5
Kaiser	64	32	16
Parks–McClellan	45	23	11.25

7.11 SUMMARY

In this chapter, we have considered a variety of design techniques for both infinite-duration and finite-duration impulse-response discrete-time filters. Our emphasis was on the frequency-domain specification of the desired filter characteristics, since this is most common in practice. Our objective was to give a general picture of the wide range of possibilities available for discrete-time filter design, while also giving sufficient detail about some of the techniques so that they may be applied directly, without further reference to the extensive literature on discrete-time filter design. In the FIR case, considerable detail was presented on both the window method and the Parks–McClellan algorithmic method of filter design.

The chapter concluded with some remarks on the choice between the two classes of digital filters. The main point of that discussion was that the choice is not always clear cut and may depend on a multitude of factors that are often difficult to quantify or discuss in general terms. However, it should be clear from this chapter and Chapter 6 that digital filters are characterized by great flexibility in design and implementation. This flexibility makes it possible to implement rather sophisticated signal-processing schemes that in many cases would be difficult, if not impossible, to implement by analog means.

Problems

Basic Problems with Answers

7.1. Consider a causal continuous-time system with impulse response $h_c(t)$ and system function

$$H_c(s) = \frac{s+a}{(s+a)^2+b^2}.$$

(a) Use impulse invariance to determine $H_1(z)$ for a discrete-time system such that $h_1[n] = h_c(nT)$.

(b) Use step invariance to determine $H_2(z)$ for a discrete-time system such that $s_2[n] = s_c(nT)$, where

$$s_2[n] = \sum_{k=-\infty}^{n} h_2[k] \quad \text{and} \quad s_c(t) = \int_{-\infty}^{t} h_c(\tau)d\tau.$$

(c) Determine the step response $s_1[n]$ of system 1 and the impulse response $h_2[n]$ of system 2. Is it true that $h_2[n] = h_1[n] = h_c(nT)$? Is it true that $s_1[n] = s_2[n] = s_c(nT)$?

7.2. A discrete-time lowpass filter is to be designed by applying the impulse invariance method to a continuous-time Butterworth filter having magnitude-squared function

$$|H_c(j\Omega)|^2 = \frac{1}{1 + (\Omega/\Omega_c)^{2N}}.$$

The specifications for the discrete-time system are those of Example 7.2, i.e.,

$$0.89125 \le |H(e^{j\omega})| \le 1, \quad 0 \le |\omega| \le 0.2\pi,$$
$$|H(e^{j\omega})| \le 0.17783, \quad 0.3\pi \le |\omega| \le \pi.$$

Assume, as in that example, that aliasing will not be a problem; i.e., design the continuous-time Butterworth filter to meet passband and stopband specifications as determined by the desired discrete-time filter.

(a) Sketch the tolerance bounds on the magnitude of the frequency response, $|H_c(j\Omega)|$, of the continuous-time Butterworth filter such that after application of the impulse invariance method (i.e., $h[n] = T_d h_c(nT_d)$), the resulting discrete-time filter will satisfy the given design specifications. Do not assume that $T_d = 1$ as in Example 7.2.

(b) Determine the integer order N and the quantity $T_d\Omega_c$ such that the continuous-time Butterworth filter exactly meets the specifications determined in part (a) at the passband edge.

(c) Note that if $T_d = 1$, your answer in part (b) should give the values of N and Ω_c obtained in Example 7.2. Use this observation to determine the system function $H_c(s)$ for $T_d \neq 1$ and to argue that the system function $H(z)$ which results from impulse invariance design with $T_d \neq 1$ is the same as the result for $T_d = 1$ given by Eq. (7.17).

7.3. We wish to use impulse invariance or the bilinear transformation to design a discrete-time filter that meets specifications of the following form:

$$1 - \delta_1 \le |H(e^{j\omega})| \le 1 + \delta_1, \quad 0 \le |\omega| \le \omega_p,$$
$$|H(e^{j\omega})| \le \delta_2, \quad \omega_s \le |\omega| \le \pi. \tag{P7.3-1}$$

For historical reasons, most of the design formulas, tables, or charts for continuous-time filters are normally specified with a peak gain of unity in the passband; i.e.,

$$1 - \tilde{\delta}_1 \le |H_c(j\Omega)| \le 1, \quad 0 \le |\Omega| \le \Omega_p,$$
$$|H_c(\Omega)| \le \tilde{\delta}_2, \quad \Omega_s \le |\Omega|. \tag{P7.3-2}$$

Useful design charts for continuous-time filters specified in this form were given by Rabiner, Kaiser, Herrmann, and Dolan (1974).

(a) To use such tables and charts to design discrete-time systems with a peak gain of $(1+\delta_1)$, it is necessary to convert the discrete-time specifications into specifications of the form of Eq. (P7.3-2). This can be done by dividing the discrete-time specifications by $(1+\delta_1)$. Use this approach to obtain an expression for $\tilde{\delta}_1$ and $\tilde{\delta}_2$ in terms of δ_1 and δ_2.

(b) In Example 7.2, we designed a discrete-time filter with a maximum passband gain of unity. This filter can be converted to a filter satisfying a set of specifications such as those in Eq. (P7.3-1) by multiplying by a constant of the form $(1+\delta_1)$. Find the required value of δ_1 and the corresponding value of δ_2 for this example, and use Eq. (7.17) to determine the coefficients of the system function of the new filter.

(c) Repeat part (b) for the filter in Example 7.3.

7.4. The system function of a discrete-time system is

$$H(z) = \frac{2}{1 - e^{-0.2}z^{-1}} - \frac{1}{1 - e^{-0.4}z^{-1}}.$$

(a) Assume that this discrete-time filter was designed by the impulse invariance method with $T_d = 2$; i.e., $h[n] = 2h_c(2n)$, where $h_c(t)$ is real. Find the system function $H_c(s)$ of a continuous-time filter that could have been the basis for the design. Is your answer unique? If not, find another system function $H_c(s)$.

(b) Assume that $H(z)$ was obtained by the bilinear transform method with $T_d = 2$. Find the system function $H_c(s)$ that could have been the basis for the design. Is your answer unique? If not, find another $H_c(s)$.

7.5. We wish to use the Kaiser window method to design a discrete-time filter with generalized linear phase that meets specifications of the following form:

$$\begin{aligned} |H(e^{j\omega})| &\le 0.01, & 0 \le |\omega| \le 0.25\pi, \\ 0.95 \le |H(e^{j\omega})| &\le 1.05, & 0.35\pi \le |\omega| \le 0.6\pi, \\ |H(e^{j\omega})| &\le 0.01, & 0.65\pi \le |\omega| \le \pi. \end{aligned}$$

(a) Determine the minimum length $(M + 1)$ of the impulse response and the value of the Kaiser window parameter β for a filter that meets the preceding specifications.

(b) What is the delay of the filter?

(c) Determine the ideal impulse response $h_d[n]$ to which the Kaiser window should be applied.

7.6. We wish to use the Kaiser window method to design a symmetric real-valued FIR filter with zero phase that meets the following specifications:

$$\begin{aligned} 0.9 < H(e^{j\omega}) &< 1.1, & 0 \le |\omega| \le 0.2\pi, \\ -0.06 < H(e^{j\omega}) &< 0.06, & 0.3\pi \le |\omega| \le 0.475\pi, \\ 1.9 < H(e^{j\omega}) &< 2.1, & 0.525\pi \le |\omega| \le \pi. \end{aligned}$$

This specification is to be met by applying the Kaiser window to the ideal real-valued impulse response associated with the ideal frequency response $H_d(e^{j\omega})$ given by

$$H_d(e^{j\omega}) = \begin{cases} 1, & 0 \le |\omega| \le 0.25\pi, \\ 0, & 0.25\pi \le |\omega| \le 0.5\pi, \\ 2, & 0.5\pi \le |\omega| \le \pi. \end{cases}$$

(a) What is the maximum value of δ that can be used to meet this specification? What is the corresponding value of β? Clearly explain your reasoning.

(b) What is the maximum value of $\Delta\omega$ that can be used to meet the specification? What is the corresponding value of $M + 1$, the length of the impulse response? Clearly explain your reasoning.

7.7. We are interested in implementing a continuous-time LTI lowpass filter $H(j\Omega)$ using the system shown in Figure 4.10 when the discrete-time system has frequency response $H_d(e^{j\omega})$. The sampling time $T = 10^{-4}$ second and the input signal $x_c(t)$ is appropriately bandlimited with $X_c(j\Omega) = 0$ for $|\Omega| \ge 2\pi(5000)$.

Let the specifications on $|H(j\Omega)|$ be

$$\begin{aligned} 0.99 \le |H(j\Omega)| &\le 1.01, & |\Omega| &\le 2\pi(1000), \\ |H(j\Omega)| &\le 0.01, & |\Omega| &\ge 2\pi(1100). \end{aligned}$$

Determine the corresponding specifications on the discrete-time frequency response $H_d(e^{j\omega})$.

7.8. We wish to design an optimal (Parks-McClellan) zero-phase Type 1 FIR lowpass filter with passband frequency $\omega_p = 0.3\pi$ and stopband frequency $\omega_s = 0.6\pi$ with equal error weighting in the passband and stopband. The impulse response of the desired filter has length 11; i.e., $h[n] = 0$ for $n < -5$ or $n > 5$. Figure P7.8 shows the frequency response $H(e^{j\omega})$ for two different filters. For each filter, specify how many alternations the filter has, and state whether it satisfies the alternation theorem as the optimal filter in the minimax sense meeting the preceding specifications.

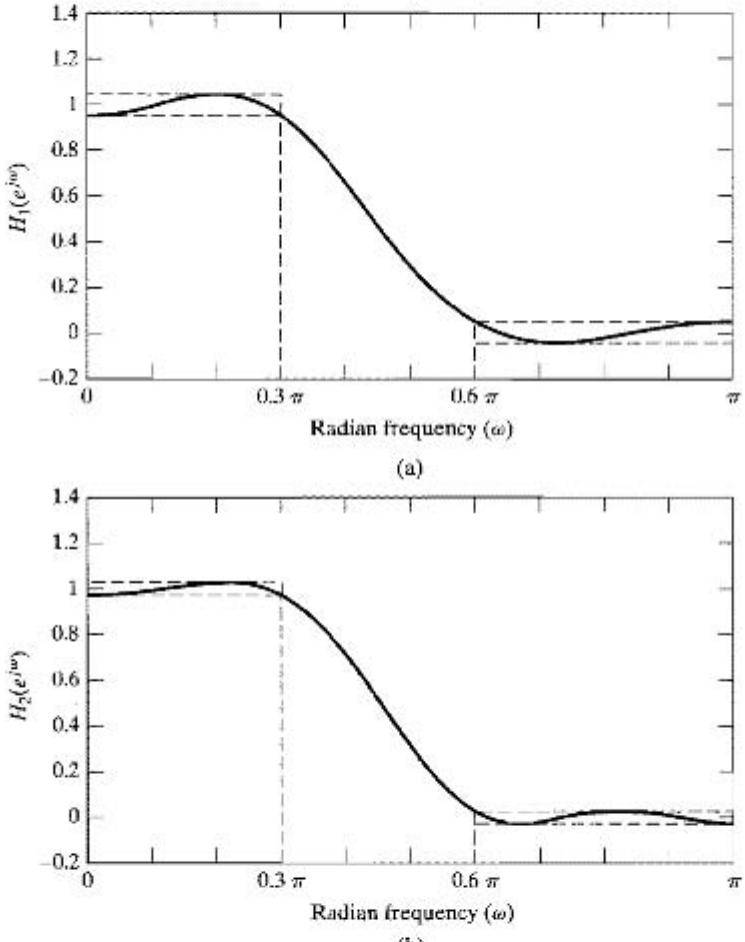

Figure P7.8

7.9. Suppose we design a discrete-time filter using the impulse invariance technique with an ideal continuous-time lowpass filter as a prototype. The prototype filter has a cutoff frequency of $\Omega_c = 2\pi(1000)$ rad/s, and the impulse invariance transformation uses $T = 0.2$ ms. What is the cutoff frequency ω_c for the resulting discrete-time filter?

7.10. We wish to design a discrete-time lowpass filter using the bilinear transformation on a continuous-time ideal lowpass filter. Assume that the continuous-time prototype filter has cutoff frequency $\Omega_c = 2\pi(2000)$ rad/s, and we choose the bilinear transformation parameter $T = 0.4$ ms. What is the cutoff frequency ω_c for the resulting discrete-time filter?

7.11. Suppose that we have an ideal discrete-time lowpass filter with cutoff frequency $\omega_c = \pi/4$. In addition, we are told that this filter resulted from applying impulse invariance to a continuous-time prototype lowpass filter using $T = 0.1$ ms. What was the cutoff frequency Ω_c for the prototype continuous-time filter?

7.12. An ideal discrete-time highpass filter with cutoff frequency $\omega_c = \pi/2$ was designed using the bilinear transformation with $T = 1$ ms. What was the cutoff frequency Ω_c for the prototype continuous-time ideal highpass filter?

7.13. An ideal discrete-time lowpass filter with cutoff frequency $\omega_c = 2\pi/5$ was designed using impulse invariance from an ideal continuous-time lowpass filter with cutoff frequency $\Omega_c = 2\pi(4000)$ rad/s. What was the value of T? Is this value unique? If not, find another value of T consistent with the information given.

7.14. The bilinear transformation is used to design an ideal discrete-time lowpass filter with cutoff frequency $\omega_c = 3\pi/5$ from an ideal continuous-time lowpass filter with cutoff frequency $\Omega_c = 2\pi(300)$ rad/s. Give a choice for the parameter T that is consistent with this information. Is this choice unique? If not, give another choice that is consistent with the information.

7.15. We wish to design an FIR lowpass filter satisfying the specifications

$$\begin{aligned} 0.95 < H(e^{j\omega}) < 1.05, &\qquad 0 \le |\omega| \le 0.25\pi, \\ -0.1 < H(e^{j\omega}) < 0.1, &\qquad 0.35\pi \le |\omega| \le \pi, \end{aligned}$$

by applying a window $w[n]$ to the impulse response $h_d[n]$ for the ideal discrete-time lowpass filter with cutoff $\omega_c = 0.3\pi$. Which of the windows listed in Section 7.5.1 can be used to meet this specification? For each window that you claim will satisfy this specification, give the minimum length $M + 1$ required for the filter.

7.16. We wish to design an FIR lowpass filter satisfying the specifications

$$\begin{aligned} 0.98 < H(e^{j\omega}) < 1.02, &\qquad 0 \le |\omega| \le 0.63\pi, \\ -0.15 < H(e^{j\omega}) < 0.15, &\qquad 0.65\pi \le |\omega| \le \pi, \end{aligned}$$

by applying a Kaiser window to the impulse response $h_d[n]$ for the ideal discrete-time lowpass filter with cutoff $\omega_c = 0.64\pi$. Find the values of β and M required to satisfy this specification.

7.17. Suppose that we wish to design a bandpass filter satisfying the following specification:

$$\begin{aligned} -0.02 < |H(e^{j\omega})| < 0.02, &\qquad 0 \le |\omega| \le 0.2\pi, \\ 0.95 < |H(e^{j\omega})| < 1.05, &\qquad 0.3\pi \le |\omega| \le 0.7\pi, \\ -0.001 < |H(e^{j\omega})| < 0.001, &\qquad 0.75\pi \le |\omega| \le \pi. \end{aligned}$$

The filter will be designed by applying impulse invariance with $T = 5$ ms to a prototype continuous-time filter. State the specifications that should be used to design the prototype continuous-time filter.

7.18. Suppose that we wish to design a highpass filter satisfying the following specification:

$$\begin{aligned} -0.04 < |H(e^{j\omega})| < 0.04, &\qquad 0 \le |\omega| \le 0.2\pi, \\ 0.995 < |H(e^{j\omega})| < 1.005, &\qquad 0.3\pi \le |\omega| \le \pi. \end{aligned}$$

The filter will be designed using the bilinear transformation and $T = 2$ ms with a prototype continuous-time filter. State the specifications that should be used to design the prototype continuous-time filter to ensure that the specifications for the discrete-time filter are met.

7.19. We wish to design a discrete-time ideal bandpass filter that has a passband $\pi/4 \le \omega \le \pi/2$ by applying impulse invariance to an ideal continuous-time bandpass filter with passband $2\pi(300) \le \Omega \le 2\pi(600)$. Specify a choice for T that will produce the desired filter. Is your choice of T unique?

7.20. Specify whether the following statement is true or false. Justify your answer.

Statement: If the bilinear transformation is used to transform a continuous-time all-pass system to a discrete-time system, the resulting discrete-time system will also be an all-pass system.

Basic Problems

7.21. An engineer is asked to evaluate the signal processing system shown in Figure P7.21-1 and improve it if necessary. The input $x[n]$ is obtained by sampling a continuous-time signal at a sampling rate of $1/T = 100$ Hz.

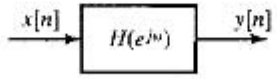

Figure P7.21-1

The goal is for $H(e^{j\omega})$ to be a linear-phase FIR filter, and ideally it should have the following amplitude response (so it can function as a bandlimited differentiator):

$$\text{amplitude of } H_{id}(e^{j\omega}) = \begin{cases} -\omega/T & \omega < 0 \\ \omega/T & \omega \ge 0 \end{cases}$$

(a) For one implementation of $H(e^{j\omega})$, referred to as $H_1(e^{j\omega})$, the designer, motivated by the definition

$$\frac{d(x(t))}{dt} = \lim_{\Delta t \to 0} \frac{x(t) - x(t - \Delta t)}{\Delta t},$$

chooses the system impulse response $h_1[n]$ so that the input–output relationship is

$$y[n] = \frac{x[n] - x[n-1]}{T}$$

Plot the amplitude response of $H_1(e^{j\omega})$ and discuss how well it matches the ideal response. You may find the following expansions helpful:

$$\sin(\theta) = \theta - \frac{1}{3!}\theta^3 + \frac{1}{5!}\theta^5 - \frac{1}{7!}\theta^7 + \cdots$$

$$\cos(\theta) = 1 - \frac{1}{2!}\theta^2 + \frac{1}{4!}\theta^4 - \frac{1}{6!}\theta^6 + \cdots$$

(b) We want to cascade $H_1(e^{j\omega})$ with another *linear-phase* FIR filter $G(e^{j\omega})$, to ensure that for the combination of the two filters, the group delay is an integer number of samples. Should the length of the impulse response $g[n]$ be an even or an odd integer? Explain.

(c) Another method for designing the discrete-time H filter is the method of impulse invariance. In this method, the ideal bandlimited continuous-time impulse response, as given in Eq. (P7.21-1), is sampled.

$$h(t) = \frac{\Omega_c \pi t \cos(\Omega_c t) - \pi \sin(\Omega_c t)}{\pi^2 t^2} \qquad \text{(P7.21-1)}$$

(In a typical application, Ω_c might be slightly less than π/T, making $h(t)$ the impulse response of a differentiator which is bandlimited to $|\Omega| < \pi/T$.) Based on this impulse

response, we would have to create a new filter H_2 which is also FIR and linear phase. Therefore, the impulse response, $h_2[n]$, should preserve the odd symmetry of $h(t)$ about $t = 0$. Using the plot in Figure P7.21-2, indicate the location of samples that result if the impulse response is sampled at 100 Hz, and an impulse response of length 9 is obtained using a rectangular window.

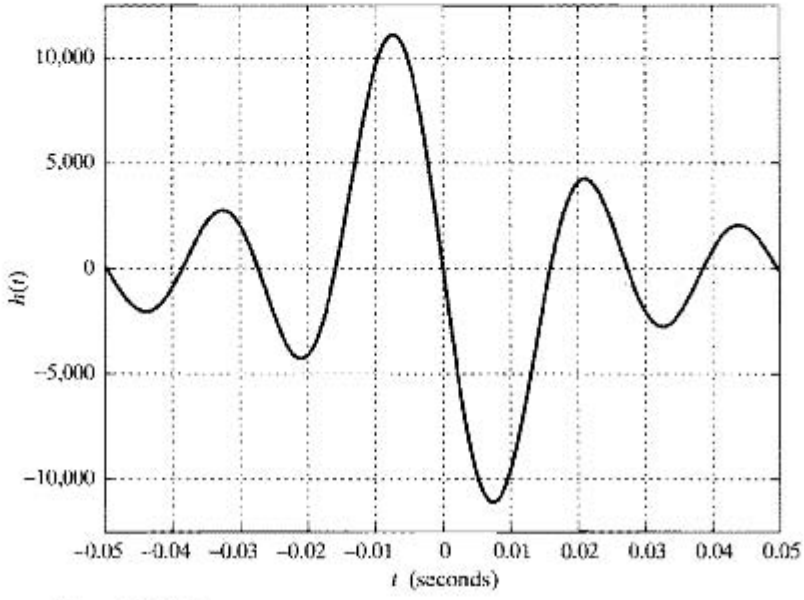

Figure P7.21-2

(d) Again using the plot in Figure P7.21-2, indicate the location of samples if the impulse response $h_2[n]$ is designed to have length 8, again preserving the odd symmetry of $h(t)$ about $t = 0$.

(e) Since the desired magnitude response of $H(e^{j\omega})$ is large near $\omega = \pi$, you do not want H_2 to have a zero at $\omega = \pi$. Would you use an impulse response with an even or an odd number of samples? Explain.

7.22. In the system shown in Figure P7.22, the discrete-time system is a linear-phase FIR lowpass filter designed by the Parks–McClellan algorithm with $\delta_1 = 0.01$, $\delta_2 = 0.001$, $\omega_p = 0.4\pi$, and $\omega_s = 0.6\pi$. The length of the impulse response is 28 samples. The sampling rate for the ideal C/D and D/C converters is $1/T = 10000$ samples/sec.

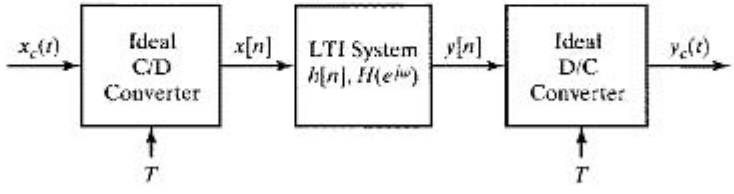

Figure P7.22

(a) What property should the input signal have so that the overall system behaves as an LTI system with $Y_c(j\Omega) = H_{eff}(j\Omega)X_c(j\Omega)$?

(b) For the conditions found in (a), determine the approximation error specifications satisfied by $|H_{eff}(j\Omega)|$. Give your answer as either an equation or a plot as a function of Ω.

(c) What is the overall delay from the continuous-time input to the continuous-time output (in seconds) of the system in Figure P7.22?

7.23. Consider a continuous-time system with system function

$$H_c(s) = \frac{1}{s}.$$

This system is called an *integrator*, since the output $y_c(t)$ is related to the input $x_c(t)$ by

$$y_c(t) = \int_{-\infty}^{t} x_c(\tau)d\tau.$$

Suppose a discrete-time system is obtained by applying the bilinear transformation to $H_c(s)$.

(a) What is the system function $H(z)$ of the resulting discrete-time system? What is the impulse response $h[n]$?

(b) If $x[n]$ is the input and $y[n]$ is the output of the resulting discrete-time system, write the difference equation that is satisfied by the input and output. What problems do you anticipate in implementing the discrete-time system using this difference equation?

(c) Obtain an expression for the frequency response $H(e^{j\omega})$ of the system. Sketch the magnitude and phase of the discrete-time system for $0 \leq |\omega| \leq \pi$. Compare them with the magnitude and phase of the frequency response $H_c(j\Omega)$ of the continuous-time integrator. Under what conditions could the discrete-time "integrator" be considered a good approximation to the continuous-time integrator?

Now consider a continuous-time system with system function

$$G_c(s) = s.$$

This system is a *differentiator*; i.e., the output is the derivative of the input. Suppose a discrete-time system is obtained by applying the bilinear transformation to $G_c(s)$.

(d) What is the system function $G(z)$ of the resulting discrete-time system? What is the impulse response $g[n]$?

(e) Obtain an expression for the frequency response $G(e^{j\omega})$ of the system. Sketch the magnitude and phase of the discrete-time system for $0 \leq |\omega| \leq \pi$. Compare them with the magnitude and phase of the frequency response $G_c(j\Omega)$ of the continuous-time differentiator. Under what conditions could the discrete-time "differentiator" be considered a good approximation to the continuous-time differentiator?

(f) The continuous-time integrator and differentiator are exact inverses of one another. Is the same true of the discrete-time approximations obtained by using the bilinear transformation?

7.24. Suppose we have an even-symmetric FIR filter $h[n]$ of length $2L + 1$, i.e.,

$$h[n] = 0 \text{ for } |n| > L,$$

$$h[n] = h[-n].$$

The frequency response $H(e^{j\omega})$, i.e., the DTFT of $h[n]$, is plotted over $-\pi \leq \omega \leq \pi$ in Figure P7.24.

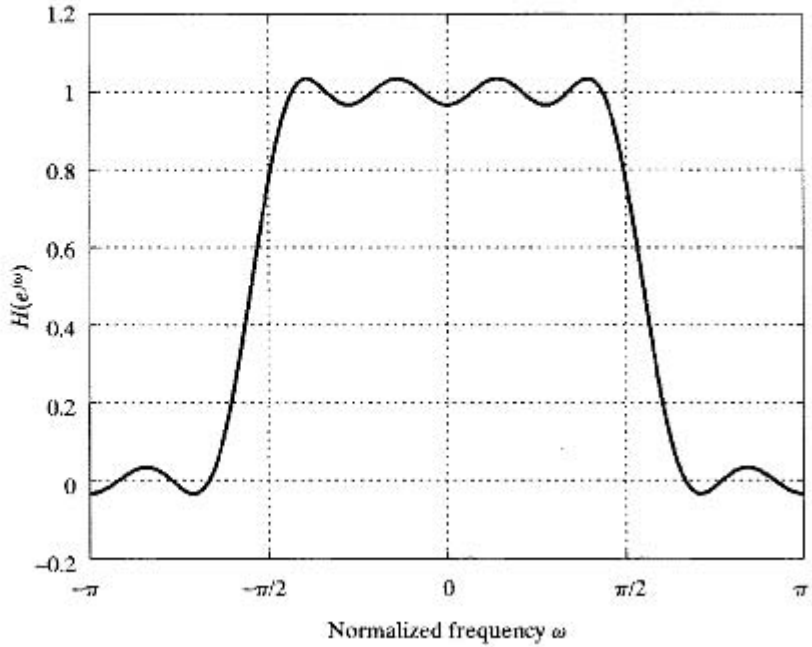

Figure P7.24

What can be inferred from Figure P7.24 about the possible range of values of L? Clearly explain the reason(s) for your answer. Do not make any assumptions about the design procedure that might have been used to obtain $h[n]$.

7.25. Let $h_d[n]$ denote the impulse response of an ideal desired system with corresponding frequency response $H_d(e^{j\omega})$, and let $h[n]$ and $H(e^{j\omega})$ denote the impulse response and frequency response, respectively, of an FIR approximation to the ideal system. Assume that $h[n] = 0$ for $n < 0$ and $n > M$. We wish to choose the $(M + 1)$ samples of the impulse response so as to minimize the mean-square error of the frequency response defined as

$$\varepsilon^2 = \frac{1}{2\pi}\int_{-\pi}^{\pi} |H_d(e^{j\omega}) - H(e^{j\omega})|^2 d\omega.$$

(a) Use Parseval's relation to express the error function in terms of the sequences $h_d[n]$ and $h[n]$.

(b) Using the result of part (a), determine the values of $h[n]$ for $0 \le n \le M$ that minimize ε^2.

(c) The FIR filter determined in part (b) could have been obtained by a windowing operation. That is, $h[n]$ could have been obtained by multiplying the desired infinite-length sequence $h_d[n]$ by a certain finite-length sequence $w[n]$. Determine the necessary window $w[n]$ such that the optimal impulse response is $h[n] = w[n]h_d[n]$.

Advanced Problems

7.26. *Impulse invariance* and the *bilinear transformation* are two methods for designing discrete-time filters. Both methods transform a continuous-time system function $H_c(s)$ into a discrete-time system function $H(z)$. Answer the following questions by indicating which method(s) will yield the desired result:

(a) A minimum-phase continuous-time system has all its poles and zeros in the left-half s-plane. If a minimum-phase continuous-time system is transformed into a discrete-time system, which method(s) will result in a minimum-phase discrete-time system?

(b) If the continuous-time system is an all-pass system, its poles will be at locations s_k in the left-half s-plane, and its zeros will be at corresponding locations $-s_k$ in the right-half s-plane. Which design method(s) will result in an all-pass discrete-time system?

(c) Which design method(s) will guarantee that

$$H(e^{j\omega})\big|_{\omega=0} = H_c(j\Omega)\big|_{\Omega=0}?$$

(d) If the continuous-time system is a bandstop filter, which method(s) will result in a discrete-time bandstop filter?

(e) Suppose that $H_1(z)$, $H_2(z)$, and $H(z)$ are transformed versions of $H_{c1}(s)$, $H_{c2}(s)$, and $H_c(s)$, respectively. Which design method(s) will guarantee that $H(z) = H_1(z)H_2(z)$ whenever $H_c(s) = H_{c1}(s)H_{c2}(s)$?

(f) Suppose that $H_1(z)$, $H_2(z)$, and $H(z)$ are transformed versions of $H_{c1}(s)$, $H_{c2}(s)$, and $H_c(s)$, respectively. Which design method(s) will guarantee that $H(z) = H_1(z)+H_2(z)$ whenever $H_c(s) = H_{c1}(s) + H_{c2}(s)$?

(g) Assume that two continuous-time system functions satisfy the condition

$$\frac{H_{c1}(j\Omega)}{H_{c2}(j\Omega)} = \begin{cases} e^{-j\pi/2}, & \Omega > 0, \\ e^{j\pi/2}, & \Omega < 0. \end{cases}$$

If $H_1(z)$ and $H_2(z)$ are transformed versions of $H_{c1}(s)$ and $H_{c2}(s)$, respectively, which design method(s) will result in discrete-time systems such that

$$\frac{H_1(e^{j\omega})}{H_2(e^{j\omega})} = \begin{cases} e^{-j\pi/2}, & 0 < \omega < \pi, \\ e^{j\pi/2}, & -\pi < \omega < 0? \end{cases}$$

(Such systems are called "90-degree phase splitters.")

7.27. Suppose that we are given an ideal lowpass discrete-time filter with frequency response

$$H(e^{j\omega}) = \begin{cases} 1, & |\omega| < \pi/4, \\ 0, & \pi/4 < |\omega| \le \pi. \end{cases}$$

We wish to derive new filters from this prototype by manipulations of the impulse response $h[n]$.

(a) Plot the frequency response $H_1(e^{j\omega})$ for the system whose impulse response is $h_1[n] = h[2n]$.

(b) Plot the frequency response $H_2(e^{j\omega})$ for the system whose impulse response is

$$h_2[n] = \begin{cases} h[n/2], & n = 0, \pm 2, \pm 4, \ldots, \\ 0, & \text{otherwise.} \end{cases}$$

(c) Plot the frequency response $H_3(e^{j\omega})$ for the system whose impulse response is $h_3[n] = e^{j\pi n}h[n] = (-1)^n h[n]$.

7.28. Consider a continuous-time lowpass filter $H_c(s)$ with passband and stopband specifications

$$\begin{aligned} 1 - \delta_1 \le |H_c(j\Omega)| &\le 1 + \delta_1, & |\Omega| &\le \Omega_p, \\ |H_c(j\Omega)| &\le \delta_2, & \Omega_s &\le |\Omega|. \end{aligned}$$

This filter is transformed to a lowpass discrete-time filter $H_1(z)$ by the transformation

$$H_1(z) = H_c(s)\big|_{s=(1-z^{-1})/(1+z^{-1})},$$

and the same continuous-time filter is transformed to a highpass discrete-time filter by the transformation

$$H_2(z) = H_c(s)\big|_{s=(1+z^{-1})/(1-z^{-1})}.$$

(a) Determine a relationship between the passband cutoff frequency Ω_p of the continuous-time lowpass filter and the passband cutoff frequency ω_{p1} of the discrete-time lowpass filter.

(b) Determine a relationship between the passband cutoff frequency Ω_p of the continuous-time lowpass filter and the passband cutoff frequency ω_{p2} of the discrete-time highpass filter.

(c) Determine a relationship between the passband cutoff frequency ω_{p1} of the discrete-time lowpass filter and the passband cutoff frequency ω_{p2} of the discrete-time highpass filter.

(d) The network in Figure P7.28 depicts an implementation of the discrete-time lowpass filter with system function $H_1(z)$. The coefficients A, B, C, and D are real. How should these coefficients be modified to obtain a network that implements the discrete-time highpass filter with system function $H_2(z)$?

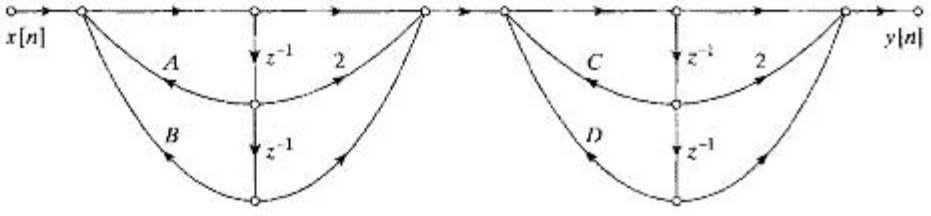

Figure P7.28

7.29. A discrete-time system with system function $H(Z)$ and impulse response $h[n]$ has frequency response

$$H(e^{j\theta}) = \begin{cases} A, & |\theta| < \theta_c, \\ 0, & \theta_c < |\theta| \leq \pi, \end{cases}$$

where $0 < \theta_c < \pi$. This filter is transformed into a new filter by the transformation $Z = -z^2$; i.e.,

$$H_1(z) = H(Z)\big|_{Z=-z^2} = H(-z^2).$$

(a) Obtain a relationship between the frequency variable θ for the original lowpass system $H(Z)$ and the frequency variable ω for the new system $H_1(z)$.

(b) Sketch and carefully label the frequency response $H_1(e^{j\omega})$ for the new filter.

(c) Obtain a relationship expressing $h_1[n]$ in terms of $h[n]$.

(d) Assume that $H(Z)$ can be realized by the set of difference equations

$$g[n] = x[n] - a_1 g[n-1] - b_1 f[n-2],$$

$$f[n] = a_2 g[n-1] + b_2 f[n-1],$$

$$y[n] = c_1 f[n] - c_2 g[n-1],$$

where $x[n]$ is the input and $y[n]$ is the output of the system. Determine a set of difference equations that will realize the transformed system $H_1(z) = H(-z^2)$.

7.30. Consider designing a discrete-time filter with system function $H(z)$ from a continuous-time filter with rational system function $H_c(s)$ by the transformation

$$H(z) = H_c(s)\big|_{s=\beta[(1-z^{-\alpha})/(1+z^{-\alpha})]},$$

where α is a nonzero integer and β is real.

(a) If $\alpha > 0$, for what values of β does a stable, causal continuous-time filter with rational $H_c(s)$ always lead to a stable, causal discrete-time filter with rational $H(z)$?

(b) If $\alpha < 0$, for what values of β does a stable, causal continuous-time filter with rational $H_c(s)$ always lead to a stable, causal discrete-time filter with rational $H(z)$?

(c) For $\alpha = 2$ and $\beta = 1$, determine to what contour in the z-plane the $j\Omega$-axis of the s-plane maps.

(d) Suppose that the continuous-time filter is a stable lowpass filter with passband frequency response such that

$$1 - \delta_1 \le |H_c(j\Omega)| \le 1 + \delta_1 \qquad \text{for} \quad |\Omega| \le 1.$$

If the discrete-time system $H(z)$ is obtained by the transformation set forth at the beginning of this problem, with $\alpha = 2$ and $\beta = 1$, determine the values of ω in the interval $|\omega| \le \pi$ for which

$$1 - \delta_1 \le |H(e^{j\omega})| \le 1 + \delta_1.$$

7.31. Suppose that we have used the Parks–McClellan algorithm to design a causal FIR linear-phase lowpass filter. The system function of this system is denoted $H(z)$. The *length* of the impulse response is 25 samples, i.e., $h[n] = 0$ for $n < 0$ and for $n > 24$, and $h[0] \neq 0$. The desired response and weighting function used were

$$H_d(e^{j\omega}) = \begin{cases} 1 & |\omega| \le 0.3\pi \\ 0 & 0.4\pi \le |\omega| \le \pi \end{cases} \qquad W(e^{j\omega}) = \begin{cases} 1 & |\omega| \le 0.3\pi \\ 2 & 0.4\pi \le |\omega| \le \pi. \end{cases}$$

In each case below, determine whether the statement is true or false or that insufficient information is given. Justify your conclusions.

(a) $h[n + 12] = h[12 - n]$ or $h[n + 12] = -h[12 - n]$ for $-\infty < n < \infty$.

(b) The system has a stable and causal inverse.

(c) We know that $H(-1) = 0$.

(d) The maximum weighted approximation error is the same in all approximation bands.

(e) If z_0 is a zero of $H(z)$, then $1/z_0$ is a pole of $H(z)$.

(f) The system can be implemented by a network (flow graph) that has no feedback paths.

(g) The group delay is equal to 24 for $0 < \omega < \pi$.

(h) If the coefficients of the system function are quantized to 10 bits each, the system is still optimum in the Chebyshev sense for the original desired response and weighting function.

(i) If the coefficients of the system function are quantized to 10 bits each, the system is still guaranteed to be a linear-phase filter.

(j) If the coefficients of the system function are quantized to 10 bits each, the system may become unstable.

7.32. You are required to design an FIR filter, $h[n]$, with the following magnitude specifications:

- Passband edge: $\omega_p = \pi/100$.
- Stopband edge: $\omega_s = \pi/50$.
- Maximum stopband gain: $\delta_s \leq -60$ dB relative to passband.

It is suggested that you try using a Kaiser window. The Kaiser window design rules for shape parameter β and filter length M are provided in Section 7.5.3.

(a) What values of β and M are necessary to meet the required specifications?

You show the resulting filter to your boss, and he is unsatisfied. He asks you to reduce the computations required for the filter. You bring in a consultant who suggests that you design the filter as a cascade of two stages: $h'[n] = p[n] * q[n]$. To design $p[n]$ he suggests first designing a filter, $g[n]$, with passband edge $\omega'_p = 10\omega_p$, stopband edge $\omega'_s = 10\omega_s$ and stopband gain $\delta'_s = \delta_s$. The filter $p[n]$ is then obtained by expanding $g[n]$ by a factor of 10:

$$p[n] = \begin{cases} g[n/10], & \text{when } n/10 \text{ is an integer,} \\ 0, & \text{otherwise.} \end{cases}$$

(b) What values of β' and M' are necessary to meet the required specifications for $g[n]$?

(c) Sketch $P(e^{j\omega})$ from $\omega = 0$ to $\omega = \pi/4$. You do not need to draw the exact shape of the frequency response; instead, you should show which regions of the frequency response are near 0 dB, and which regions are at or below -60 dB. Label all band edges in your sketch.

(d) What specifications should be used in designing $q[n]$ to guarantee that $h'[n] = p[n] * q[n]$ meets or exceeds the original requirements? Specify the passband edge, ω''_p, stopband edge, ω''_s, and stopband attenuation, δ''_s, required for $q[n]$.

(e) What values of β'' and M'' are necessary to meet the required specifications for $q[n]$? How many nonzero samples will $h'[n] = q[n] * p[n]$ have?

(f) The filter $h'[n]$ from parts (b)–(e) is implemented by first directly convolving the input with $q[n]$ and then directly convolving the results with $p[n]$. The filter $h[n]$ from part (a) is implemented by directly convolving the input with $h[n]$. Which of these two implementations requires fewer multiplications? Explain. Note: you should not count multiplications by 0 as an operation.

7.33. Consider a real, bandlimited signal $x_a(t)$ whose Fourier transform $X_a(j\Omega)$ has the following property:

$$X_a(j\Omega) = 0 \qquad \text{for} \qquad |\Omega| > 2\pi \cdot 10000 .$$

That is, the signal is bandlimited to 10 kHz.

We wish to process $x_a(t)$ with a highpass analog filter whose magnitude response satisfies the following specifications (see Figure P7.33):

$$\begin{cases} 0 \leq |H_a(j\Omega)| \leq 0.1 & \text{for } 0 \leq |\Omega| \leq 2\pi \cdot 4000 = \Omega_s \\ 0.9 \leq |H_a(j\Omega)| \leq 1 & \text{for } \Omega_p = 2\pi \cdot 8000 \leq |\Omega|, \end{cases}$$

where Ω_s and Ω_p denote the stopband and passband frequencies, respectively.

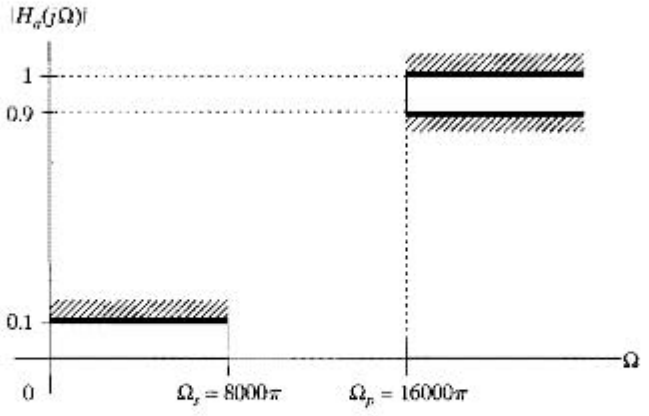

Figure P7.33

(a) Suppose the analog filter $H_a(j\Omega)$ is implemented by discrete-time processing, according to the diagram shown in Figure 7.2.

The sampling frequency $f_s = \frac{1}{T}$ is 24 kHz for both the ideal C/D and D/C converters. Determine the appropriate filter specification for $|H(e^{j\omega})|$, the magnitude response of the digital filter.

(b) Using the bilinear transformation $s = \dfrac{1 - z^{-1}}{1 + z^{-1}}$, we want to design a digital filter whose magnitude response specifications were found in part (a). Find the specifications of $|G_{HP}(j\Omega_1)|$, the magnitude response of the highpass analog filter that is related to the digital filter through the bilinear transformation. Again, provide a fully labelled sketch of the magnitude response specifications on $|G_{HP}(j\Omega_1)|$.

(c) Using the frequency transformation $s_1 = \dfrac{1}{s_2}$, (i.e., replacing the Laplace transform variable s by its reciprocal), design the highpass analog filter $G_{HP}(j\Omega_1)$ from the lowest-order Butterworth filter, whose magnitude-squared frequency response is given below:

$$|G(j\Omega_2)|^2 = \frac{1}{1 + (\Omega_2/\Omega_c)^{2N}} .$$

In particular, find the lowest filter order N and its corresponding cutoff frequency Ω_c, such that the original filter's passband specification ($|H_a(j\Omega_p)| = 0.9$) is met *exactly*. In a diagram, label the salient features of the Butterworth filter magnitude response that you have designed.

(d) Draw the pole–zero diagram of the (lowpass) Butterworth filter $G(s_2)$, and find an expression for its transfer function.

7.34. A zero-phase FIR filter $h[n]$ has associated DTFT $H(e^{j\omega})$, shown in Figure P7.34.

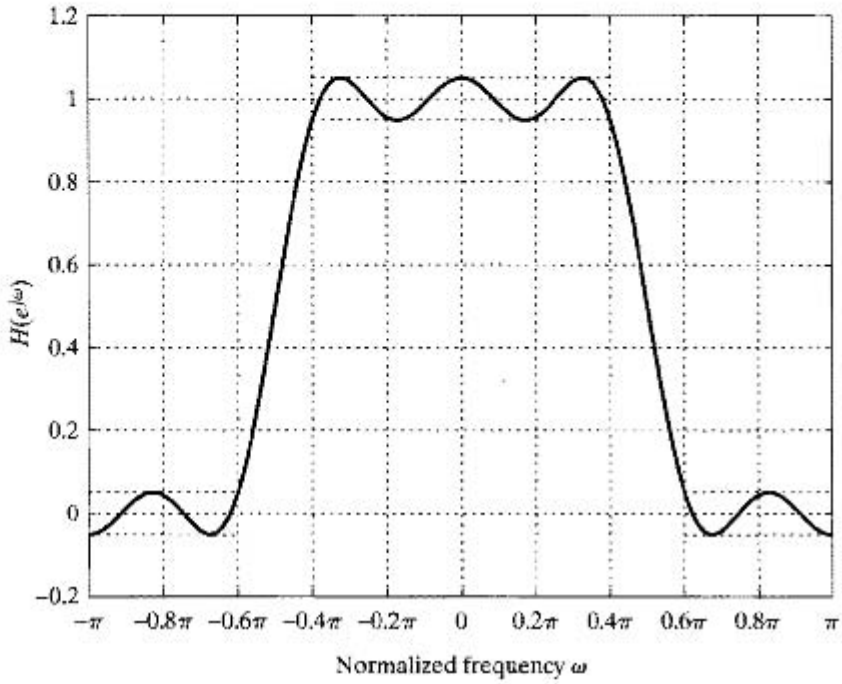

Figure P7.34

The filter is known to have been designed using the Parks–McClellan (PM) algorithm. The input parameters to the PM algorithm are known to have been:

- Passband edge: $\omega_p = 0.4\pi$
- Stopband edge: $\omega_s = 0.6\pi$
- Ideal passband gain: $G_p = 1$
- Ideal stopband gain: $G_s = 0$
- Error weighting function $W(\omega) = 1$

The length of the impulse response $h[n]$, is $M + 1 = 2L + 1$ and

$$h[n] = 0 \text{ for } |n| > L.$$

The value of L is not known.

It is claimed that there are two filters, each with frequency response identical to that shown in Figure P7.34, and each having been designed by the Parks–McClellan algorithm with *different* values for the input parameter L.

- **Filter 1:** $L = L_1$
- **Filter 2:** $L = L_2 > L_1$.

Both filters were designed using exactly the same Parks–McClellan algorithm and input parameters, *except* for the value of L.

(a) What are possible values for L_1?
(b) What are possible values for $L_2 > L_1$?

(c) Are the impulse responses $h_1[n]$ and $h_2[n]$ of the two filters identical?

(d) The alternation theorem guarantees "*uniqueness* of the r^{th}-order polynomial." If your answer to (c) is yes, explain why the alternation theorem is not violated. If your answer is no, show how the two filters, $h_1[n]$ and $h_2[n]$, are related.

7.35. We are given an FIR bandpass filter $h[n]$ that is zero phase, i.e., $h[n] = h[-n]$. Its associated DTFT $H(e^{j\omega})$ is shown in Figure P7.35.

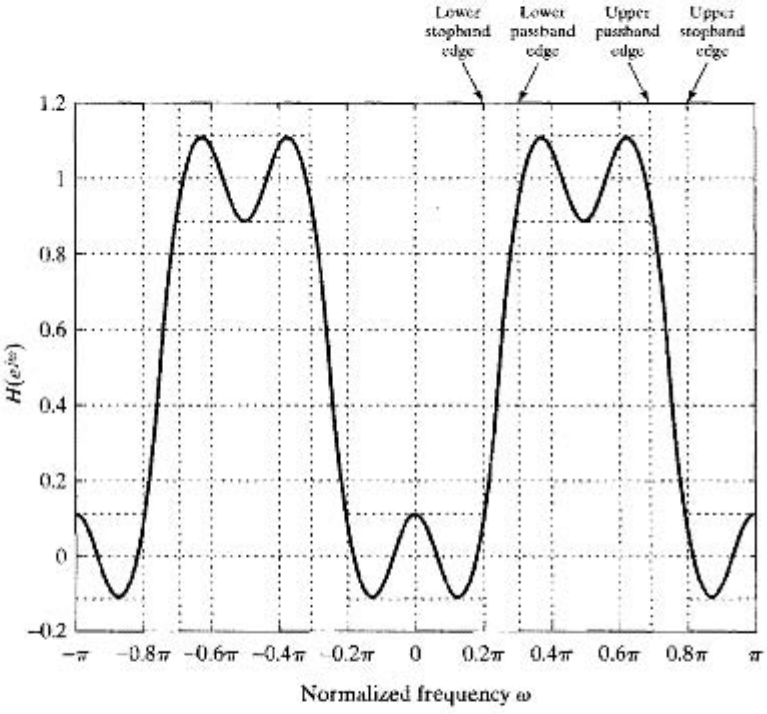

Figure P7.35

The filter is known to have been designed using the Parks–McClellan algorithm. The input parameters to the Parks–McClellan algorithm are known to have been:

- Lower stopband edge: $\omega_1 = 0.2\pi$
- Lower passband edge: $\omega_2 = 0.3\pi$
- Upper passband edge: $\omega_3 = 0.7\pi$
- Upper stopband edge: $\omega_4 = 0.8\pi$
- Ideal passband gain: $G_p = 1$
- Ideal stopband gain: $G_s = 0$
- Error weighting function $W(\omega) = 1$

The value of the input parameter $M+1$, which represents the maximum number of nonzero impulse response values (equivalently the filter length), is not known.

It is claimed that there are two filters, each with a frequency response identical to that shown in Figure P7.35, but having *different* impulse response lengths $M + 1 = 2L + 1$.

- **Filter 1:** $M = M_1 = 14$
- **Filter 2:** $M = M_2 \neq M_1$

Both filters were designed using exactly the same Parks–McClellan algorithm and input parameters, *except* for the value of M.

(a) What are possible values for M_2?

(b) The alternation theorem guarantees "*uniqueness* of the r^{th}-order polynomial." Explain why the alternation theorem is not violated.

7.36. The graphs in Figure P7.36 depict four frequency-response magnitude plots of linear-phase FIR filters, labelled $|A_e^i(e^{j\omega})|$, $i = 1, 2, 3, 4$. One or more of these plots may belong to equiripple linear-phase FIR filters designed by the Parks–McClellan algorithm. The maximum approximation errors in the passband and the stopband, as well as the desired cutoff frequencies of those bands, are also shown in the plots. Please note that the approximation error and filter length specifications may have been chosen differently to ensure that the cutoff frequencies are the same in each design.

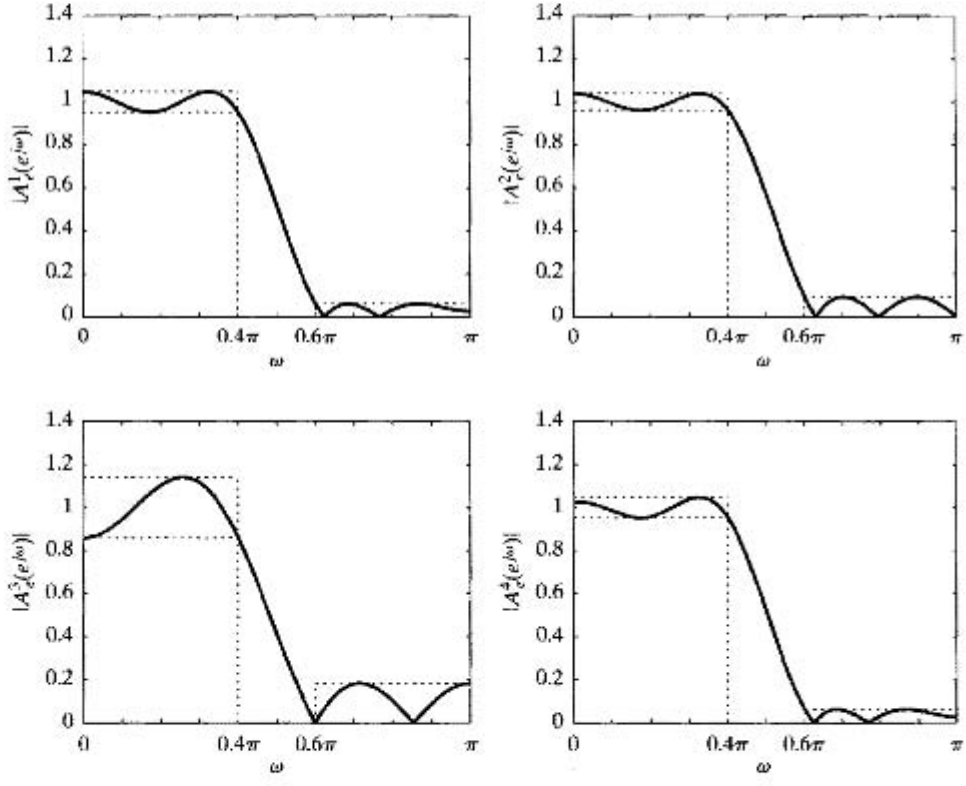

Figure P7.36

(a) What type(s) (I, II, III, IV) of linear-phase FIR filters can $|A_e^i(e^{j\omega})|$ correspond to, for $i = 1, 2, 3, 4$? Please note that there may be more than one linear-phase FIR filter type corresponding to each $|A_e^i(e^{j\omega})|$. If you feel this is the case, list all possible choices.

(b) How many alternations does each $|A_e^i(e^{j\omega})|$ exhibit, for $i = 1, 2, 3, 4$?

(c) For each i, $i = 1, 2, 3, 4$, can $|A_e^i(e^{j\omega})|$ belong to an output of the Parks–McClellan algorithm?

(d) If you claimed that a given $|A_e^i(e^{j\omega})|$ could correspond to an output of the Parks–McClellan algorithm, and that it could be type I, what is the length of the impulse response of $|A_e^i(e^{j\omega})|$?

7.37. Consider the two-stage system shown in Figure P7.37 for interpolating a sequence $x[n] = x_c(nT)$ to a sampling rate that is 15 times as high as the input sampling rate; i.e., we desire $y[n] = x_c(nT/15)$.

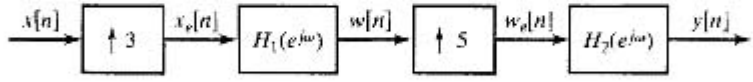

Figure P7.37

Assume that the input sequence $x[n] = x_c(nT)$ was obtained by sampling a bandlimited continuous-time signal whose Fourier transform satisfies the following condition: $|X_c(j\Omega)| = 0$ for $|\Omega| \geq 2\pi(3600)$. Assume that the original sampling period was $T = 1/8000$.

(a) Make a sketch of the Fourier transform $X_c(j\Omega)$ of a "typical" bandlimited input signal and the corresponding discrete-time Fourier transforms $X(e^{j\omega})$ and $X_e(e^{j\omega})$.

(b) To implement the interpolation system, we must, of course, use nonideal filters. Use your plot of $X_e(e^{j\omega})$ obtained in part (a) to determine the passband and stopband cutoff frequencies (ω_{p1} and ω_{s1}) required to preserve the original band of frequencies essentially unmodified while significantly attenuating the images of the baseband spectrum. (That is, we desire that $w[n] \approx x_c(nT/3)$.) Assuming that this can be achieved with passband approximation error $\delta_1 = 0.005$ (for filter passband gain of 1) and stopband approximation error $\delta_2 = 0.01$, plot the specifications for the design of the filter $H_1(e^{j\omega})$ for $-\pi \leq \omega \leq \pi$.

(c) Assuming that $w[n] = x_c(nT/3)$, make a sketch of $W_e(e^{j\omega})$ and use it to determine the passband and stopband cutoff frequencies ω_{p2} and ω_{s2} required for the second filter.

(d) Use the formula of Eq. (7.117) to determine the filter orders M_1 and M_2 for Parks–McClellan filters that have the passband and stopband cutoff frequencies determined in parts (b) and (c) with $\delta_1 = 0.005$ and $\delta_2 = 0.01$ for both filters.

(e) Determine how many multiplications are required to compute 15 samples of the output for this case.

7.38. The system of Figure 7.2 is used to perform filtering of continuous-time signals with a digital filter. The sampling rate of the C/D and D/C converters is $f_s = 1/T = 10,000$ samples/sec.

A Kaiser window $w_K[n]$ of length $M + 1 = 23$ and $\beta = 3.395$ is used to design a linear-phase lowpass filter with frequency response $H_{lp}(e^{j\omega})$. When used in the system of Figure 7.1 so that $H(e^{j\omega}) = H_{lp}(e^{j\omega})$, the overall effective frequency response (from input $x_a(t)$ to output $y_a(t)$) meets the following specifications:

$$\begin{aligned} &0.99 \leq |H_{\text{eff}}(j\Omega)| \leq 1.01, && 0 \leq |\Omega| \leq 2\pi(2000) \\ &|H_{\text{eff}}(j\Omega)| \leq 0.01 && 2\pi(3000) \leq |\Omega| \leq 2\pi(5000). \end{aligned}$$

(a) The linear phase of the FIR filter introduces a time delay t_d. Find the time delay through the system (in milliseconds).

(b) Now a highpass filter is designed with the *same* Kaiser window by applying it to the ideal impulse response $h_d[n]$ whose corresponding frequency response is

$$H_d(e^{j\omega}) = \begin{cases} 0 & |\omega| < 0.25\pi \\ 2e^{-j\omega n_d} & 0.25\pi < |\omega| \le \pi. \end{cases}$$

That is, a linear-phase FIR highpass filter with impulse response $h_{\text{hp}}[n] = w_K[n]h_d[n]$ and frequency response $H_{\text{hp}}(e^{j\omega})$ was obtained by multiplying $h_d[n]$ by the same Kaiser window $w_K[n]$ that was used to design the first mentioned lowpass filter. The resulting FIR highpass discrete-time filter meets a set of specifications of the following form:

$$\begin{aligned} |H_{\text{hp}}(e^{j\omega})| &\le \delta_1 & 0 \le |\omega| \le \omega_1 \\ G - \delta_2 \le |H_{\text{hp}}(e^{j\omega})| &\le G + \delta_2 & \omega_2 \le |\omega| \le \pi \end{aligned}$$

Use information from the lowpass filter specifications to determine the values of ω_1, ω_2, δ_1, δ_2, and G.

7.39. Figure P7.39 is the ideal, desired frequency response amplitude for a bandpass filter to be designed as a Type 1 FIR filter $h[n]$, with DTFT $H(e^{j\omega})$ that approximates $H_d(e^{j\omega})$ and meets the following constraints:

$$-\delta_1 \le H(e^{j\omega}) \le \delta_1, \quad 0 \le |\omega| \le \omega_1$$

$$1 - \delta_2 \le H(e^{j\omega}) \le 1 + \delta_2, \quad \omega_2 \le |\omega| \le \omega_3$$

$$-\delta_3 \le H(e^{j\omega}) \le \delta_3, \quad \omega_4 \le |\omega| \le \pi$$

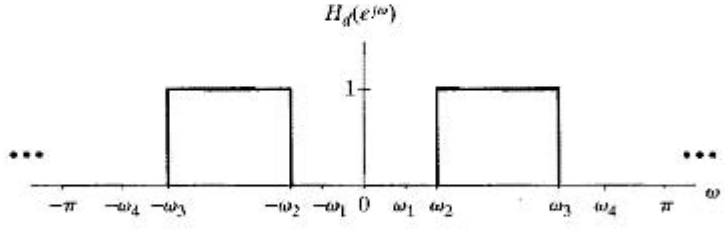

Figure P7.39

The resulting filter $h[n]$ is to minimize the maximum weighted error and therefore must satisfy the alternation theorem.

Determine and sketch an appropriate choice for the weighting function to use with the Parks–McClellan algorithm.

7.40. **(a)** Figure P7.40-1 shows the frequency response $A_e(e^{j\omega})$ of a lowpass Type I Parks–McClellan filter based on the following specifications. Consequently it satisfies the alternation theorem.

Passband edge: $\omega_p = 0.45\pi$
Stopband edge: $\omega_s = 0.50\pi$
Desired passband magnitude: 1
Desired stopband magnitude: 0

The weighting function used in both the passband and the stopband is $W(\omega) = 1$.

What can you conclude about the maximum possible number of nonzero values in the impulse response of the filter?

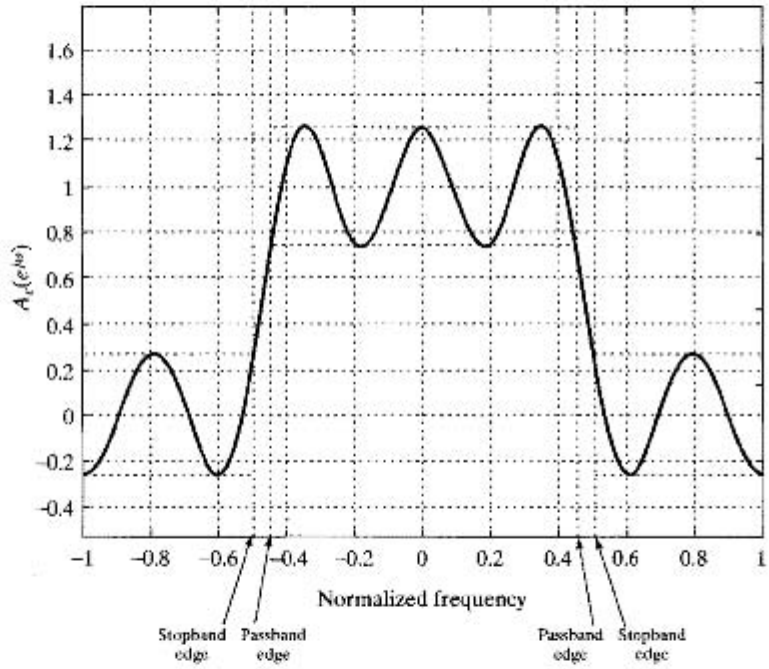

Figure P7.40-1

(b) Figure P7.40-2 shows another frequency response $B_e(e^{j\omega})$ for a Type I FIR filter. $B_e(e^{j\omega})$ is obtained from $A_e(e^{j\omega})$ from part (a) as follows:

$$B_e(e^{j\omega}) = k_1 \left(A_e(e^{j\omega})\right)^2 + k_2,$$

where k_1 and k_2 are constants. Observe that $B_e(e^{j\omega})$ displays equiripple behavior, with different maximum error in the passband and stopband.

Does this filter satisfy the alternation theorem with the passband and stopband edge frequencies indicated and with passband ripple and stopband ripple indicated by the dashed lines?

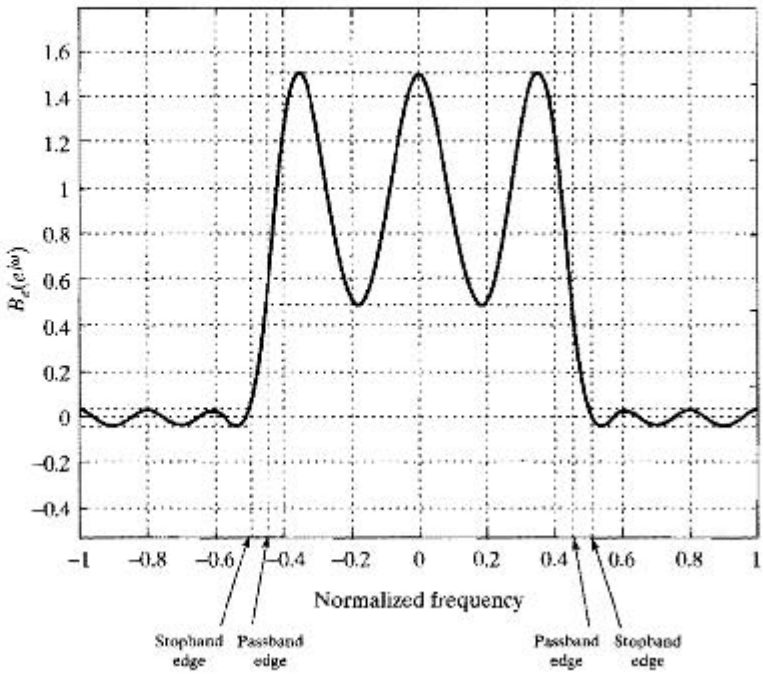

Figure P7.40-2

7.41. Assume that $H_c(s)$ has an r^{th}-order pole at $s = s_0$, so that $H_c(s)$ can be expressed as

$$H_c(s) = \sum_{k=1}^{r} \frac{A_k}{(s - s_0)^k} + G_c(s),$$

where $G_c(s)$ has only 1^{st}-order poles. Assume $H_c(s)$ is causal.

(a) Give a formula for determining the constants A_k from $H_c(s)$.

(b) Obtain an expression for the impulse response $h_c(t)$ in terms of s_0 and $g_c(t)$, the inverse Laplace transform of $G_c(s)$.

7.42. As discussed in Chapter 12, an *ideal discrete-time Hilbert transformer* is a system that introduces -90 degrees ($-\pi/2$ radians) of phase shift for $0 < \omega < \pi$ and $+90$ degrees ($+\pi/2$ radians) of phase shift for $-\pi < \omega < 0$. The magnitude of the frequency response is constant (unity) for $0 < \omega < \pi$ and for $-\pi < \omega < 0$. Such systems are also called *ideal 90-degree phase shifters.*

(a) Give an equation for the ideal desired frequency response $H_d(e^{j\omega})$ of an ideal discrete-time Hilbert transformer that also includes constant (nonzero) group delay. Plot the phase response of this system for $-\pi < \omega < \pi$.

(b) What type(s) of FIR linear-phase systems (I, II, III, or IV) can be used to approximate the ideal Hilbert transformer in part (a)?

(c) Suppose that we wish to use the window method to design a linear-phase approximation to the ideal Hilbert transformer. Use $H_d(e^{j\omega})$ given in part (a) to determine the ideal impulse response $h_d[n]$ if the FIR system is to be such that $h[n] = 0$ for $n < 0$ and $n > M$.

(d) What is the delay of the system if $M = 21$? Sketch the magnitude of the frequency response of the FIR approximation for this case, assuming a rectangular window.

(e) What is the delay of the system if $M = 20$? Sketch the magnitude of the frequency response of the FIR approximation for this case, assuming a rectangular window.

7.43. The commonly used windows presented in Section 7.5.1 can all be expressed in terms of rectangular windows. This fact can be used to obtain expressions for the Fourier transforms of the Bartlett window and the raised-cosine family of windows, which includes the Hanning, Hamming, and Blackman windows.

(a) Show that the $(M+1)$-point Bartlett window, defined by Eq. (7.60b), can be expressed as the convolution of two smaller rectangular windows. Use this fact to show that the Fourier transform of the $(M+1)$-point Bartlett window is

$$W_B(e^{j\omega}) = e^{-j\omega M/2}(2/M)\left(\frac{\sin(\omega M/4)}{\sin(\omega/2)}\right)^2 \qquad \text{for } M \text{ even,}$$

or

$$W_B(e^{j\omega}) = e^{-j\omega M/2}(2/M)\left(\frac{\sin[\omega(M+1)/4]}{\sin(\omega/2)}\right)\left(\frac{\sin[\omega(M-1)/4]}{\sin(\omega/2)}\right) \qquad \text{for } M \text{ odd.}$$

(b) It can easily be seen that the $(M+1)$-point raised-cosine windows defined by Eqs. (7.60c)–(7.60e) can all be expressed in the form

$$w[n] = [A + B\cos(2\pi n/M) + C\cos(4\pi n/M)]w_R[n],$$

where $w_R[n]$ is an $(M+1)$-point rectangular window. Use this relation to find the Fourier transform of the general raised-cosine window.

(c) Using appropriate choices for A, B, and C and the result determined in part (b), sketch the magnitude of the Fourier transform of the Hanning window.

7.44. Consider the following ideal frequency response for a multiband filter:

$$H_d(e^{j\omega}) = \begin{cases} e^{-j\omega M/2}, & 0 \le |\omega| < 0.3\pi, \\ 0, & 0.3\pi < |\omega| < 0.6\pi, \\ 0.5e^{-j\omega M/2}, & 0.6\pi < |\omega| \le \pi. \end{cases}$$

The impulse response $h_d[n]$ is multiplied by a Kaiser window with $M = 48$ and $\beta = 3.68$, resulting in a linear-phase FIR system with impulse response $h[n]$.

(a) What is the delay of the filter?

(b) Determine the ideal desired impulse response $h_d[n]$.

(c) Determine the set of approximation error specifications that is satisfied by the FIR filter; i.e., determine the parameters $\delta_1, \delta_2, \delta_3, B, C, \omega_{p1}, \omega_{s1}, \omega_{s2}$, and ω_{p2} in

$$\begin{aligned} B - \delta_1 \le |H(e^{j\omega})| &\le B + \delta_1, & 0 \le \omega \le \omega_{p1}, \\ |H(e^{j\omega})| &\le \delta_2, & \omega_{s1} \le \omega \le \omega_{s2}, \\ C - \delta_3 \le |H(e^{j\omega})| &\le C + \delta_3, & \omega_{p2} \le \omega \le \pi. \end{aligned}$$

7.45. The frequency response of a desired filter $h_d[n]$ is shown in Figure P7.45. In this problem, we wish to design an $(M+1)$-point causal linear-phase FIR filter $h[n]$ that minimizes the integral-squared error

$$\epsilon_d^2 = \frac{1}{2\pi}\int_{-\pi}^{\pi} |A(e^{j\omega}) - H_d(e^{j\omega})|^2 d\omega,$$

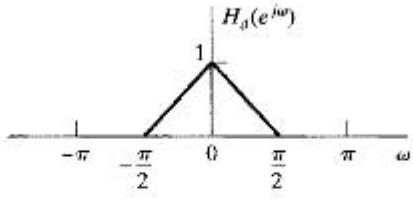

Figure P7.45

where the frequency response of the filter $h[n]$ is

$$H(e^{j\omega}) = A(e^{j\omega})e^{-j\omega M/2}$$

and M is an even integer.

(a) Determine $h_d[n]$.

(b) What symmetry should $h[n]$ have in the range $0 \leq n \leq M$? Briefly explain your reasoning.

(c) Determine $h[n]$ in the range $0 \leq n \leq M$.

(d) Determine an expression for the minimum integral-squared error ϵ^2 as a function of $h_d[n]$ and M.

7.46. Consider a type I linear-phase FIR lowpass filter with impulse response $h_{LP}[n]$ of length $(M+1)$ and frequency response

$$H_{LP}(e^{j\omega}) = A_e(e^{j\omega})e^{-j\omega M/2}.$$

The system has the amplitude function $A_e(e^{j\omega})$ shown in Figure P7.46.

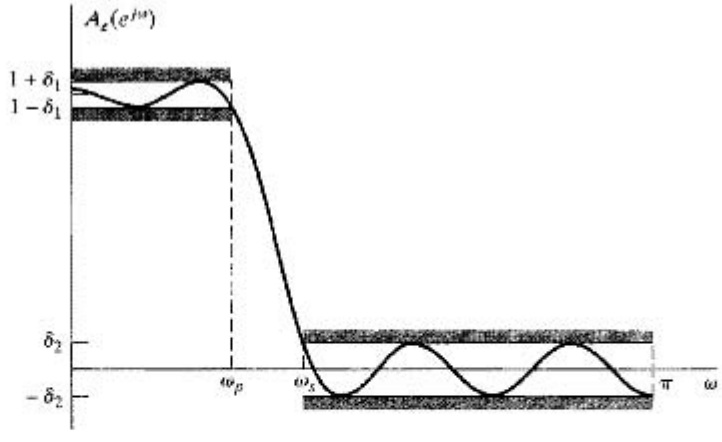

Figure P7.46

This amplitude function is the optimal (in the Parks–McClellan sense) approximation to unity in the band $0 \leq \omega \leq \omega_p$, where $\omega_p = 0.27\pi$, and the optimal approximation to zero in the band $\omega_s \leq \omega \leq \pi$, wherein $\omega_s = 0.4\pi$.

(a) What is the value of M?

Suppose now that a highpass filter is derived from this lowpass filter by defining

$$h_{HP}[n] = (-1)^{n+1}h_{LP}[n] = -e^{j\pi n}h_{LP}[n].$$

(b) Show that the resulting frequency response is of the form $H_{HP}(e^{j\omega}) = B_e(e^{j\omega})e^{-j\omega M/2}$.

(c) Sketch $B_e(e^{j\omega})$ for $0 \le \omega \le \pi$.

(d) It is asserted that for the given value of M (as found in part (a)), the resulting highpass filter is the optimum approximation to zero in the band $0 \le \omega \le 0.6\pi$ and to unity in the band $0.73\pi \le \omega \le \pi$. Is this assertion correct? Justify your answer.

7.47. Design a three-point optimal (in the minimax sense) causal lowpass filter with $\omega_s = \pi/2$, $\omega_p = \pi/3$, and $K = 1$. Specify the impulse response $h[n]$ of the filter you design. *Note:* $\cos(\pi/2) = 0$ and $\cos(\pi/3) = 0.5$.

Extension Problems

7.48. If an LTI continuous-time system has a rational system function, then its input and output satisfy an ordinary linear differential equation with constant coefficients. A standard procedure in the simulation of such systems is to use finite-difference approximations to the derivatives in the differential equations. In particular, since, for continuous differentiable functions $y_c(t)$,

$$\frac{dy_c(t)}{dt} = \lim_{T \to 0} \left[\frac{y_c(t) - y_c(t - T)}{T} \right],$$

it seems plausible that if T is "small enough," we should obtain a good approximation if we replace $dy_c(t)/dt$ by $[y_c(t) - y_c(t - T)]/T$.

While this simple approach may be useful for simulating continuous-time systems, it is *not* generally a useful method for designing discrete-time systems for filtering applications. To understand the effect of approximating differential equations by difference equations, it is helpful to consider a specific example. Assume that the system function of a continuous-time system is

$$H_c(s) = \frac{A}{s + c},$$

where A and c are constants.

(a) Show that the input $x_c(t)$ and the output $y_c(t)$ of the system satisfy the differential equation

$$\frac{dy_c(t)}{dt} + cy_c(t) = Ax_c(t).$$

(b) Evaluate the differential equation at $t = nT$, and substitute

$$\left.\frac{dy_c(t)}{dt}\right|_{t=nT} \approx \frac{y_c(nT) - y_c(nT - T)}{T},$$

i.e., replace the first derivative by the *first backward difference*.

(c) Define $x[n] = x_c(nT)$ and $y[n] = y_c(nT)$. With this notation and the result of part (b), obtain a difference equation relating $x[n]$ and $y[n]$, and determine the system function $H(z) = Y(z)/X(z)$ of the resulting discrete-time system.

(d) Show that, for this example,

$$H(z) = H_c(s)|_{s=(1-z^{-1})/T};$$

i.e., show that $H(z)$ can be obtained directly from $H_c(s)$ by the mapping

$$s = \frac{1 - z^{-1}}{T}.$$

(It can be demonstrated that if higher-order derivatives are approximated by repeated application of the first backward difference, then the result of part (d) holds for higher-order systems as well.)

(e) For the mapping of part (d), determine the contour in the z-plane to which the $j\Omega$-axis of the s-plane maps. Also, determine the region of the z-plane that corresponds to the left half of the s-plane. If the continuous-time system with system function $H_c(s)$ is stable, will the discrete-time system obtained by first backward difference approximation also be stable? Will the frequency response of the discrete-time system be a faithful reproduction of the frequency response of the continuous-time system? How will the stability and frequency response be affected by the choice of T?

(f) Assume that the first derivative is approximated by the *first forward difference;* i.e.,

$$\left.\frac{dy_c(t)}{dt}\right|_{t=nT} \approx \frac{y_c(nT+T)-y_c(nT)}{T}.$$

Determine the corresponding mapping from the s-plane to the z-plane, and repeat part (e) for this mapping.

7.49. Consider an LTI continuous-time system with rational system function $H_c(s)$. The input $x_c(t)$ and the output $y_c(t)$ satisfy an ordinary linear differential equation with constant coefficients. One approach to simulating such systems is to use numerical techniques to integrate the differential equation. In this problem, we demonstrate that if the trapezoidal integration formula is used, this approach is equivalent to transforming the continuous-time system function $H_c(s)$ to a discrete-time system function $H(z)$ using the bilinear transformation.

To demonstrate this statement, consider the continuous-time system function

$$H_c(s) = \frac{A}{s+c},$$

where A and c are constants. The corresponding differential equation is

$$\dot{y}_c(t) + cy_c(t) = Ax_c(t),$$

where

$$\dot{y}_c(t) = \frac{dy_c(t)}{dt}.$$

(a) Show that $y_c(nT)$ can be expressed in terms of $\dot{y}_c(t)$ as

$$y_c(nT) = \int_{(nT-T)}^{nT} \dot{y}_c(\tau)d\tau + y_c(nT-T).$$

The definite integral in this equation represents the area beneath the function $\dot{y}_c(t)$ for the interval from $(nT-T)$ to nT. Figure P7.49 shows a function $\dot{y}_c(t)$ and a shaded trapezoid-shaped region whose area approximates the area beneath the curve. This approximation to the integral is known as the *trapezoidal approximation.* Clearly, as T approaches zero, the approximation improves. Use the trapezoidal approximation to obtain an expression for $y_c(nT)$ in terms of $y_c(nT-T)$, $\dot{y}_c(nT)$, and $\dot{y}_c(nT-T)$.

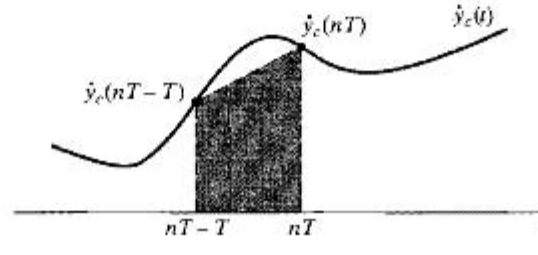

Figure P7.49

(b) Use the differential equation to obtain an expression for $\dot{y}_c(nT)$, and substitute this expression into the expression obtained in part (a).

(c) Define $x[n] = x_c(nT)$ and $y[n] = y_c(nT)$. With this notation and the result of part (b), obtain a difference equation relating $x[n]$ and $y[n]$, and determine the system function $H(z) = Y(z)/X(z)$ of the resulting discrete-time system.

(d) Show that, for this example,

$$H(z) = H_c(s)\big|_{s=(2/T)[(1-z^{-1})/(1+z^{-1})]};$$

i.e., show that $H(z)$ can be obtained directly from $H_c(s)$ by the bilinear transformation. (For higher-order differential equations, repeated trapezoidal integration applied to the highest order derivative of the output will result in the same conclusion for a general continuous-time system with rational system function.)

7.50. In this problem, we consider a method of filter design that might be called *autocorrelation invariance*. Consider a stable continuous-time system with impulse response $h_c(t)$ and system function $H_c(s)$. The autocorrelation function of the system impulse response is defined as

$$\phi_c(\tau) = \int_{-\infty}^{\infty} h_c(t)h_c(t+\tau)d\tau,$$

and for a real impulse response, it is easily shown that the Laplace transform of $\phi_c(\tau)$ is $\Phi_c(s) = H_c(s)H_c(-s)$. Similarly, consider a discrete-time system with impulse response $h[n]$ and system function $H(z)$. The autocorrelation function of a discrete-time system impulse response is defined as

$$\phi[m] = \sum_{n=-\infty}^{\infty} h[n]h[n+m],$$

and for a real impulse response, $\Phi(z) = H(z)H(z^{-1})$.

Autocorrelation invariance implies that a discrete-time filter is defined by equating the autocorrelation function of the discrete-time system to the sampled autocorrelation function of a continuous-time system; i.e.,

$$\phi[m] = T_d\phi_c(mT_d), \qquad -\infty < m < \infty.$$

The following design procedure is proposed for autocorrelation invariance when $H_c(s)$ is a rational function having N 1st-order poles at s_k, $k = 1, 2, \ldots, N$, and $M < N$ zeros:

1. Obtain a partial fraction expansion of $\Phi_c(s)$ in the form

$$\Phi_c(s) = \sum_{k=1}^{N}\left(\frac{A_k}{s-s_k} + \frac{B_k}{s+s_k}\right).$$

2. Form the z-transform

$$\Phi(z) = \sum_{k=1}^{N}\left(\frac{T_dA_k}{1-e^{s_kT_d}z^{-1}} + \frac{T_dB_k}{1-e^{-s_kT_d}z^{-1}}\right).$$

3. Find the poles and zeros of $\Phi(z)$, and form a minimum-phase system function $H(z)$ from the poles and zeros of $\Phi(z)$ that are *inside* the unit circle.

(a) Justify each step in the proposed design procedure; i.e., show that the autocorrelation function of the resulting discrete-time system is a sampled version of the autocorrelation function of the continuous-time system. To verify the procedure, it may be helpful to try it out on the 1st-order system with impulse response

$$h_c(t) = e^{-\alpha t}u(t)$$

and corresponding system function

$$H_c(s) = \frac{1}{s+\alpha}.$$

(b) What is the relationship between $|H(e^{j\omega})|^2$ and $|H_c(j\Omega)|^2$? What types of frequency-response functions would be appropriate for autocorrelation invariance design?

(c) Is the system function obtained in Step 3 unique? If not, describe how to obtain additional autocorrelation-invariant discrete-time systems.

7.51. Let $H_{lp}(Z)$ denote the system function for a discrete-time lowpass filter. The implementations of such a system can be represented by linear signal flow graphs consisting of adders, gains, and unit delay elements as in Figure P7.51-1. We want to implement a lowpass filter for which the cutoff frequency can be varied by changing a single parameter. The proposed strategy is to replace each unit delay element in a flow graph representing $H_{lp}(Z)$ by the network shown in Figure P7.51-2, where α is real and $|\alpha| < 1$.

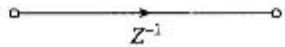

Figure P7.51-1

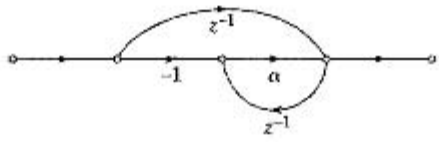

Figure P7.51-2

(a) Let $H(z)$ denote the system function for the filter that results when the network of Figure P7.51-2 is substituted for each unit delay branch in the network that implements $H_{lp}(Z)$. Show that $H(z)$ and $H_{lp}(Z)$ are related by a mapping of the Z-plane into the z-plane.

(b) If $H(e^{j\omega})$ and $H_{lp}(e^{j\theta})$ are the frequency responses of the two systems, determine the relationship between the frequency variables ω and θ. Sketch ω as a function of θ for $\alpha = 0.5$, and -0.5, and show that $H(e^{j\omega})$ is a lowpass filter. Also, if θ_p is the passband cutoff frequency for the original lowpass filter $H_{lp}(Z)$, obtain an equation for ω_p, the cutoff frequency of the new filter $H(z)$, as a function of α and θ_p.

(c) Assume that the original lowpass filter has the system function

$$H_{lp}(Z) = \frac{1}{1-0.9Z^{-1}}.$$

Draw the flow graph of an implementation of $H_{lp}(Z)$, and also draw the flow graph of the implementation of $H(z)$ obtained by replacing the unit delay elements in the first flow graph by the network in Figure P7.51-2. Does the resulting network correspond to a computable difference equation?

(d) If $H_{lp}(Z)$ corresponds to an FIR system implemented in direct form, would the flow graph manipulation lead to a computable difference equation? If the FIR system $H_{lp}(Z)$ was a linear-phase system, would the resulting system $H(z)$ also be a linear-phase system? If the FIR system has an impulse response of length $M+1$ samples what would be the length of the impulse response of the transformed system?

(e) To avoid the difficulties that arose in part (c), it is suggested that the network of Figure P7.51-2 be cascaded with a unit delay element, as depicted in Figure P7.51-3. Repeat the analysis of part (a) when the network of Figure P7.51-3 is substituted for each unit delay element. Determine an equation that expresses θ as a function of ω, and show that if $H_{lp}(e^{j\omega})$ is a lowpass filter, then $H(e^{j\omega})$ is not a lowpass filter.

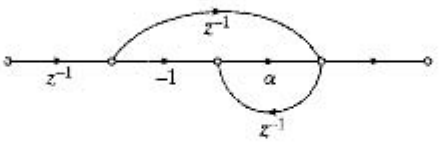

Figure P7.51-3

7.52. If we are given a basic filter module (a hardware or computer subroutine), it is sometimes possible to use it repetitively to implement a new filter with sharper frequency-response characteristics. One approach is to cascade the filter with itself two or more times, but it can easily be shown that, while stopband errors are squared (thereby reducing them if they are less than 1), this approach will increase the passband approximation error. Another approach, suggested by Tukey (1977), is shown in the block diagram of Figure P7.52-1. Tukey called this approach "twicing."

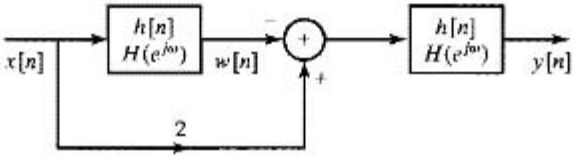

Figure P7.52-1

(a) Assume that the basic system has a symmetric finite-duration impulse response; i.e.,

$$h[n] = \begin{cases} h[-n], & -L \le n \le L, \\ 0 & \text{otherwise.} \end{cases}$$

Determine whether the overall impulse response $g[n]$ is (i) FIR and (ii) symmetric.

(b) Suppose that $H(e^{j\omega})$ satisfies the following approximation error specifications:

$$(1-\delta_1) \le H(e^{j\omega}) \le (1+\delta_1), \qquad 0 \le \omega \le \omega_p,$$
$$-\delta_2 \le H(e^{j\omega}) \le \delta_2, \qquad \omega_s \le \omega \le \pi.$$

It can be shown that if the basic system has these specifications, the overall frequency response $G(e^{j\omega})$ (from $x[n]$ to $y[n]$) satisfies specifications of the form

$$A \le G(e^{j\omega}) \le B, \qquad 0 \le \omega \le \omega_p,$$
$$C \le G(e^{j\omega}) \le D, \qquad \omega_s \le \omega \le \pi.$$

Determine A, B, C, and D in terms of δ_1 and δ_2. If $\delta_1 \ll 1$ and $\delta_2 \ll 1$, what are the approximate maximum passband and stopband approximation errors for $G(e^{j\omega})$?

(c) As determined in part (b), Tukey's twicing method improves the passband approximation error, but increases the stopband error. Kaiser and Hamming (1977) generalized the twicing method so as to improve *both* the passband and the stopband. They called their approach "sharpening." The simplest sharpening system that improves both passband and stopband is shown in Figure P7.52-2. Assume again that the impulse response of the basic system is as given in part (a). Repeat part (b) for the system of Figure P7.52-2.

(d) The basic system was assumed to be noncausal. If the impulse response of the basic system is a causal linear-phase FIR system such that

$$h[n] = \begin{cases} h[M-n], & 0 \le n \le M, \\ 0, & \text{otherwise,} \end{cases}$$

how should the systems of Figures P7.52-1 and P7.52-2 be modified? What type(s) (I, II, III, or IV) of causal linear-phase FIR system(s) can be used? What are the lengths of the impulse responses $g[n]$ for the systems in Figures P7.52-1 and P7.52-2 (in terms of L)?

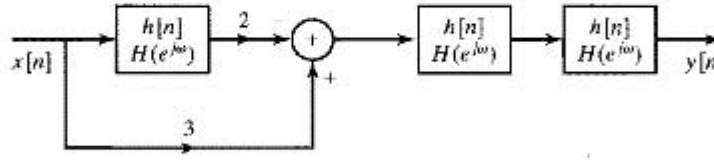

Figure P7.52-2

7.53. Consider the design of a lowpass linear-phase FIR filter by means of the Parks–McClellan algorithm. Use the alternation theorem to argue that the approximation must decrease monotonically in the "don't care" region between the passband and the stopband approximation intervals. *Hint*: Show that all the local maxima and minima of the trigonometric polynomial must be in either the passband or the stopband to satisfy the alternation theorem.

7.54. Figure P7.54 shows the frequency response $A_e(e^{j\omega})$ of a discrete-time FIR system for which the impulse response is

$$h_e[n] = \begin{cases} h_e[-n], & -L \le n \le L, \\ 0, & \text{otherwise.} \end{cases}$$

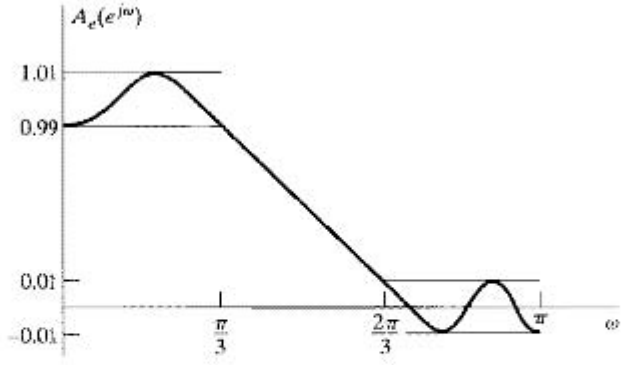

Figure P7.54

(a) Show that $A_e(e^{j\omega})$ cannot correspond to an FIR filter generated by the Parks–McClellan algorithm with a passband edge frequency of $\pi/3$, a stopband edge frequency of $2\pi/3$, and an error-weighting function of unity in the passband and stopband. Clearly explain your reasoning. *Hint*: The alternation theorem states that the best approximation is unique.

(b) Based on Figure P7.54 and the statement that $A_e(e^{j\omega})$ cannot correspond to an optimal filter, what can be concluded about the value of L?

7.55. Consider the system in Figure P7.55.

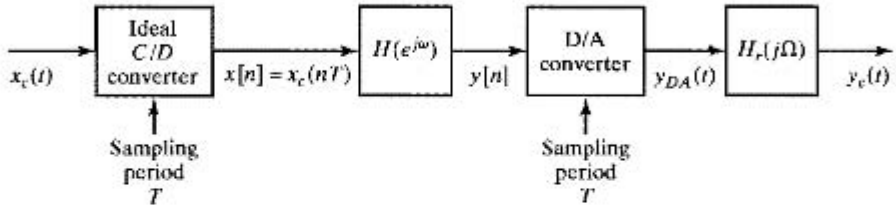

Figure P7.55

1. Assume that $X_c(j\Omega) = 0$ for $|\Omega| \geq \pi/T$ and that

$$H_r(j\Omega) = \begin{cases} 1, & |\Omega| < \pi/T, \\ 0, & |\Omega| > \pi/T, \end{cases}$$

   denotes an ideal lowpass reconstruction filter.
2. The D/A converter has a built-in zero-order-hold circuit, so that

$$y_{DA}(t) = \sum_{n=-\infty}^{\infty} y[n]h_0(t - nT),$$

   where

$$h_0(t) = \begin{cases} 1, & 0 \leq t < T, \\ 0, & \text{otherwise.} \end{cases}$$

   (We neglect quantization in the D/A converter.)
3. The second system in Figure P7.55 is a linear-phase FIR discrete-time system with frequency response $H(e^{j\omega})$.

We wish to design the FIR system using the Parks–McClellan algorithm to compensate for the effects of the zero-order-hold system.

(a) The Fourier transform of the output is $Y_c(j\Omega) = H_{\text{eff}}(j\Omega)X_c(j\Omega)$. Determine an expression for $H_{\text{eff}}(j\Omega)$ in terms of $H(e^{j\Omega T})$ and T.

(b) If the linear-phase FIR system is such that $h[n] = 0$ for $n < 0$ and $n > 51$, and $T = 10^{-4}$ s, what is the overall time delay (in ms) between $x_c(t)$ and $y_c(t)$?

(c) Suppose that when $T = 10^{-4}$ s, we want the effective frequency response to be equiripple (in both the passband and the stopband) within the following tolerances:

$$0.99 \leq |H_{\text{eff}}(j\Omega)| \leq 1.01, \qquad |\Omega| \leq 2\pi(1000),$$
$$|H_{\text{eff}}(j\Omega)| \leq 0.01, \qquad 2\pi(2000) \leq |\Omega| \leq 2\pi(5000).$$

We want to achieve this by designing an optimum linear-phase filter (using the Parks–McClellan algorithm) that includes compensation for the zero-order hold. Give an equation for the ideal response $H_d(e^{j\omega})$ that should be used. Find and sketch the weighting function $W(\omega)$ that should be used. Sketch a "typical" frequency response $H(e^{j\omega})$ that might result.

(d) How would you modify your results in part (c) to include magnitude compensation for a reconstruction filter $H_r(j\Omega)$ with zero gain above $\Omega = 2\pi(5000)$, but with sloping passband?

7.56. After a discrete-time signal is lowpass filtered, it is often downsampled or decimated, as depicted in Figure P7.56-1. Linear-phase FIR filters are frequently desirable in such applications, but if the lowpass filter in the figure has a narrow transition band, an FIR system will have a long impulse response and thus will require a large number of multiplications and additions per output sample.

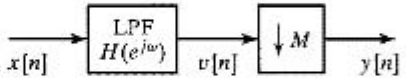

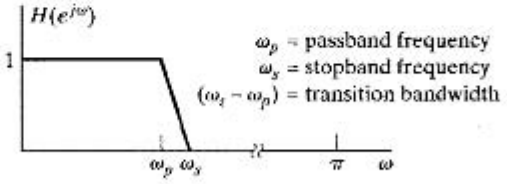

Figure P7.56-1

In this problem, we will study the merits of a multistage implementation of the system in Figure P7.56-1. Such implementations are particularly useful when ω_s is small and the decimation factor M is large. A general multistage implementation is depicted in Figure P7.56-2. The strategy is to use a wider transition band in the lowpass filters of the earlier stages, thereby reducing the length of the required filter impulse responses in those stages. As decimation occurs, the number of signal samples is reduced, and we can progressively decrease the widths of the transition bands of the filters that operate on the decimated signal. In this manner, the overall number of computations required to implement the decimator may be reduced.

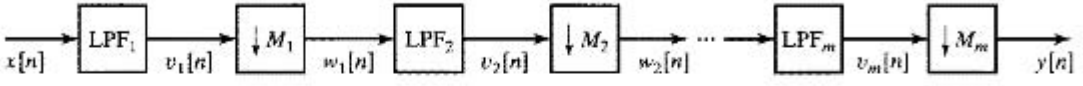

Figure P7.56-2

(a) If no aliasing is to occur as a result of the decimation in Figure P7.56-1, what is the maximum allowable decimation factor M in terms of ω_s?

(b) Let $M = 100$, $\omega_s = \pi/100$, and $\omega_p = 0.9\pi/100$ in the system of Figure P7.56-2. If $x[n] = \delta[n]$, sketch $V(e^{j\omega})$ and $Y(e^{j\omega})$.

Now consider a two-stage implementation of the decimator for $M = 100$, as depicted in Figure P7.56-3, where $M_1 = 50$, $M_2 = 2$, $\omega_{p1} = 0.9\pi/100$, $\omega_{p2} = 0.9\pi/2$, and $\omega_{s2} = \pi/2$. We must choose ω_{s1} or, equivalently, the transition band of LPF_1, $(\omega_{s1} - \omega_{p1})$, such that the two-stage implementation yields the same equivalent passband and stopband frequencies as the single-stage decimator. (We are not concerned about the detailed shape of the frequency response in the transition band, except that both systems should have a monotonically decreasing response in the transition band.)

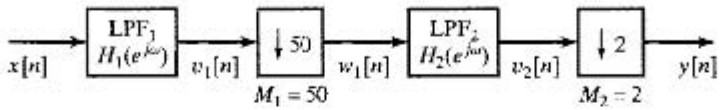

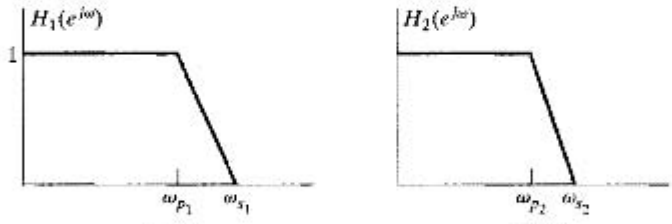

Figure P7.56-3

(c) For an arbitrary ω_{s1} and the input $x[n] = \delta[n]$, sketch $V_1(e^{j\omega})$, $W_1(e^{j\omega})$, $V_2(e^{j\omega})$, and $Y(e^{j\omega})$ for the two-stage decimator of Figure P7.56-3.

(d) Find the *largest* value of ω_{s1} such that the two-stage decimator yields the same equivalent passband and stopband cutoff frequencies as the single-stage system in part (b).

In addition to possessing a nonzero transition bandwidth, the lowpass filters must differ from the ideal by passband and stopband approximation errors of δ_p and δ_s, respectively. Assume that linear-phase equiripple FIR approximations are used. It follows from Eq. (7.117) that, for optimum lowpass filters,

$$N \approx \frac{-10\log_{10}(\delta_p\delta_s) - 13}{2.324\Delta\omega} + 1, \tag{P7.56-1}$$

where N is the length of the impulse response and $\Delta\omega = \omega_s - \omega_p$ is the transition band of the lowpass filter. Equation P7.56-1 provides the basis for comparing the two implementations of the decimator. Equation (7.76) could be used in place of Eq. (P7.56-1) to estimate the impulse-response length if the filters are designed by the Kaiser window method.

(e) Assume that $\delta_p = 0.01$ and $\delta_s = 0.001$ for the lowpass filter in the single-stage implementation. Compute the length N of the impulse response of the lowpass filter, and determine the number of multiplications required to compute each sample of the output. Take advantage of the symmetry of the impulse response of the linear-phase FIR system. (Note that in this decimation application, only every M^{th} sample of the output need be computed; i.e., the compressor commutes with the multiplications of the FIR system.)

(f) Using the value of ω_{s1} found in part (d), compute the impulse response lengths N_1 and N_2 of LPF_1 and LPF_2, respectively, in the two-stage decimator of Figure P7.56-3. Determine the total number of multiplications required to compute each sample of the output in the two-stage decimator.

(g) If the approximation error specifications $\delta_p = 0.01$ and $\delta_s = 0.001$ are used for both filters in the two-stage decimator, the overall passband ripple may be greater than 0.01, since the passband ripples of the two stages can reinforce each other; e.g., $(1+\delta_p)(1+\delta_p) > (1+\delta_p)$. To compensate for this, the filters in the two-stage implementation can each be designed to have only one-half the passband ripple of the single-stage implementation. Therefore, assume that $\delta_p = 0.005$ and $\delta_s = 0.001$ for each filter in the two-stage decimator. Calculate the impulse response lengths N_1 and N_2 of LPF_1 and LPF_2, respectively, and determine the total number of multiplications required to compute each sample of the output.

(h) Should we also reduce the specification on the stopband approximation error for the filters in the two-stage decimator?

(i) *Optional.* The combination of $M_1 = 50$ and $M_2 = 2$ may not yield the smallest total number of multiplications per output sample. Other integer choices for M_1 and M_2 are possible such that $M_1 M_2 = 100$. Determine the values of M_1 and M_2 that minimize the number of multiplications per output sample.

7.57. In this problem, we develop a technique for designing discrete-time filters with minimum phase. Such filters have all their poles and zeros inside (or on) the unit circle. (We will allow zeros on the unit circle.) Let us first consider the problem of converting a type I linear-phase FIR equiripple lowpass filter to a minimum-phase system. If $H(e^{j\omega})$ is the frequency response of a type I linear-phase filter, then

1. The corresponding impulse response
$$h[n] = \begin{cases} h[M-n], & 0 \le n \le M, \\ 0, & \text{otherwise}, \end{cases}$$
is real and M is an even integer.
2. It follows from part 1 that $H(e^{j\omega}) = A_e(e^{j\omega})e^{-j\omega n_0}$, where $A_e(e^{j\omega})$ is real and $n_0 = M/2$ is an integer.
3. The passband ripple is δ_1; i.e., in the passband, $A_e(e^{j\omega})$ oscillates between $(1+\delta_1)$ and $(1-\delta_1)$. (See Figure P7.57-1.)

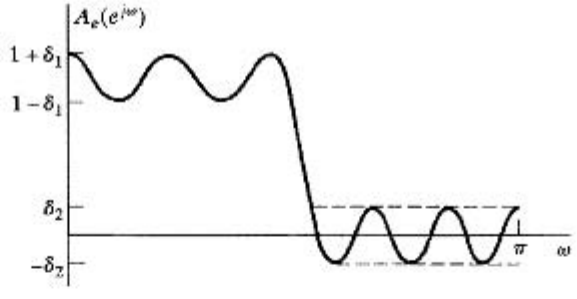

Figure P7.57-1

4. The stopband ripple is δ_2; i.e., in the stopband, $-\delta_2 \le A_e(e^{j\omega}) \le \delta_2$, and $A_e(e^{j\omega})$ oscillates between $-\delta_2$ and $+\delta_2$. (See Figure P7.57-1.)

The following technique was proposed by Herrmann and Schüssler (1970a) for converting this linear-phase system into a minimum-phase system that has a system function $H_{\min}(z)$ and unit sample response $h_{\min}[n]$ (in this problem, we assume that minimum-phase systems can have zeros *on* the unit circle):

Step 1. Create a new sequence
$$h_1[n] = \begin{cases} h[n], & n \ne n_0, \\ h[n_0] + \delta_2, & n = n_0. \end{cases}$$

Step 2. Recognize that $H_1(z)$ can be expressed in the form
$$H_1(z) = z^{-n_0} H_2(z) H_2(1/z) = z^{-n_0} H_3(z)$$
for some $H_2(z)$, where $H_2(z)$ has all its poles and zeros inside or on the unit circle and $h_2[n]$ is real.

Step 3. Define
$$H_{\min}(z) = \frac{H_2(z)}{a}.$$

The denominator constant where $a = (\sqrt{1-\delta_1+\delta_2} + \sqrt{1+\delta_1+\delta_2})/2$ normalizes the passband so that the resulting frequency response $H_{\min}(e^{j\omega})$ will oscillate about a value of unity.

(a) Show that if $h_1[n]$ is chosen as in Step 1, then $H_1(e^{j\omega})$ can be written as

$$H_1(e^{j\omega}) = e^{-j\omega n_0} H_3(e^{j\omega}),$$

where $H_3(e^{j\omega})$ is real and nonnegative for all values of ω.

(b) If $H_3(e^{j\omega}) \geq 0$, as was shown in part (a), show that there exists an $H_2(z)$ such that

$$H_3(z) = H_2(z)H_2(1/z),$$

where $H_2(z)$ is a minimum-phase system function and $h_2[n]$ is real (i.e., justify Step 2).

(c) Demonstrate that the new filter $H_{\min}(e^{j\omega})$ is an equiripple lowpass filter (i.e., that its magnitude characteristic is of the form shown in Figure P7.57-2) by evaluating δ_1' and δ_2'. What is the length of the new impulse response $h_{\min}[n]$?

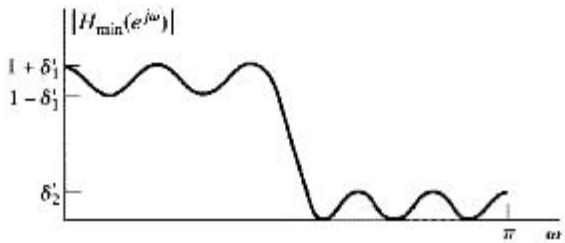

Figure P7.57-2

(d) In parts (a), (b), and (c), we assumed that we started with a type I FIR linear-phase filter. Will this technique work if we remove the linear-phase constraint? Will it work if we use a type II FIR linear-phase system?

7.58. Suppose that we have a program that finds the set of coefficients $a[n]$, $n = 0, 1, \ldots, L$, that minimizes

$$\max_{\omega \in F} \left\{ \left| W(\omega) \left[H_d(e^{j\omega}) - \sum_{n=0}^{L} a[n] \cos \omega n \right] \right| \right\},$$

given L, F, $W(\omega)$, and $H_d(e^{j\omega})$. We have shown that the solution to this optimization problem implies a noncausal FIR zero-phase system with impulse response satisfying $h_e[n] = h_e[-n]$. By delaying $h_e[n]$ by L samples, we obtain a causal type I FIR linear-phase system with frequency response

$$H(e^{j\omega}) = e^{-j\omega M/2} \sum_{n=0}^{L} a[n] \cos \omega n = \sum_{n=0}^{2L} h[n] e^{-j\omega n},$$

where the impulse response is related to the coefficients $a[n]$ by

$$a[n] = \begin{cases} 2h[M/2 - n] & \text{for } 1 \leq n \leq L, \\ h[M/2] & \text{for } n = 0, \end{cases}$$

and $M = 2L$ is the order of the system function polynomial. (The length of the impulse response is $M + 1$.)

The other three types (II, III, and IV) of linear-phase FIR filters can be designed by the available program if we make suitable modifications to the weighting function $W(\omega)$

and the desired frequency response $H_d(e^{j\omega})$. To see how to do this, it is necessary to manipulate the expressions for the frequency response into the standard form assumed by the program.

(a) Assume that we wish to design a causal type II FIR linear-phase system such that $h[n] = h[M - n]$ for $n = 0, 1, \ldots, M$, where M is an odd integer. Show that the frequency response of this type of system can be expressed as

$$H(e^{j\omega}) = e^{-j\omega M/2} \sum_{n=1}^{(M+1)/2} b[n] \cos \omega\left(n - \tfrac{1}{2}\right),$$

and determine the relationship between the coefficients $b[n]$ and $h[n]$.

(b) Show that the summation

$$\sum_{n=1}^{(M+1)/2} b[n] \cos \omega\left(n - \tfrac{1}{2}\right)$$

can be written as

$$\cos(\omega/2) \sum_{n=0}^{(M-1)/2} \tilde{b}[n] \cos \omega n$$

by obtaining an expression for $b[n]$ for $n = 1, 2, \ldots, (M + 1)/2$ in terms of $\tilde{b}[n]$ for $n = 0, 1, \ldots, (M - 1)/2$. *Hint*: Note carefully that $b[n]$ is to be expressed in terms of $\tilde{b}[n]$. Also, use the trigonometric identity $\cos\alpha \cos\beta = \frac{1}{2}\cos(\alpha + \beta) + \frac{1}{2}\cos(\alpha - \beta)$.

(c) If we wish to use the given program to design type II systems (M odd) for a given F, $W(\omega)$, and $H_d(e^{j\omega})$, show how to obtain $\tilde{L}$, $\tilde{F}$, $\tilde{W}(\omega)$, and $\tilde{H}_d(e^{j\omega})$ in terms of M, F, $W(\omega)$, and $H_d(e^{j\omega})$ such that if we run the program using $\tilde{L}$, $\tilde{F}$, $\tilde{W}(\omega)$, and $\tilde{H}_d(e^{j\omega})$, we may use the resulting set of coefficients to determine the impulse response of the desired type II system.

(d) Parts (a)–(c) can be repeated for types III and IV causal linear-phase FIR systems where $h[n] = -h[M - n]$. For these cases, you must show that, for type III systems (M even), the frequency response can be expressed as

$$\begin{aligned} H(e^{j\omega}) &= e^{-j\omega M/2} \sum_{n=1}^{M/2} c[n] \sin \omega n \\ &= e^{-j\omega M/2} \sin\omega \sum_{n=0}^{(M-2)/2} \tilde{c}[n] \cos \omega n, \end{aligned}$$

and for type IV systems (M odd),

$$\begin{aligned} H(e^{j\omega}) &= e^{-j\omega M/2} \sum_{n=1}^{(M+1)/2} d[n] \sin \omega\left(n - \tfrac{1}{2}\right) \\ &= e^{-j\omega M/2} \sin(\omega/2) \sum_{n=0}^{(M-1)/2} \tilde{d}[n] \cos \omega n. \end{aligned}$$

As in part (b), it is necessary to express $c[n]$ in terms of $\tilde{c}[n]$ and $d[n]$ in terms of $\tilde{d}[n]$ using the trigonometric identity $\sin\alpha \cos\beta = \frac{1}{2}\sin(\alpha + \beta) + \frac{1}{2}\sin(\alpha - \beta)$. McClellan and Parks (1973) and Rabiner and Gold (1975) give more details on issues raised in this problem.

7.59. In this problem, we consider a method of obtaining an implementation of a variable-cutoff linear-phase filter. Assume that we are given a zero-phase filter designed by the Parks–McClellan method. The frequency response of this filter can be represented as

$$A_e(e^{j\theta}) = \sum_{k=0}^{L} a_k(\cos\theta)^k,$$

and its system function can therefore be represented as

$$A_e(Z) = \sum_{k=0}^{L} a_k \left(\frac{Z+Z^{-1}}{2}\right)^k,$$

with $e^{j\theta} = Z$. (We use Z for the original system and z for the system to be obtained by transformation of the original system.)

(a) Using the preceding expression for the system function, draw a block diagram or flow graph of an implementation of the system that utilizes multiplications by the coefficients a_k, additions, and elemental systems having system function $(Z+Z^{-1})/2$.

(b) What is the length of the impulse response of the system? The overall system can be made causal by cascading the system with a delay of L samples. Distribute this delay as unit delays so that all parts of the network will be causal.

(c) Suppose that we obtain a new system function from $A_e(Z)$ by the substitution

$$B_e(z) = A_e(Z)\big|_{(Z+Z^{-1})/2=\alpha_0+\alpha_1[(z+z^{-1})/2]}.$$

Using the flow graph obtained in part (a), draw the flow graph of a system that implements the system function $B_e(z)$. What is the length of the impulse response of this system? Modify the network as in part (b) to make the overall system and all parts of the network causal.

(d) If $A_e(e^{j\theta})$ is the frequency response of the original filter and $B_e(e^{j\omega})$ is the frequency response of the transformed filter, determine the relationship between θ and ω.

(e) The frequency response of the original optimal filter is shown in Figure P7.59. For the case $\alpha_1 = 1 - \alpha_0$ and $0 \le \alpha_0 < 1$, describe how the frequency response $B_e(e^{j\omega})$ changes as α_0 varies. *Hint*: Plot $A_e(e^{j\theta})$ and $B_e(e^{j\omega})$ as functions of $\cos\theta$ and $\cos\omega$. Are the resulting transformed filters also optimal in the sense of having the minimum maximum weighted approximation errors in the transformed passband and stopband?

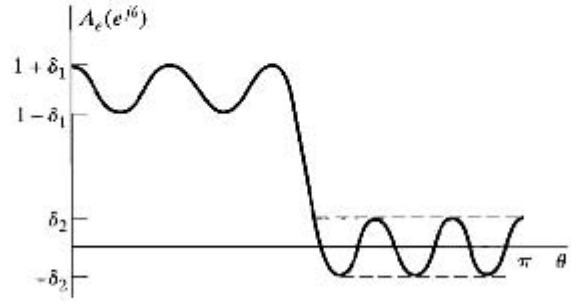

Figure P7.59

(f) *Optional.* Repeat part (e) for the case $\alpha_1 = 1 + \alpha_0$ and $-1 < \alpha_0 \le 0$.

7.60. In this problem, we consider the effect of mapping continuous-time filters to discrete-time filters by replacing derivatives in the differential equation for a continuous-time filter by central differences to obtain a difference equation. The first central difference of a sequence $x[n]$ is defined as

$$\Delta^{(1)}\{x[n]\} = x[n+1] - x[n-1],$$

and the k^{th} central difference is defined recursively as

$$\Delta^{(k)}\{x[n]\} = \Delta^{(1)}\{\Delta^{(k-1)}\{x[n]\}\}.$$

For consistency, the zero$^{\text{th}}$ central difference is defined as

$$\Delta^{(0)}\{x[n]\} = x[n].$$

(a) If $X(z)$ is the z-transform of $x[n]$, determine the z-transform of $\Delta^{(k)}\{x[n]\}$.

The mapping of an LTI continuous-time filter to an LTI discrete-time filter is as follows: Let the continuous-time filter with input $x(t)$ and output $y(t)$ be specified by a differential equation of the form

$$\sum_{k=0}^{N} a_k \frac{d^k y(t)}{dt^k} = \sum_{r=0}^{M} b_r \frac{d^r x(t)}{dt^r}.$$

Then the corresponding discrete-time filter with input $x[n]$ and output $y[n]$ is specified by the difference equation

$$\sum_{k=0}^{N} a_k \Delta^{(k)}\{y[n]\} = \sum_{r=0}^{M} b_r \Delta^{(r)}\{x[n]\}.$$

(b) If $H_c(s)$ is a rational continuous-time system function and $H_d(z)$ is the discrete-time system function obtained by mapping the differential equation to a difference equation as indicated in part (a), then

$$H_d(z) = H_c(s)\big|_{s=m(z)}.$$

Determine $m(z)$.

(c) Assume that $H_c(s)$ approximates a continuous-time lowpass filter with a cutoff frequency of $\Omega = 1$; i.e.,

$$H(j\Omega) \approx \begin{cases} 1, & |\Omega| < 1, \\ 0, & \text{otherwise.} \end{cases}$$

This filter is mapped to a discrete-time filter using central differences as discussed in part (a). Sketch the approximate frequency response that you would expect for the discrete-time filter, assuming that it is stable.

7.61. Let $h[n]$ be the optimal type I equiripple lowpass filter shown in Figure P7.61, designed with weighting function $W(e^{j\omega})$ and desired frequency response $H_d(e^{j\omega})$. For simplicity, assume that the filter is zero phase (i.e., noncausal). We will use $h[n]$ to design five different FIR filters as follows:

$$h_1[n] = h[-n],$$

$$h_2[n] = (-1)^n h[n],$$

$$h_3[n] = h[n] * h[n],$$

$$h_4[n] = h[n] - K\delta[n], \text{ where } K \text{ is a constant,}$$

$$h_5[n] = \begin{cases} h[n/2] & \text{for } n \text{ even,} \\ 0 & \text{otherwise.} \end{cases}$$

For each filter $h_i[n]$, determine whether $h_i[n]$ is optimal in the minimax sense. That is, determine whether

$$h_i[n] = \min_{h_i[n]} \max_{\omega \in F} \left(W(e^{j\omega})|H_d(e^{j\omega}) - H_i(e^{j\omega})|\right)$$

for some choices of a piecewise-constant $H_d(e^{j\omega})$ and a piecewise-constant $W(e^{j\omega})$, where F is a union of disjoint closed intervals on $0 \leq \omega \leq \pi$. If $h_i[n]$ is optimal, determine the corresponding $H_d(e^{j\omega})$ and $W(e^{j\omega})$. If $h_i[n]$ is not optimal, explain why.

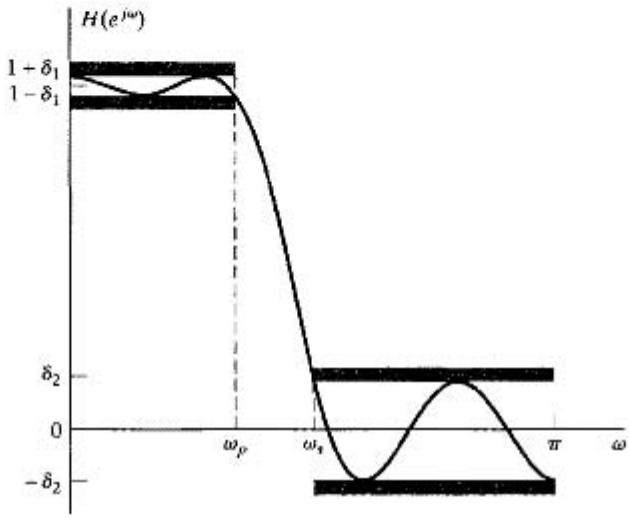

Figure P7.61

7.62. Suppose that you have used the Parks–McClellan algorithm to design a causal FIR linear-phase system. The system function of this system is denoted $H(z)$. The length of the impulse response is 25 samples, $h[n] = 0$ for $n < 0$ and for $n > 24$, and $h[0] \neq 0$. For each of the following questions, answer "true," "false," or "insufficient information given":

(a) $h[n+12] = h[12-n]$ or $h[n+12] = -h[12-n]$ for $-\infty < n < \infty$.
(b) The system has a stable and causal inverse.
(c) We know that $H(-1) = 0$.
(d) The maximum weighted approximation error is the same in all approximation bands.
(e) The system can be implemented by a signal flow graph that has no feedback paths.
(f) The group delay is positive for $0 < \omega < \pi$.

7.63. Consider the design of a type I bandpass linear-phase FIR filter using the Parks–McClellan algorithm. The impulse response length is $M+1 = 2L+1$. Recall that for type I systems, the frequency response is of the form $H(e^{j\omega}) = A_e(e^{j\omega})e^{-j\omega M/2}$, and the Parks–McClellan algorithm finds the function $A_e(e^{j\omega})$ that minimizes the maximum value of the error function

$$E(\omega) = W(\omega)[H_d(e^{j\omega}) - A_e(e^{j\omega})], \qquad \omega \in F,$$

where F is a closed subset of the interval $0 \leq \omega \leq \pi$, $W(\omega)$ is a weighting function, and $H_d(e^{j\omega})$ defines the desired frequency response in the approximation intervals F. The tolerance scheme for a bandpass filter is shown in Figure P7.63.

(a) Give the equation for the desired response $H_d(e^{j\omega})$ for the tolerance scheme in Figure P7.63.

(b) Give the equation for the weighting function $W(\omega)$ for the tolerance scheme in Figure P7.63.

(c) What is the *minimum* number of alternations of the error function for the optimum filter?

(d) What is the *maximum* number of alternations of the error function for the optimum filter?

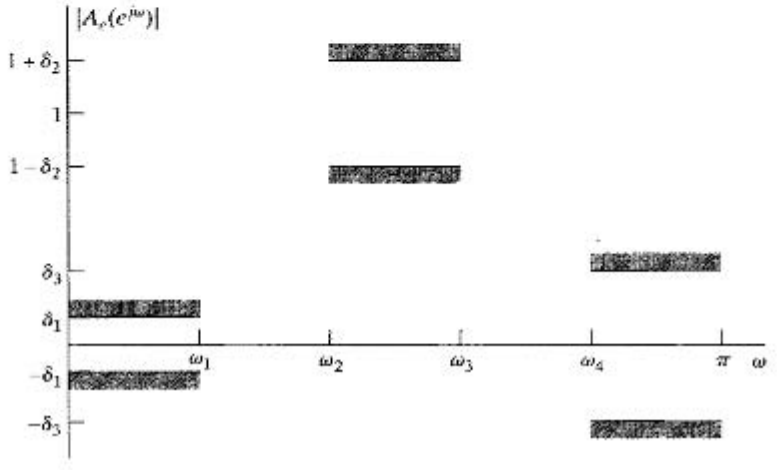

Figure P7.63

(e) Sketch a "typical" weighted error function $E(\omega)$ that could be the error function for an optimum bandpass filter if $M = 14$. Assume the *maximum* number of alternations.

(f) Now suppose that M, ω_1, ω_2, ω_3, the weighting function, and the desired function are kept the same, but ω_4 is *increased*, so that the transition band $(\omega_4 - \omega_3)$ is increased. Will the optimum filter for these new specifications *necessarily* have a *smaller* value of the maximum approximation error than the optimum filter associated with the original specifications? Clearly show your reasoning.

(g) In the lowpass filter case, all local minima and maxima of $A_e(e^{j\omega})$ must occur in the approximation bands $\omega \in F$; they *cannot* occur in the "don't care" bands. Also, in the lowpass case, the local minima and maxima that occur in the approximation bands must be alternations of the error. Show that this is not necessarily true in the bandpass filter case. Specifically, use the alternation theorem to show (i) that local maxima and minima of $A_e(e^{j\omega})$ are not restricted to the approximation bands and (ii) that local maxima and minima in the approximation bands need not be alternations.

7.64. It is often desirable to transform a prototype discrete-time lowpass filter to another kind of discrete-time frequency-selective filter. In particular, the impulse invariance approach cannot be used to convert continuous-time highpass or bandstop filters to discrete-time highpass or bandstop filters. Consequently, the traditional approach has been to design a prototype lowpass discrete-time filter using either impulse invariance or the bilinear transformation and then to use an algebraic transformation to convert the discrete-time lowpass filter into the desired frequency-selective filter.

To see how this is done, assume that we are given a lowpass system function $H_{lp}(Z)$ that we wish to transform to a new system function $H(z)$, which has either lowpass, highpass, bandpass, or bandstop characteristics when it is evaluated on the unit circle. Note that we associate the complex variable Z with the prototype lowpass filter and the complex variable z with the transformed filter. Then, we define a mapping from the Z-plane to the z-plane

of the form

$$Z^{-1} = G(z^{-1}) \tag{P7.64-1}$$

such that

$$H(z) = H_{\text{lp}}(Z)\big|_{Z^{-1}=G(z^{-1})}. \tag{P7.64-2}$$

Instead of expressing Z as a function of z, we have assumed in Eq. (P7.64-1) that Z^{-1} is expressed as a function of z^{-1}. Thus, according to Eq. (P7.64-2), in obtaining $H(z)$ from $H_{\text{lp}}(Z)$, we simply replace Z^{-1} everywhere in $H_{\text{lp}}(Z)$ by the function $G(z^{-1})$. This is a convenient representation, because $H_{\text{lp}}(Z)$ is normally expressed as a rational function of Z^{-1}.

If $H_{\text{lp}}(Z)$ is the rational system function of a causal and stable system, we naturally require that the transformed system function $H(z)$ be a rational function of z^{-1} and that the system also be causal and stable. This places the following constraints on the transformation $Z^{-1} = G(z^{-1})$:

1. $G(z^{-1})$ must be a rational function of z^{-1}.
2. The inside of the unit circle of the Z-plane must map to the inside of the unit circle of the z-plane.
3. The unit circle of the Z-plane must map onto the unit circle of the z-plane.

In this problem, you will derive and characterize the algebraic transformations necessary to convert a discrete-time lowpass filter into another lowpass filter with a different cutoff frequency or to a discrete-time highpass filter.

(a) Let θ and ω be the frequency variables (angles) in the Z-plane and z-plane, respectively, i.e., on the respective unit circles $Z = e^{j\theta}$ and $z = e^{j\omega}$. Show that, for Condition 3 to hold, $G(z^{-1})$ must be an all-pass system, i.e.,

$$|G(e^{-j\omega})| = 1. \tag{P7.64-3}$$

(b) It is possible to show that the most general form of $G(z^{-1})$ that satisfies all of the preceding three conditions is

$$Z^{-1} = G(z^{-1}) = \pm \prod_{k=1}^{N} \frac{z^{-1} - \alpha_k}{1 - \alpha_k z^{-1}}. \tag{P7.64-4}$$

From our discussion of all-pass systems in Chapter 5, it should be clear that $G(z^{-1})$, as given in Eq. (P7.64-4), satisfies Eq. (P7.64-3), i.e., is an allpass system, and thus meets Condition 3. Eq. (P7.64-4) also clearly meets Condition 1. Demonstrate that Condition 2 is satisfied if and only if $|\alpha_k| < 1$.

(c) A simple 1st-order $G(z^{-1})$ can be used to map a prototype lowpass filter $H_{\text{lp}}(Z)$ with cutoff θ_p to a new filter $H(z)$ with cutoff ω_p. Demonstrate that

$$G(z^{-1}) = \frac{z^{-1} - \alpha}{1 - \alpha z^{-1}}$$

will produce the desired mapping for some value of α. Solve for α as a function of θ_p and ω_p. Problem 7.51 uses this approach to design lowpass filters with adjustable cutoff frequencies.

(d) Consider the case of a prototype lowpass filter with $\theta_p = \pi/2$. For each of the following choices of α, specify the resulting cutoff frequency ω_p for the transformed filter:

(i) $\alpha = -0.2679$.
(ii) $\alpha = 0$.
(iii) $\alpha = 0.4142$.

(e) It is also possible to find a 1st-order all-pass system for $G(z^{-1})$ such that the prototype lowpass filter is transformed to a discrete-time highpass filter with cutoff ω_p. Note that such a transformation must map $Z^{-1} = e^{j\theta_p} \rightarrow z^{-1} = e^{j\omega_p}$ and also map $Z^{-1} = 1 \rightarrow z^{-1} = -1$; i.e., $\theta = 0$ maps to $\omega = \pi$. Find $G(z^{-1})$ for this transformation, and also, find an expression for α in terms of θ_p and ω_p.

(f) Using the same prototype filter and values for α as in part (d), sketch the frequency responses for the highpass filters resulting from the transformation you specified in part (e).

Similar, but more complicated, transformations can be used to convert the prototype lowpass filter $H_{\text{lp}}(Z)$ into bandpass and bandstop filters. Constantinides (1970) describes these transformations in more detail.